10.1071/CH18252_AC

Australian Journal of Chemistry 2018, 71(8), 610-623

Supplementary Material

N,N-Dialkyl-N′-Chlorosulfonyl Chloroformamidines in Heterocyclic Synthesis. Part XV. Some Unexpected Reactions with Anilines.

Dylan Innes,[A] Michael V. Perkins,[A] Andris J. Liepa,[B] and Craig L. Francis[B,C]

[A]School of Chemical and Physical Sciences, Flinders University, Bedford Park, SA 5042, Australia.

[B]Biomedical Synthetic Chemistry Group, CSIRO, Clayton, VIC 3168, Australia.

[C]Corresponding author. Email: craig.francis@csiro.au

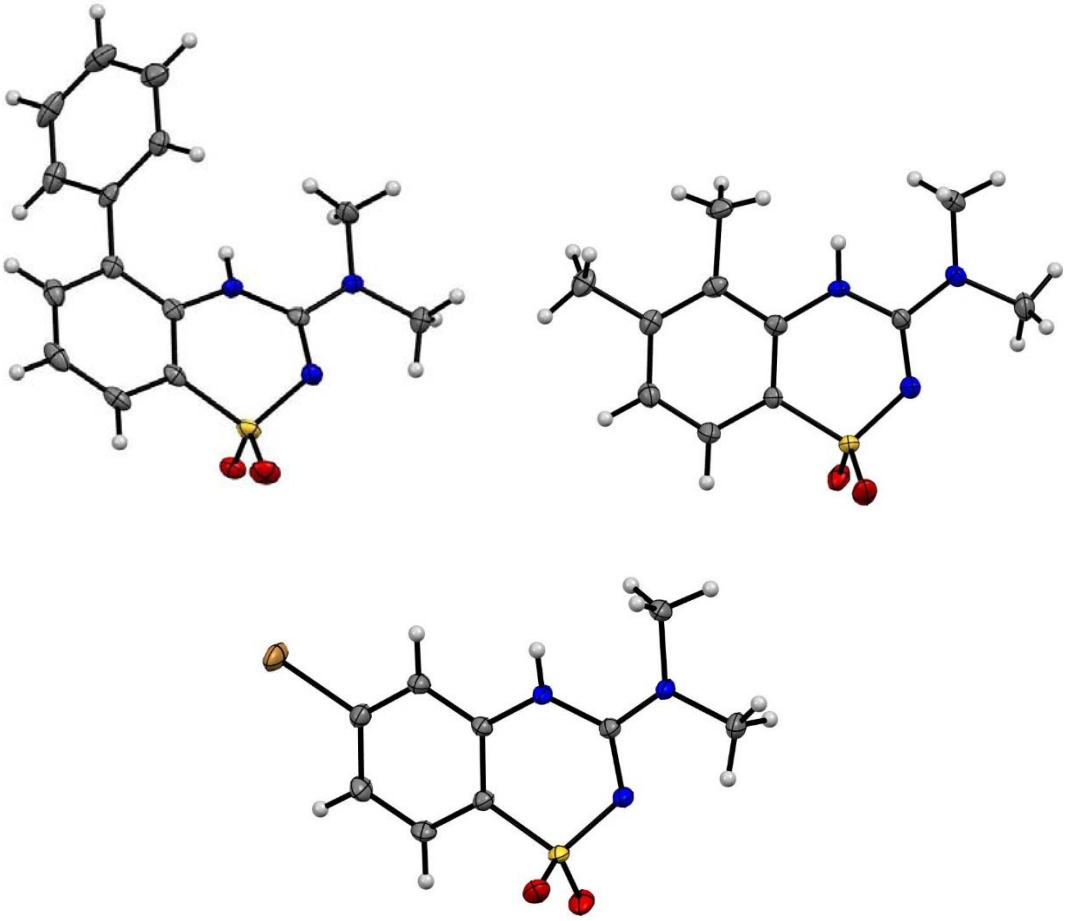

Figure S1. ORTEP diagrams of **8e** (top left), **8g** (top right), and **8k** (bottom).

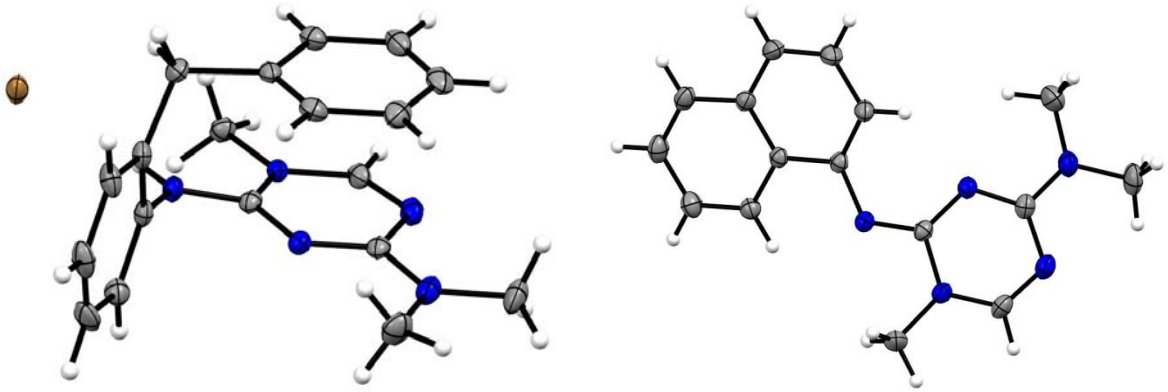

Figure S2. ORTEP diagrams of the triazines **14d**.HBr (left) and **14f** (right).

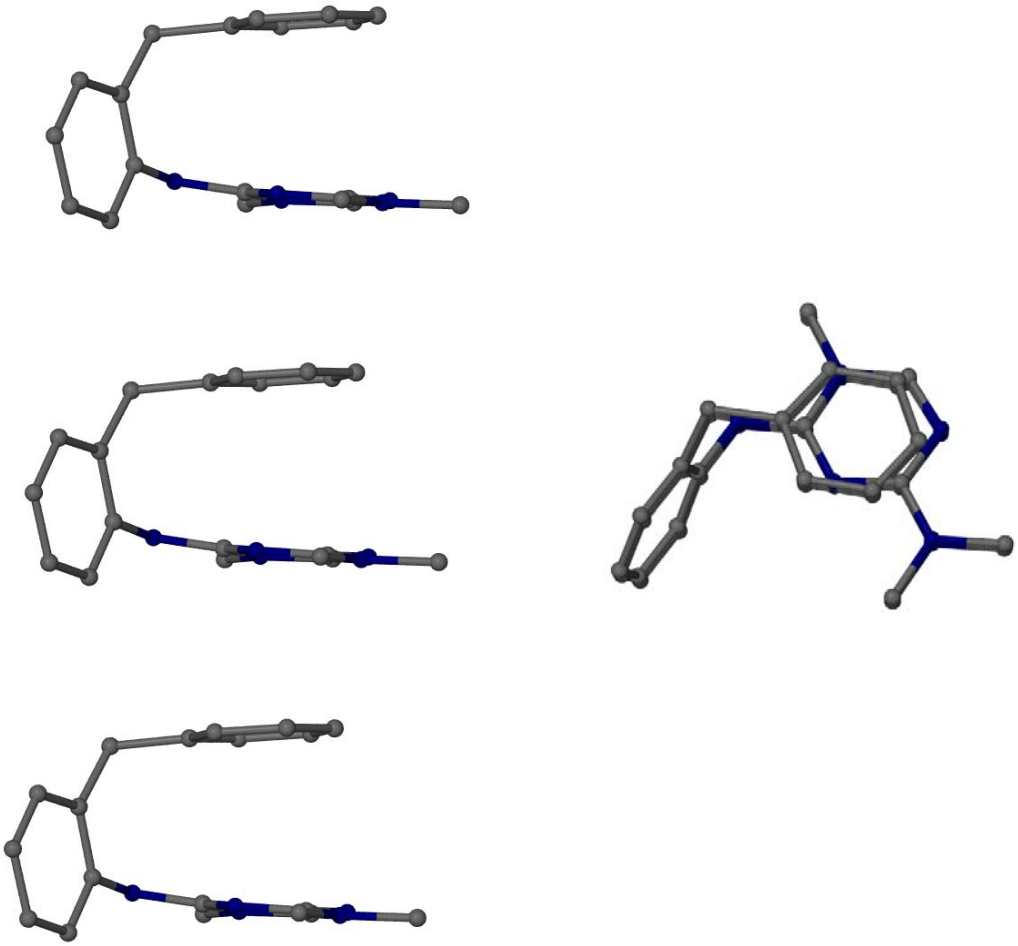

Figure S3. π-stacking or aryl and triazine rings in **14d**: side view (left), top view (right). The phenyl ring and the triazine ring are approximately parallel and partially overlap with the closest intramolecular separation at a distance of 3.191(6) Å and the closest intermolecular separation at a distance of 3.386(6) Å.

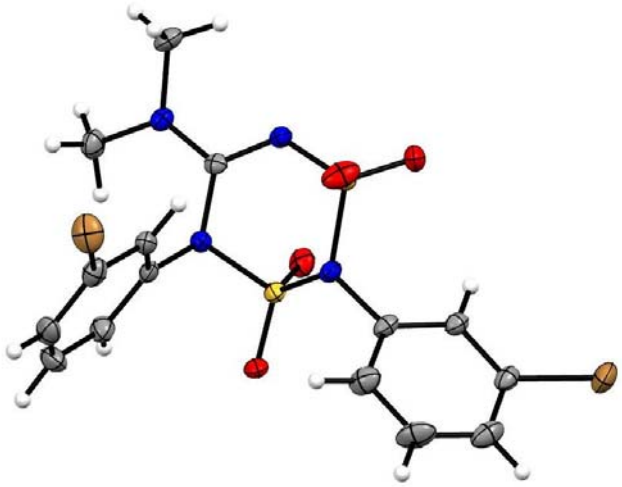

Figure S4. ORTEP diagram of **17k**.

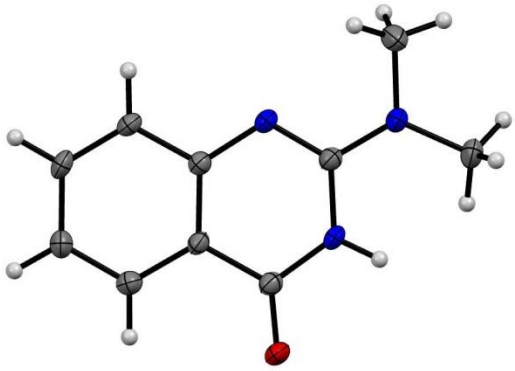

Figure S5. ORTEP diagram of quinazolinone **15**.

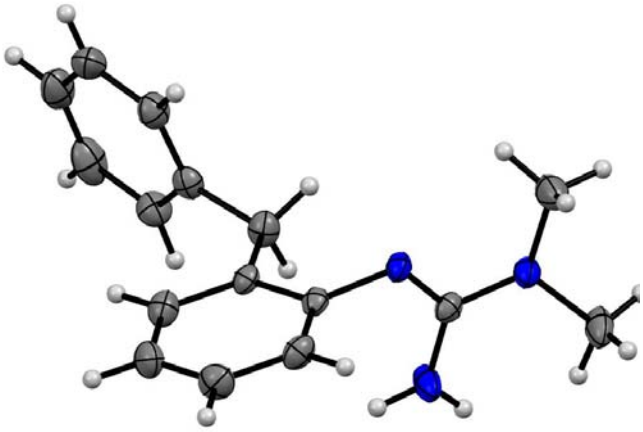

Figure S6. ORTEP diagram of the guanidine **19**. A chemically equivalent molecule has been omitted for clarity.

^{1}H NMR data for **8b** (400 MHz; DMSO-d_6)

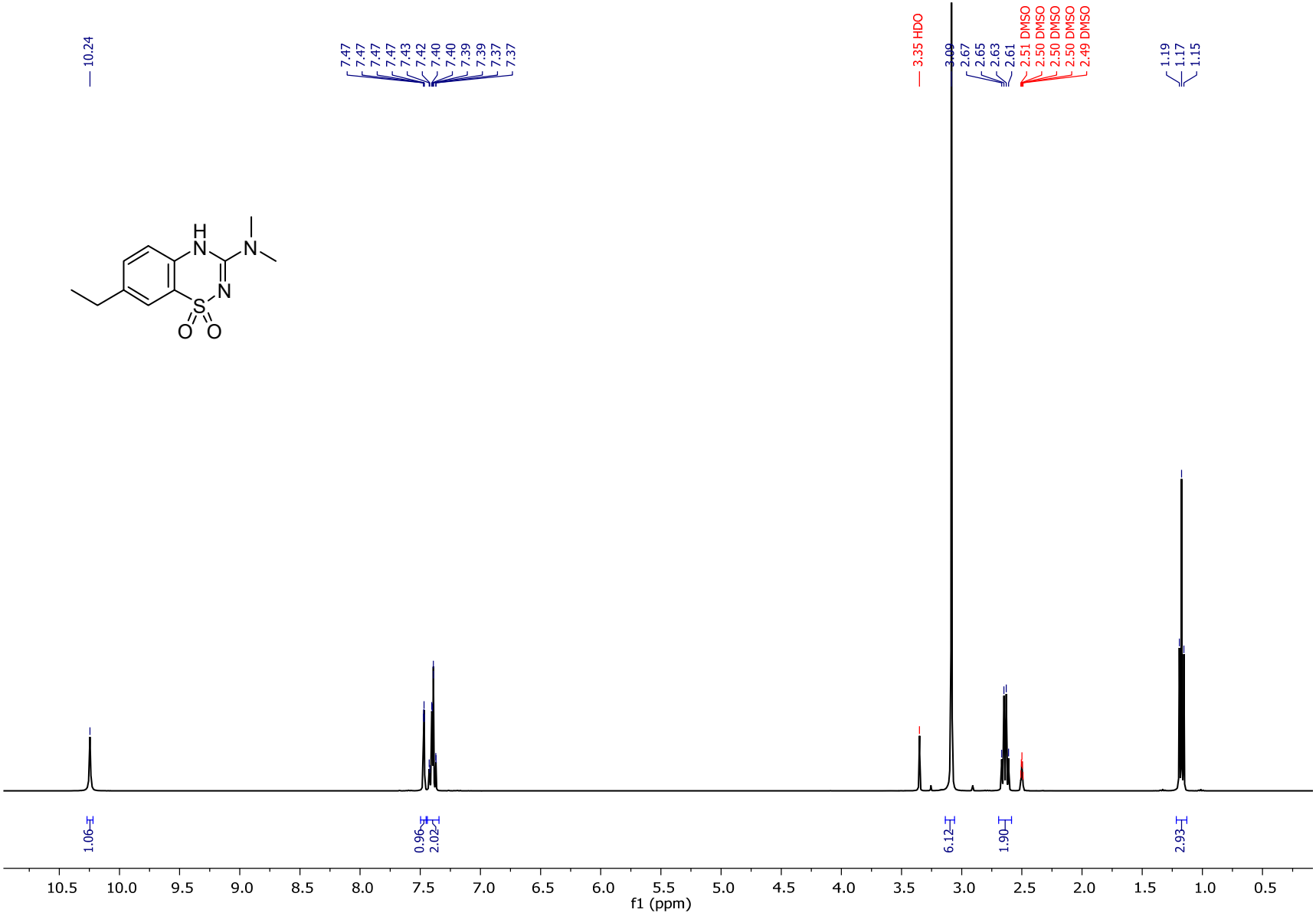

^{13}C NMR data for **8b** (100 MHz; DMSO-*d*$_6$)

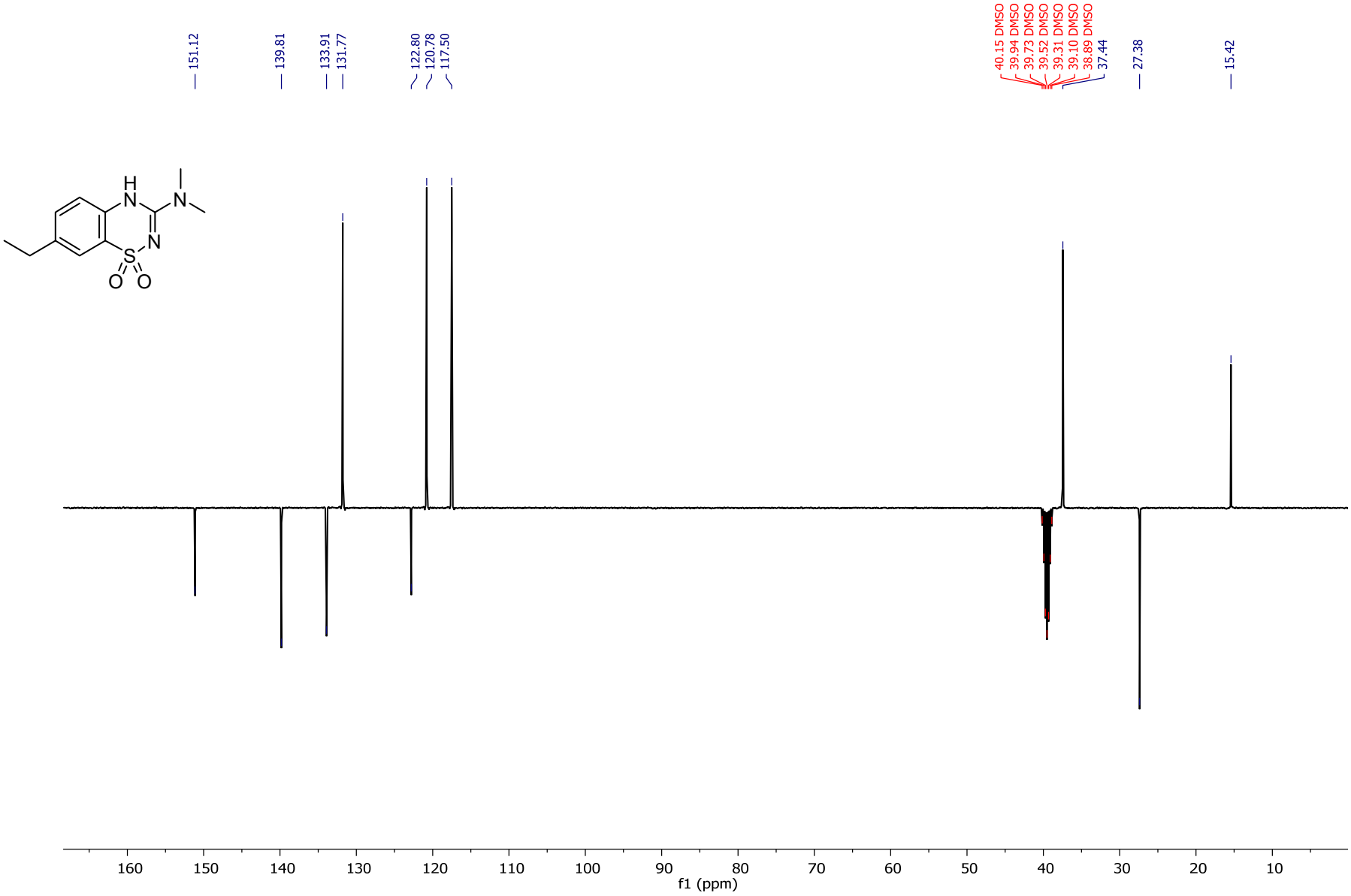

^{1}H NMR data for **9b** (400 MHz; DMSO-d_6)

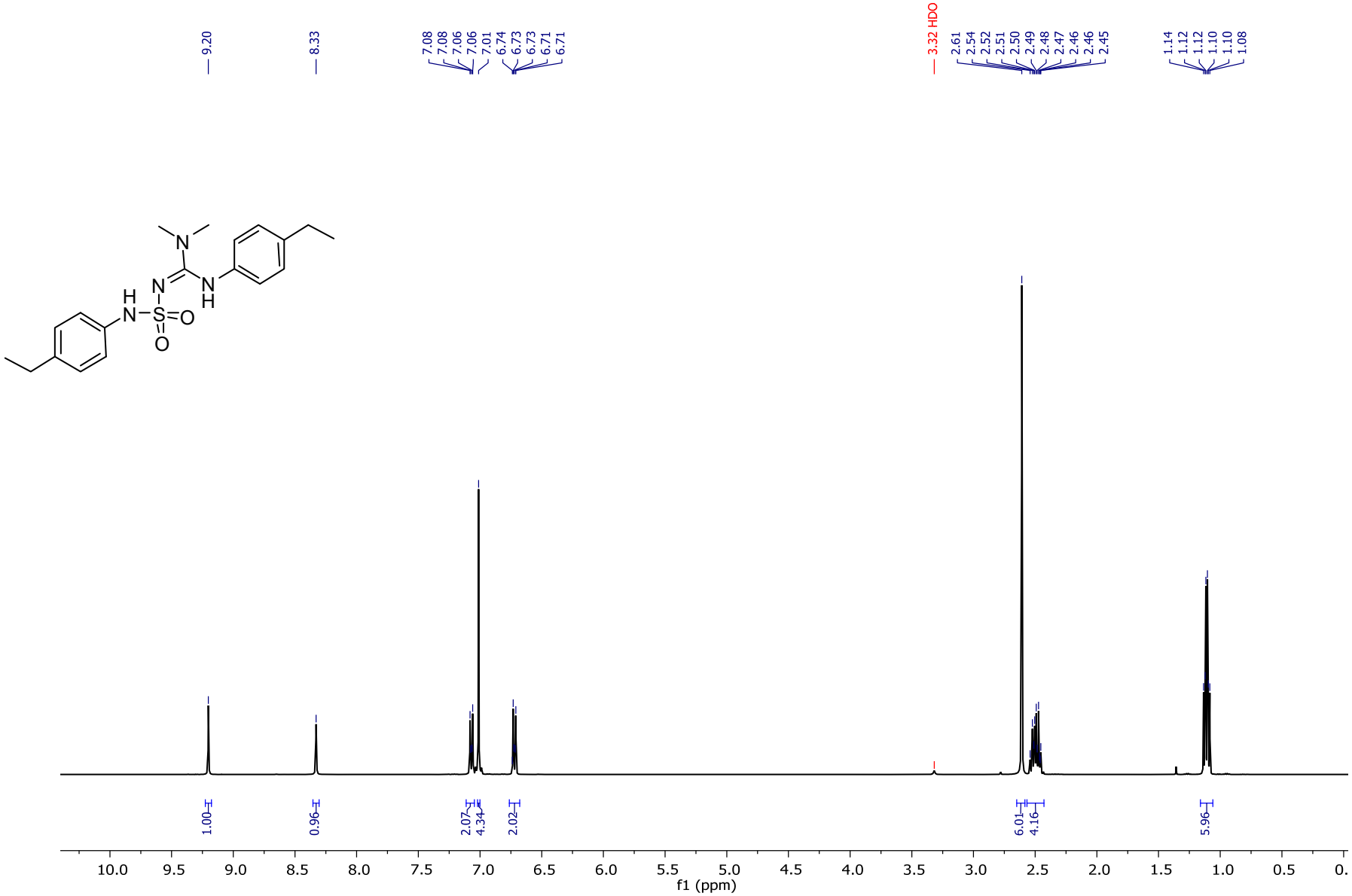

^{13}C NMR data for **9b** (100 MHz; DMSO-*d*$_6$)

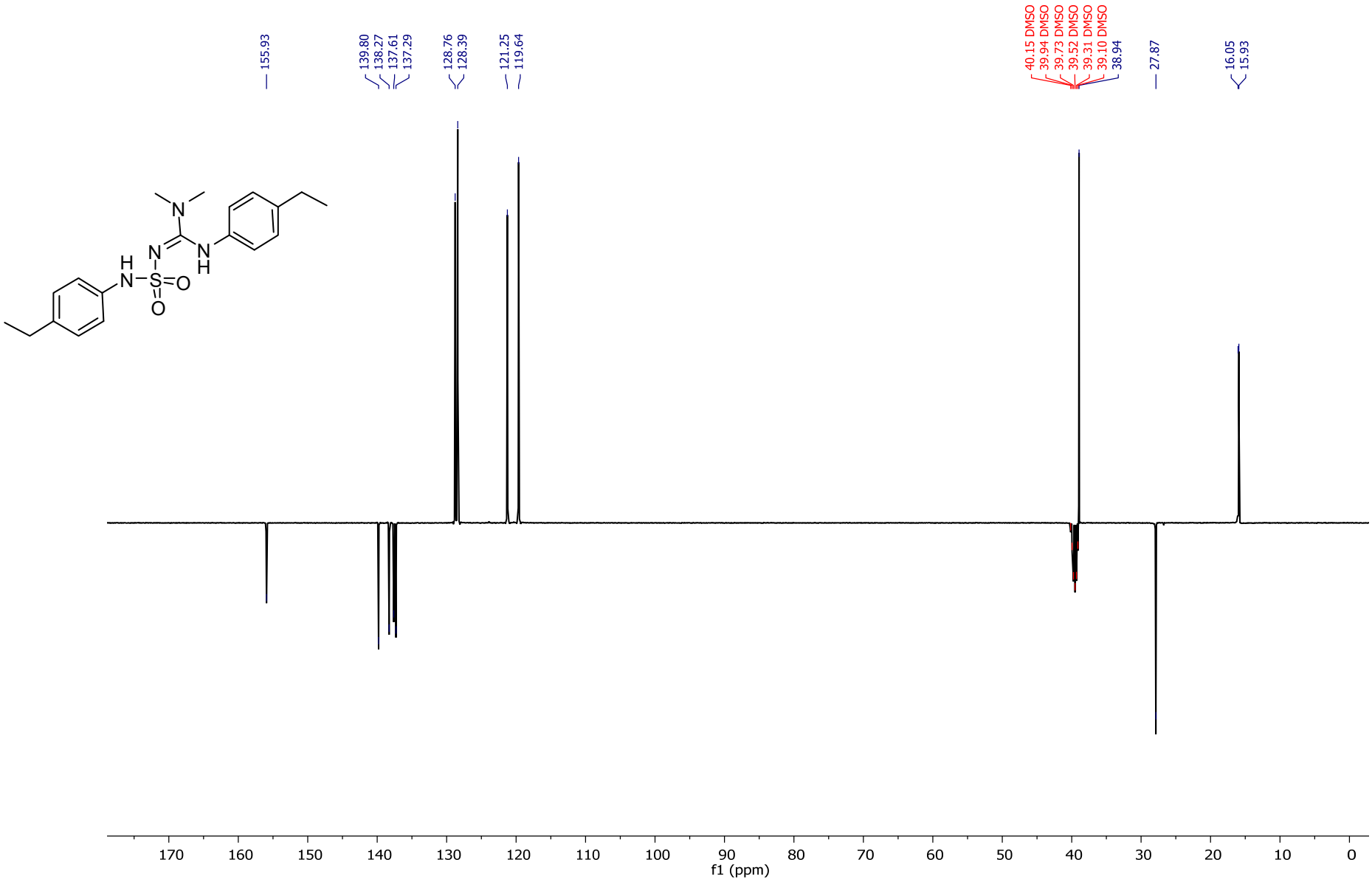

^{1}H NMR data for **11** (600 MHz; DMSO-d_6)

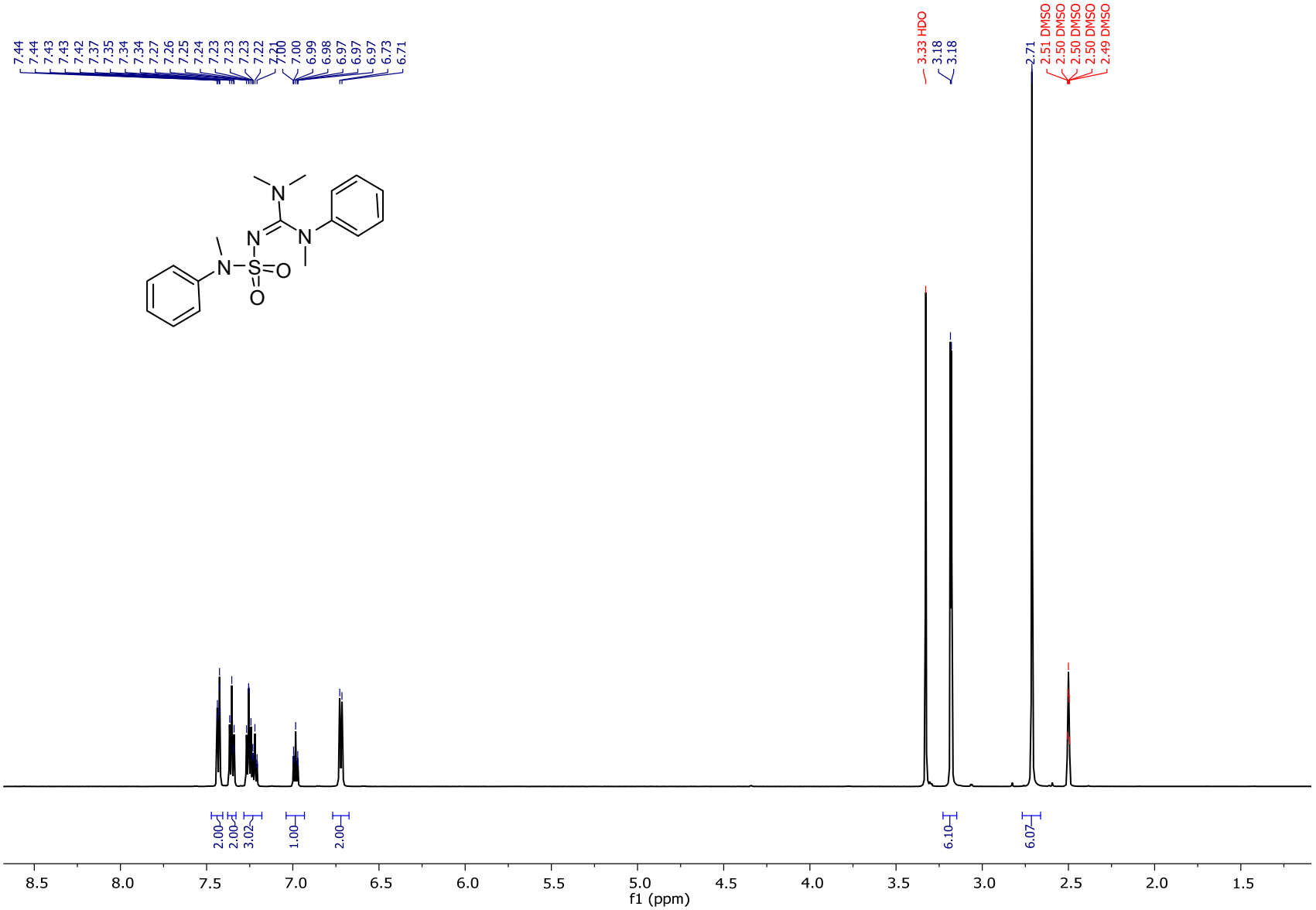

^{13}C NMR data for **11** (150 MHz; DMSO-*d*$_6$)

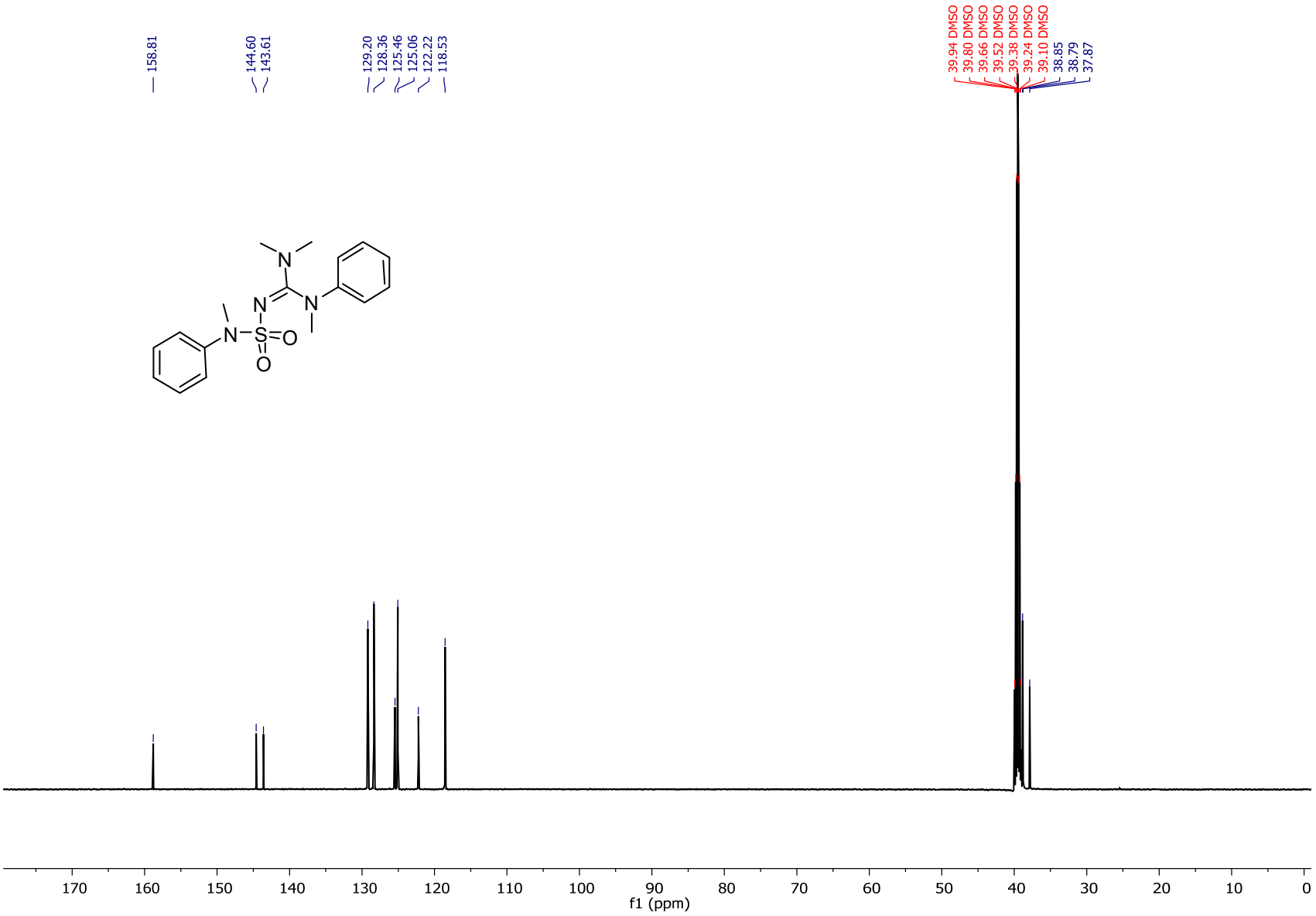

^{1}H NMR data for **14c** (600 MHz; DMSO-d_6)

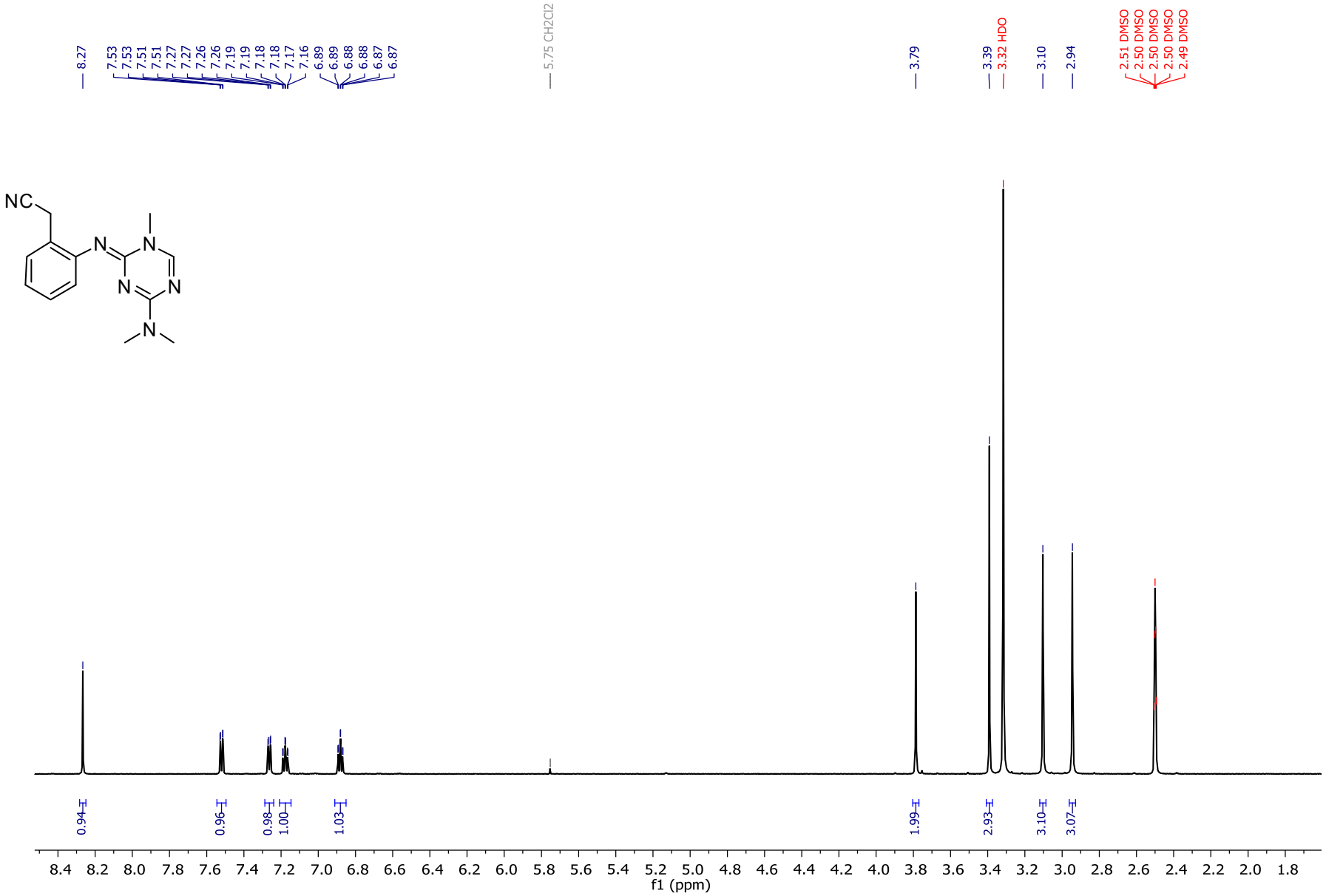

^{13}C NMR data for **14c** (150 MHz; DMSO-*d*$_6$)

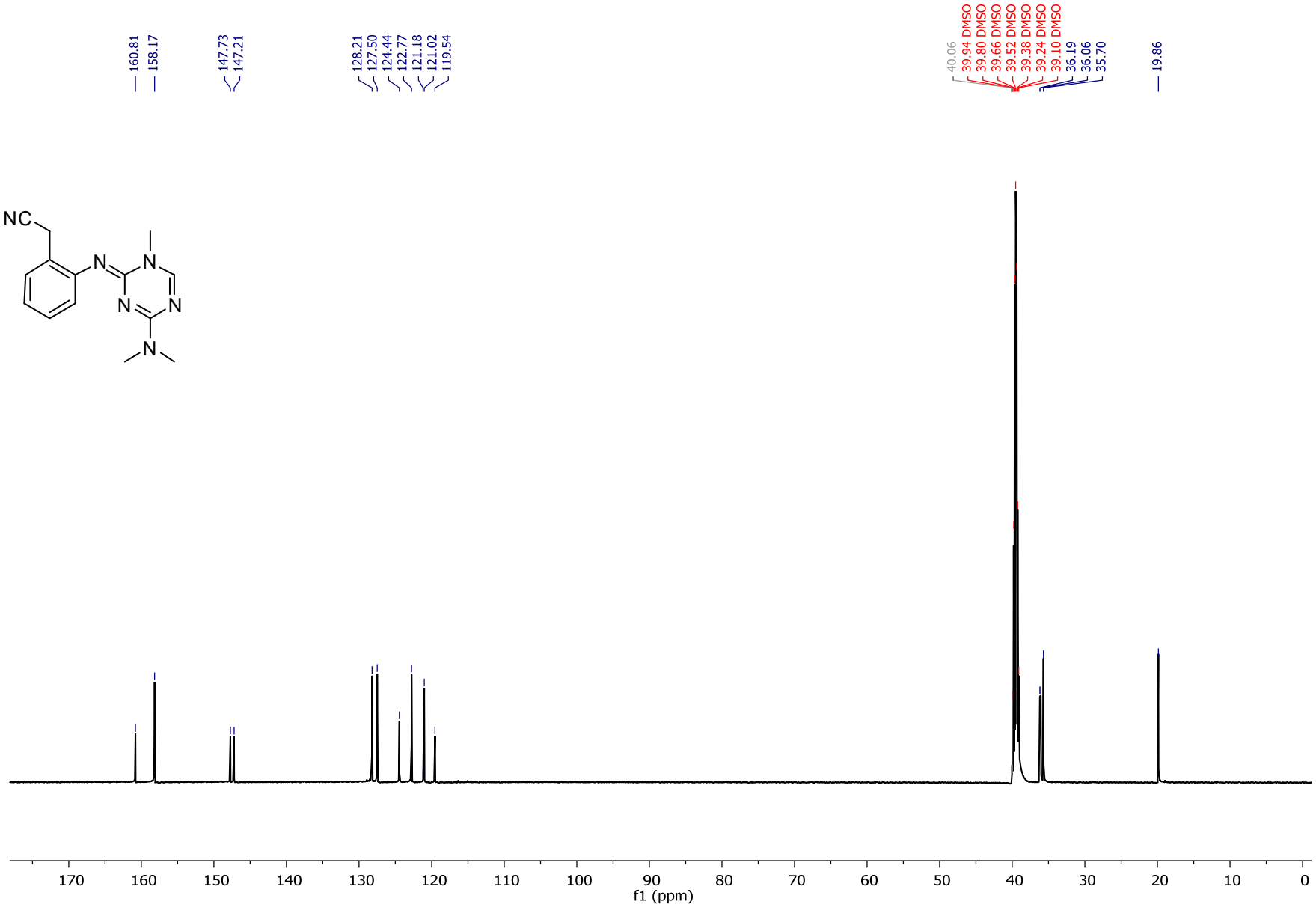

^{1}H NMR data for **15** (600 MHz; DMSO-d_6)

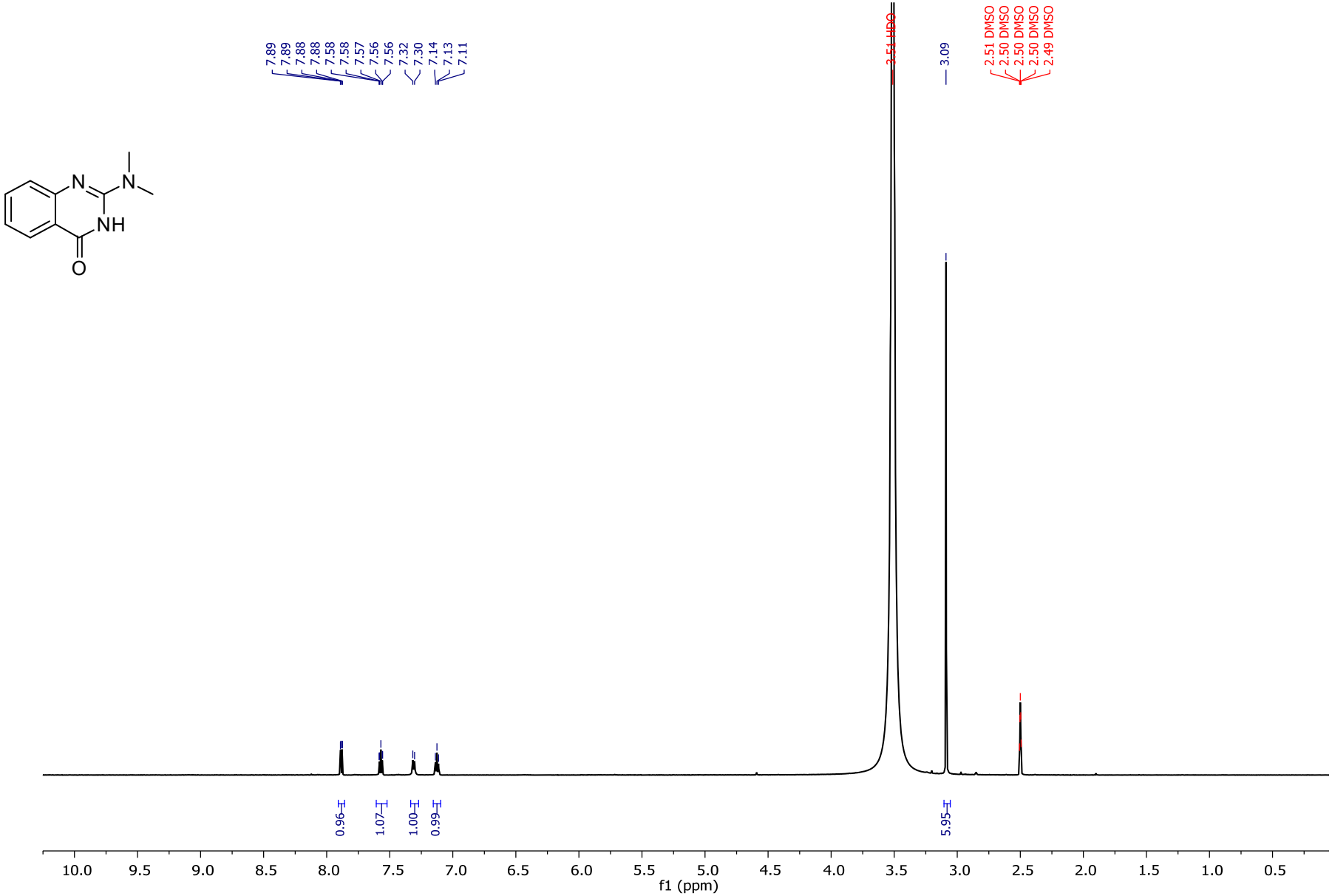

^{13}C NMR data for **15** (150 MHz; DMSO-*d*$_6$)

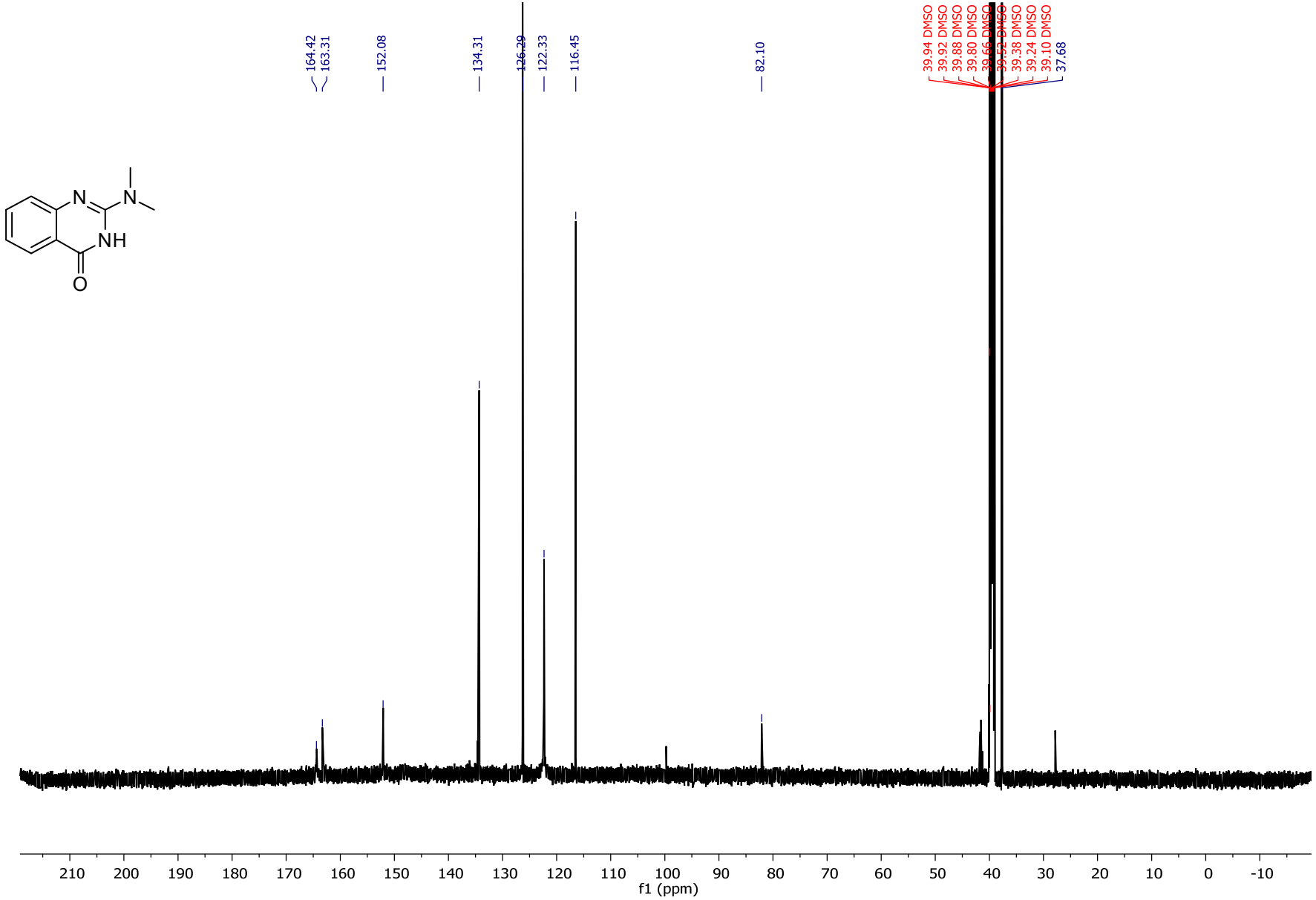

^{1}H NMR data for **14d** (600 MHz; DMSO-d_6)

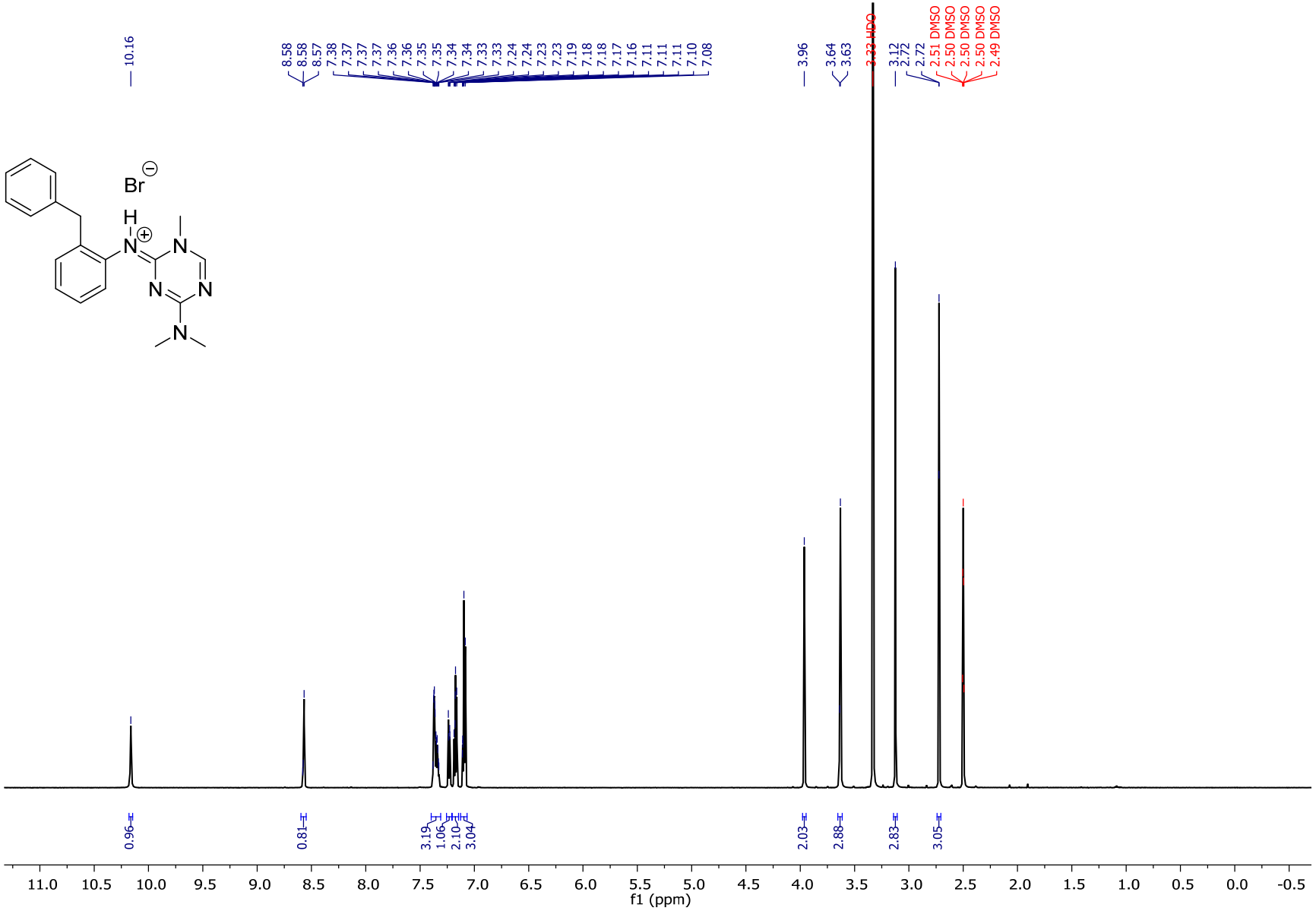

^{13}C NMR data for **14d** (150 MHz; DMSO-d_6)

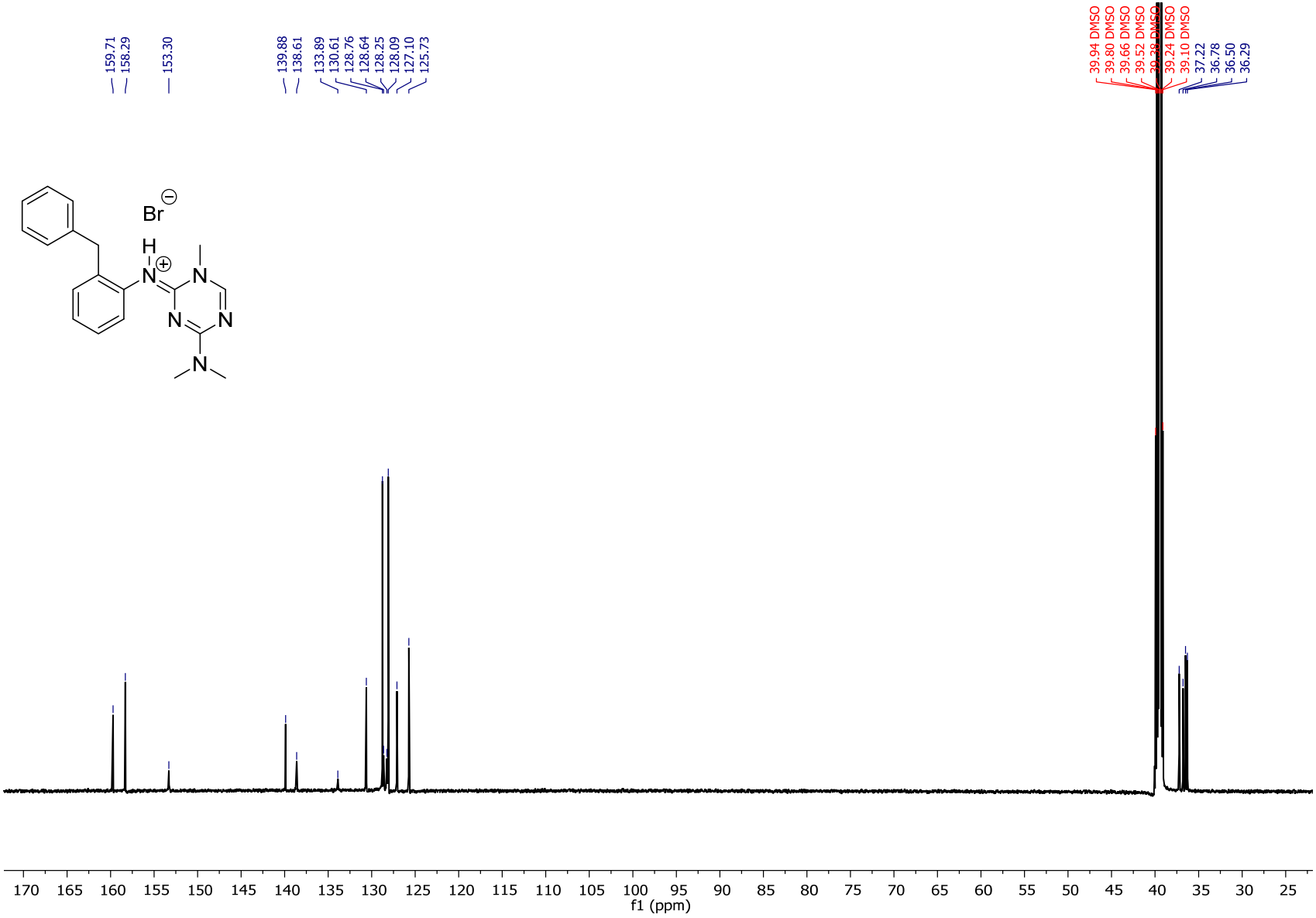

^{1}H NMR data for **8d** (600 MHz; DMSO-d_6)

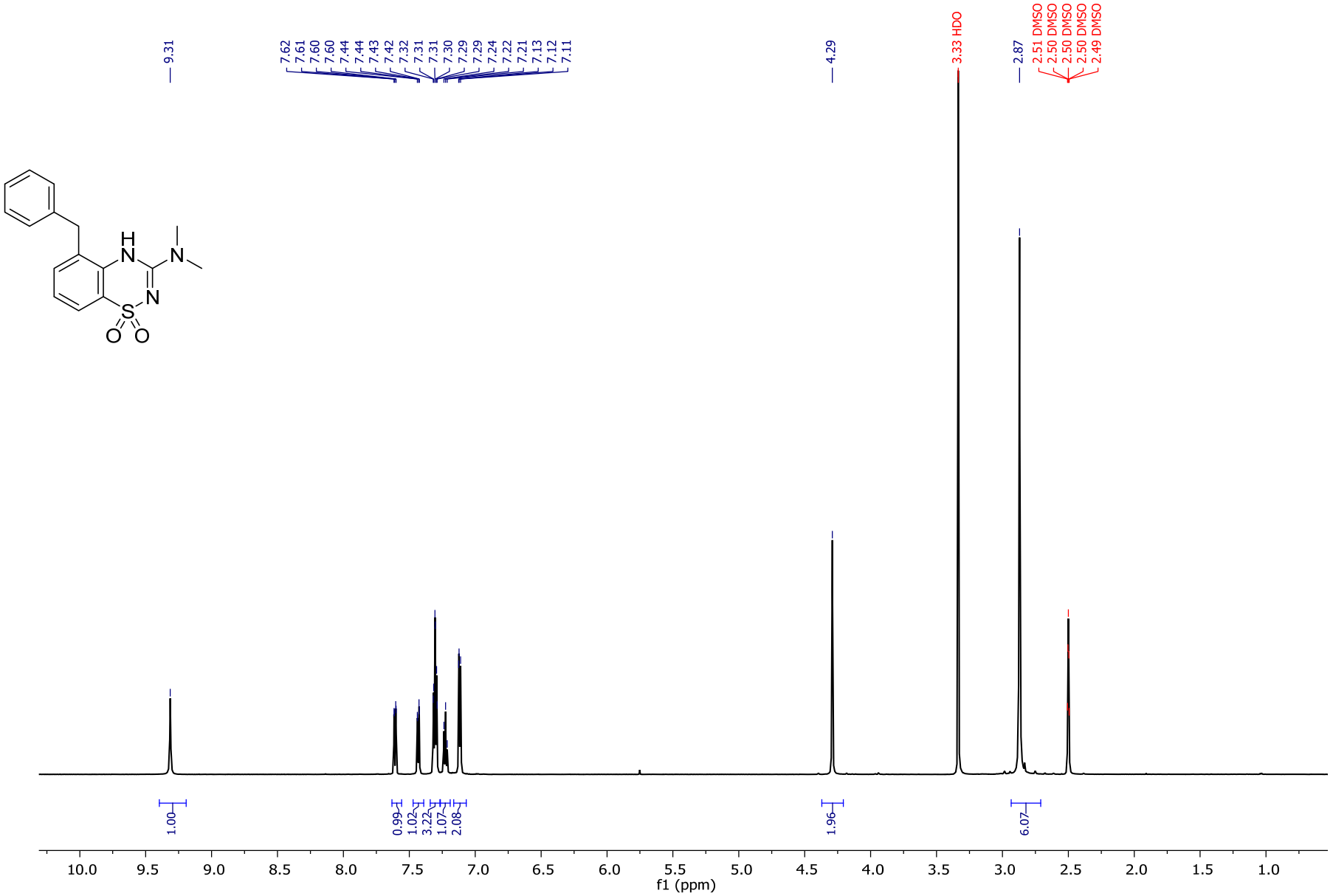

^{13}C NMR data for **8d** (150 MHz; DMSO-*d*$_6$)

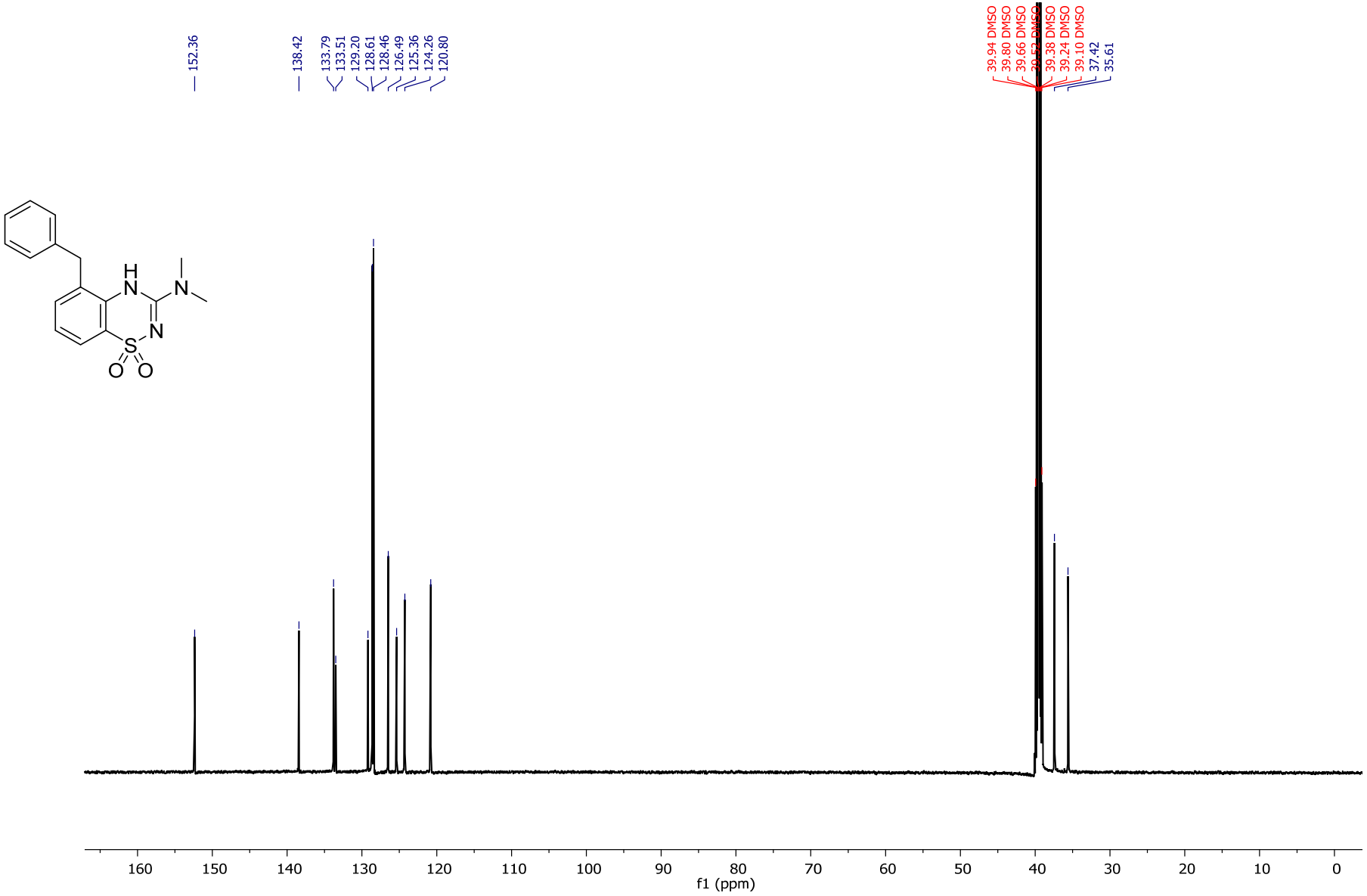

^{1}H NMR data for **17d** (600 MHz; DMSO-d$_6$)

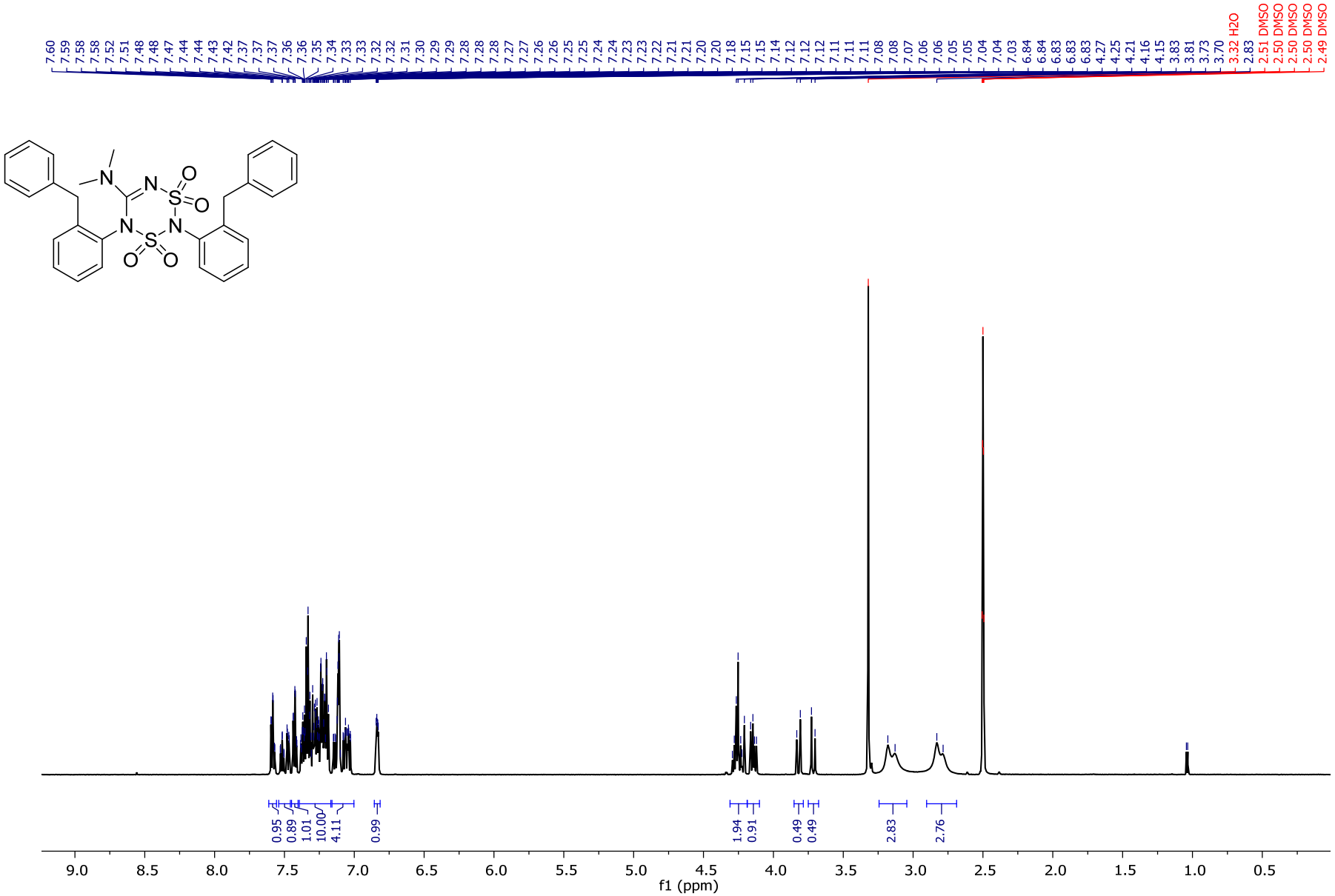

^{13}C NMR data for **17d** (150 MHz; DMSO-d_6)

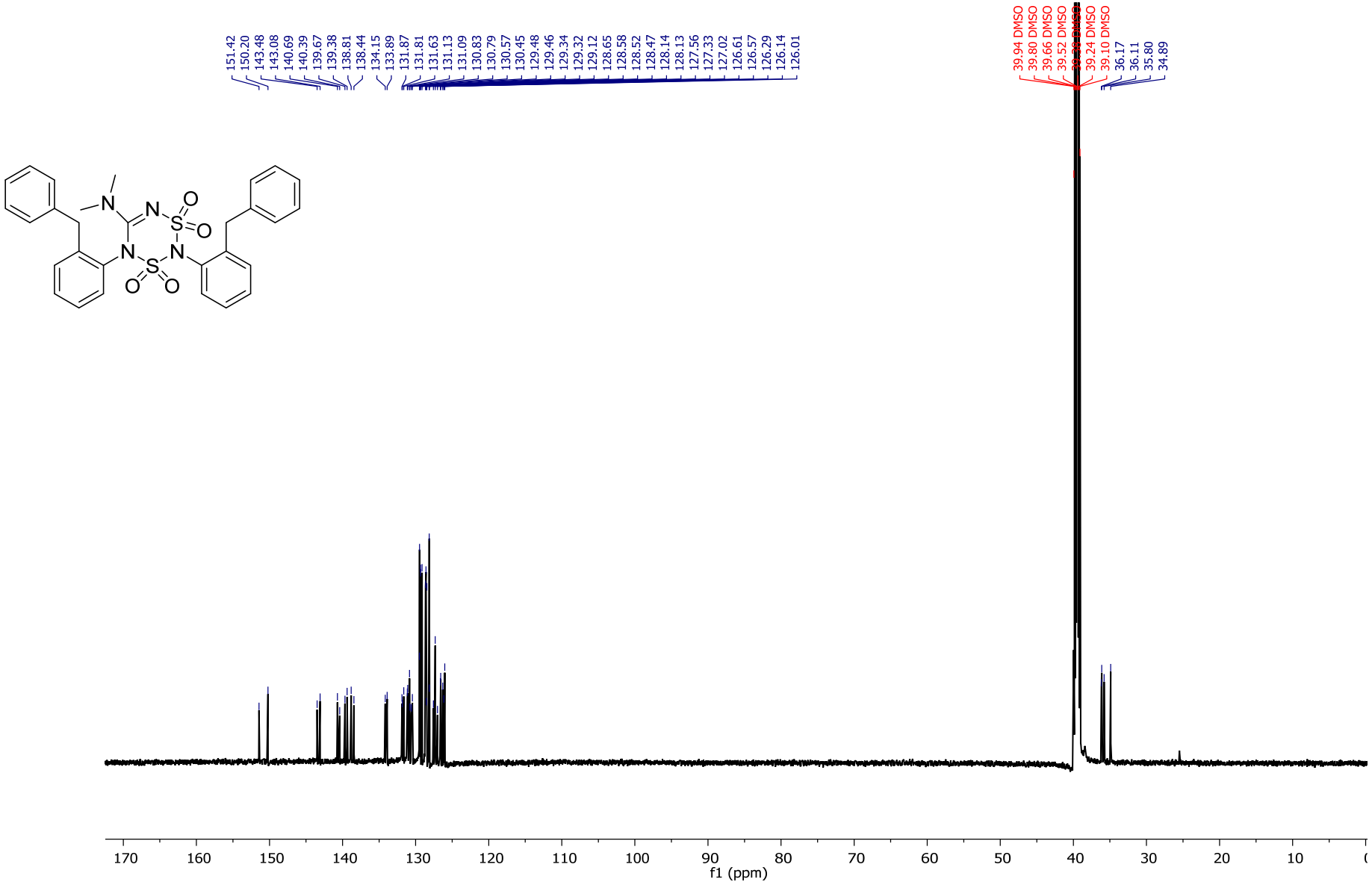

^{1}H NMR data for **16** (600 MHz; DMSO-d_6)

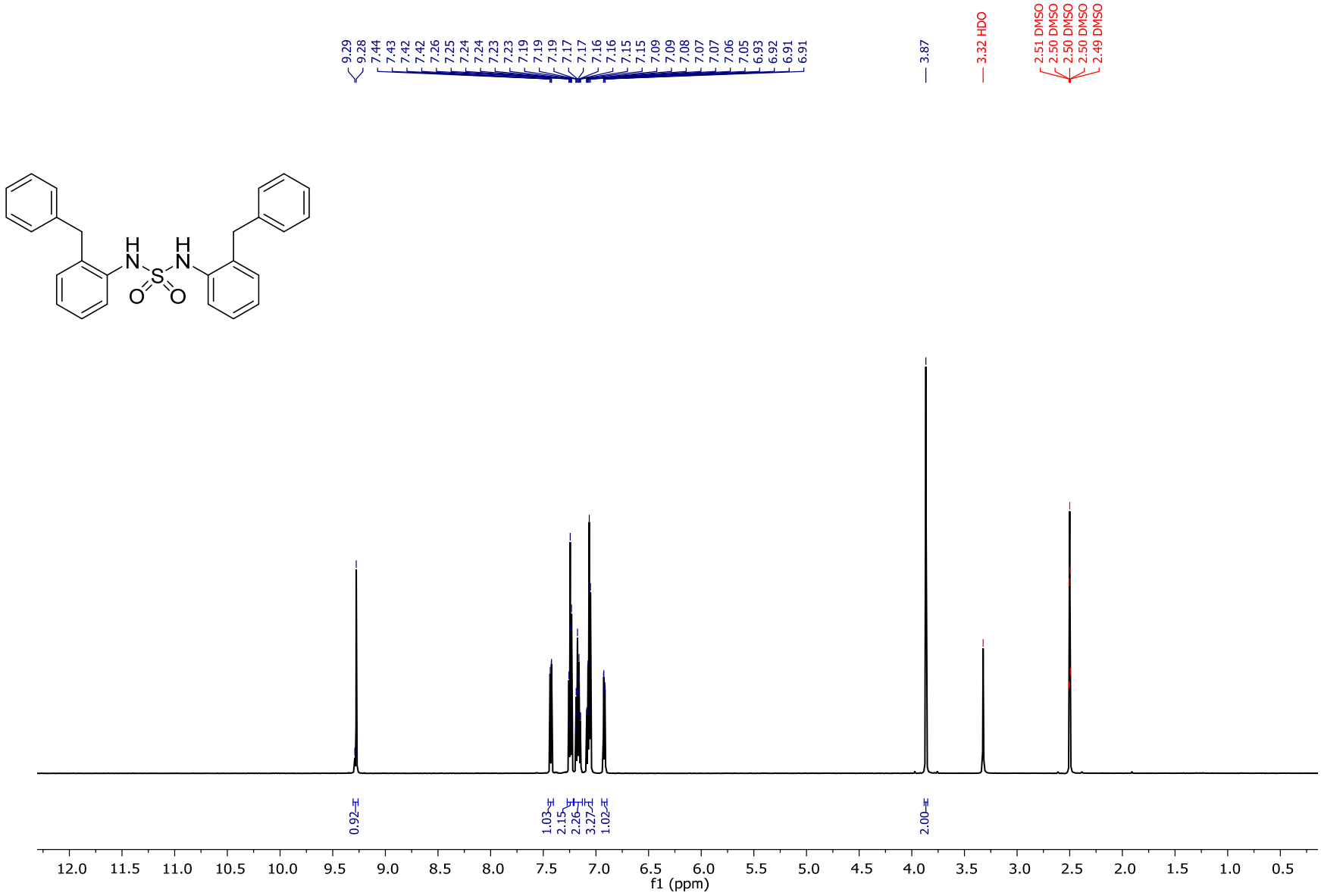

^{13}C NMR data for **16** (150 MHz; DMSO-d_6)

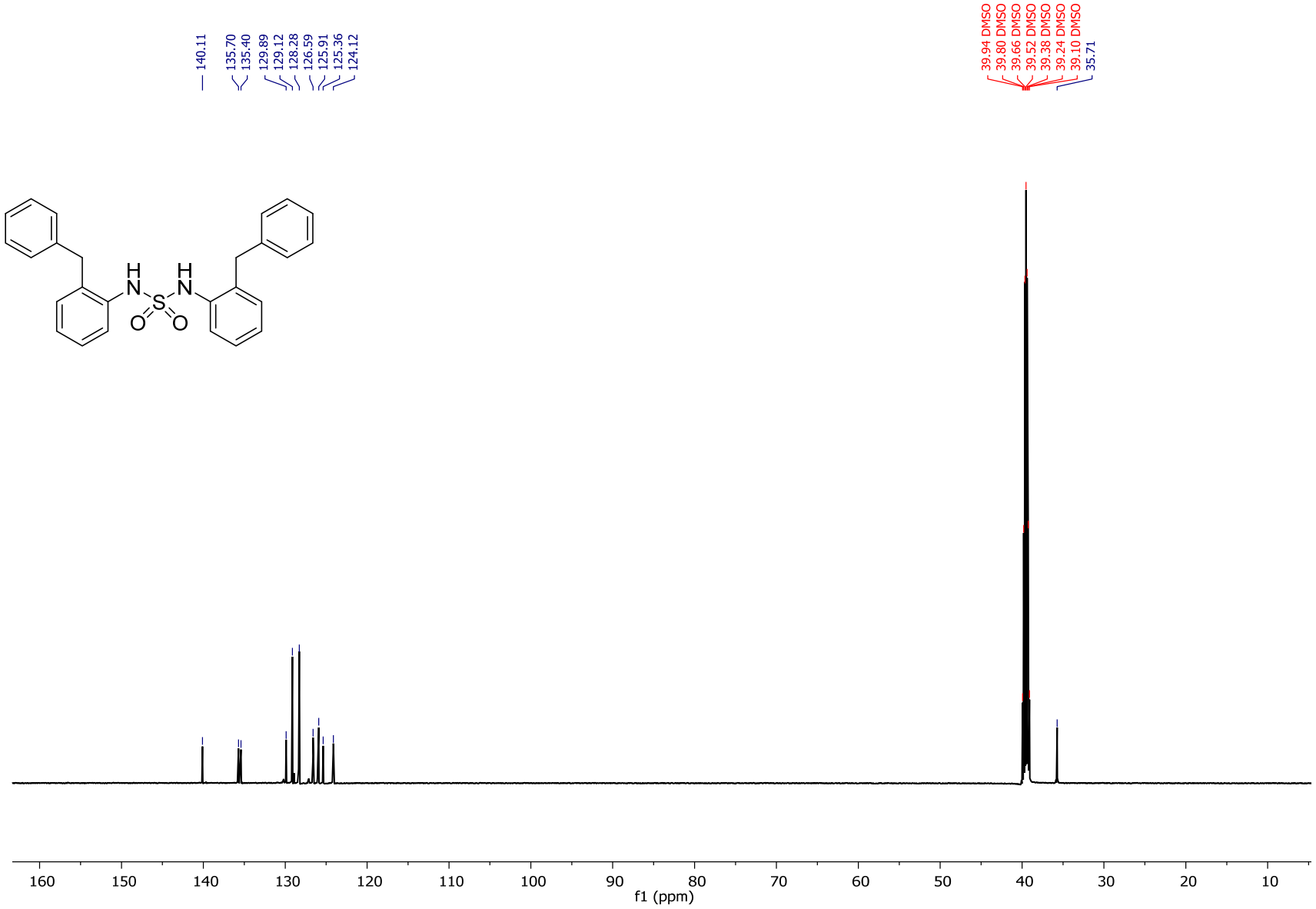

^{1}H NMR data for **18** (600 MHz; DMSO-d$_6$)

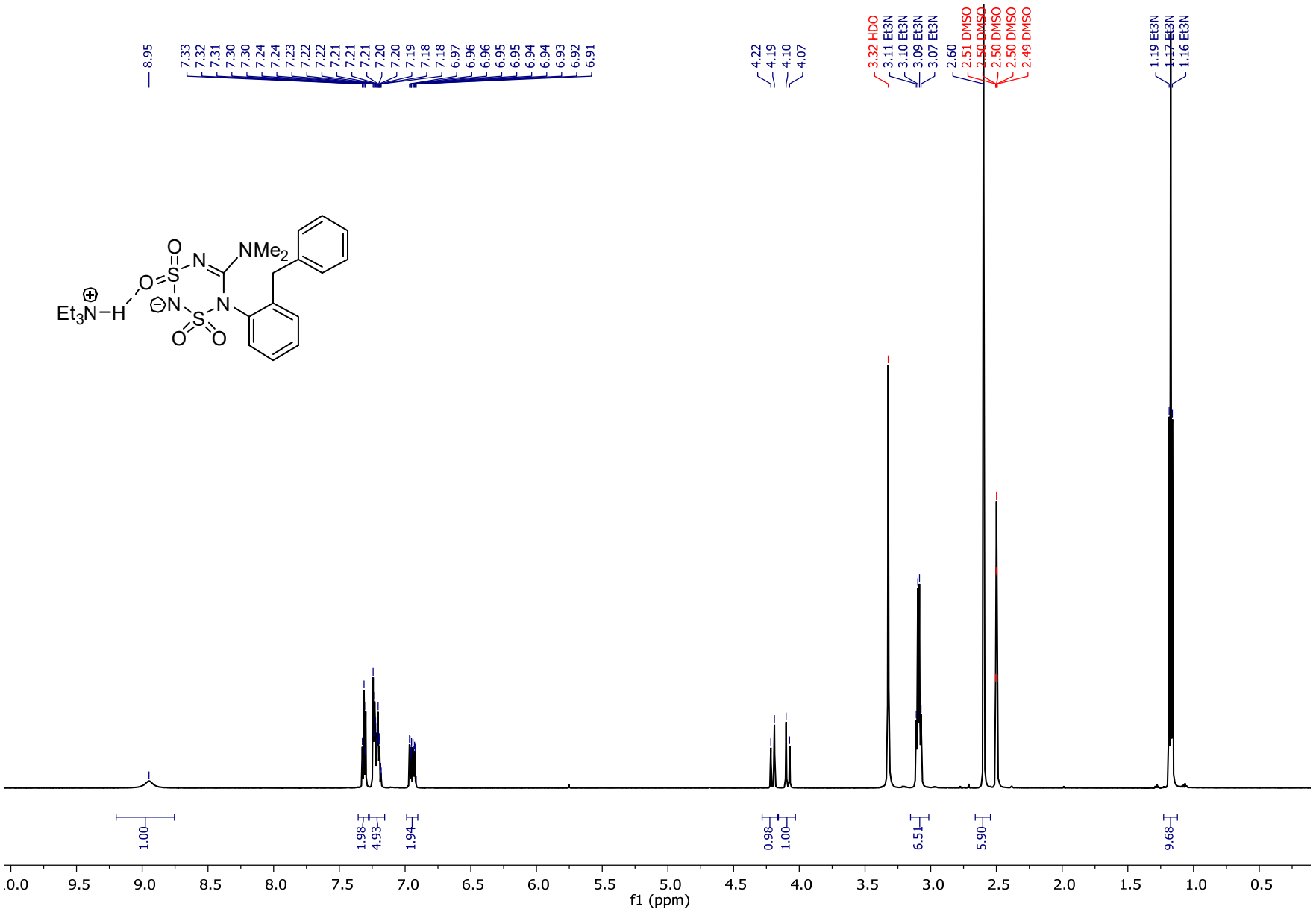

^{13}C NMR data for **18** (150 MHz; DMSO-d_6)

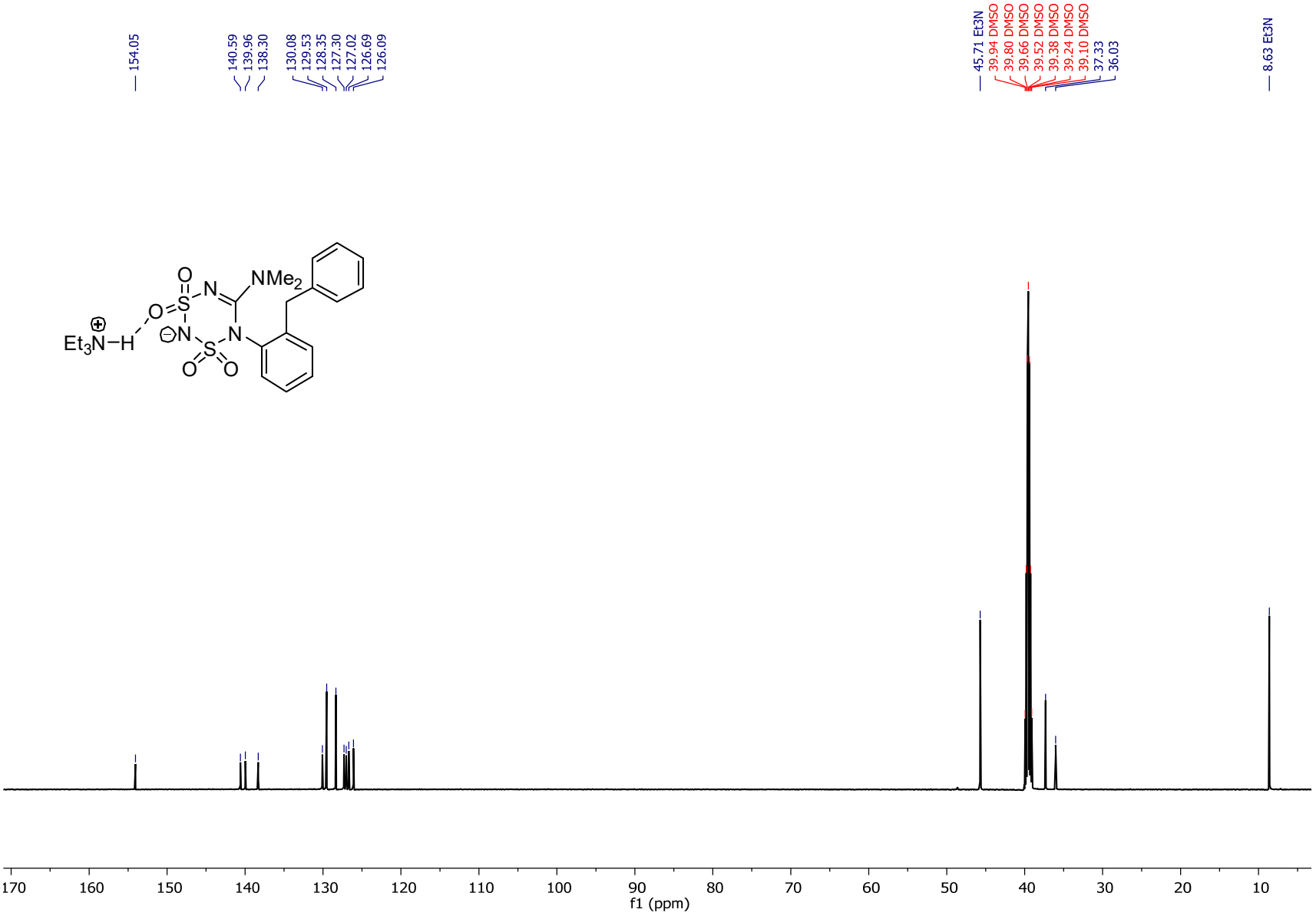

^{1}H NMR data for **19** (600 MHz; DMSO-d$_6$)

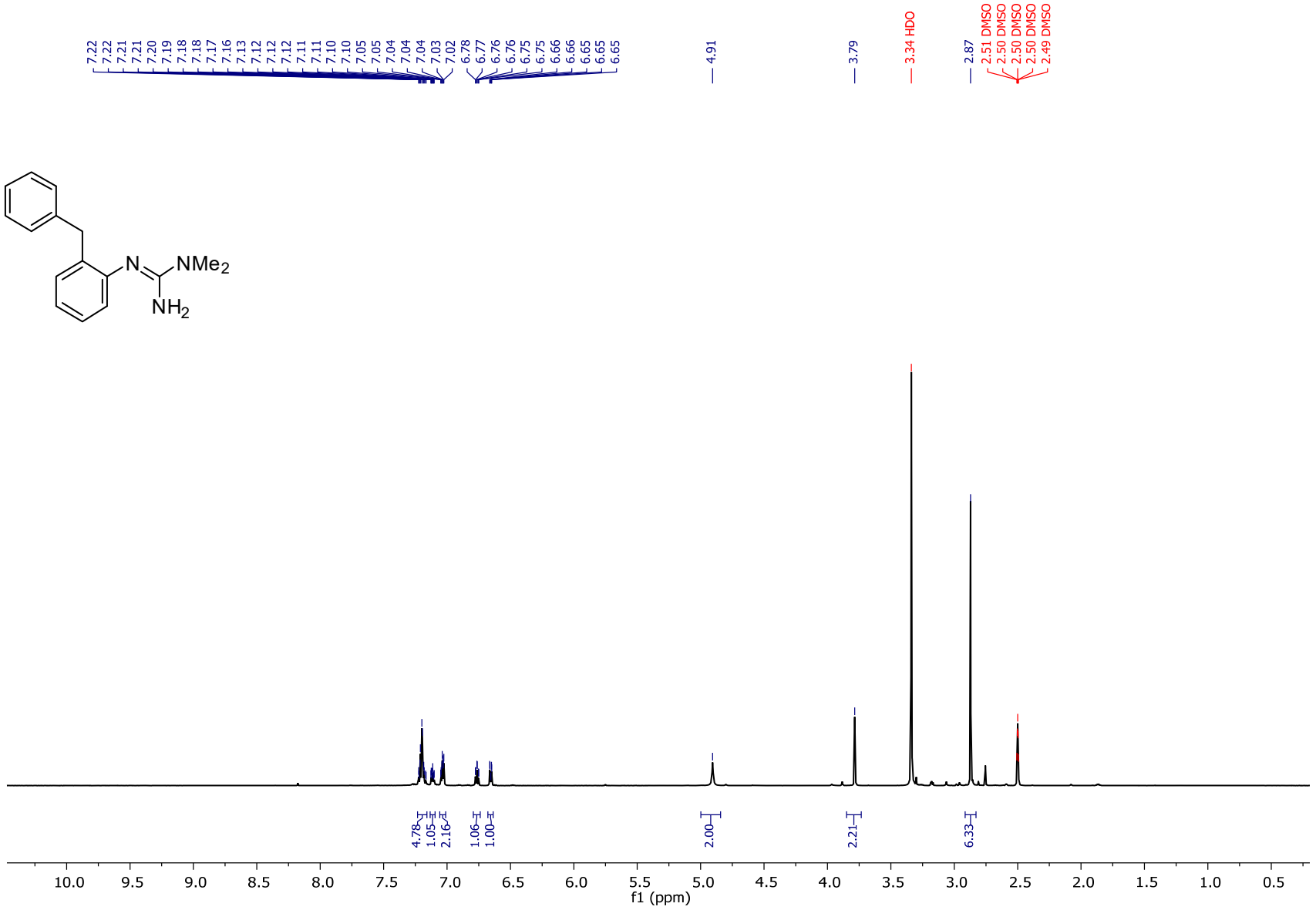

^{13}C NMR data for **19** (150 MHz; DMSO-d_6)

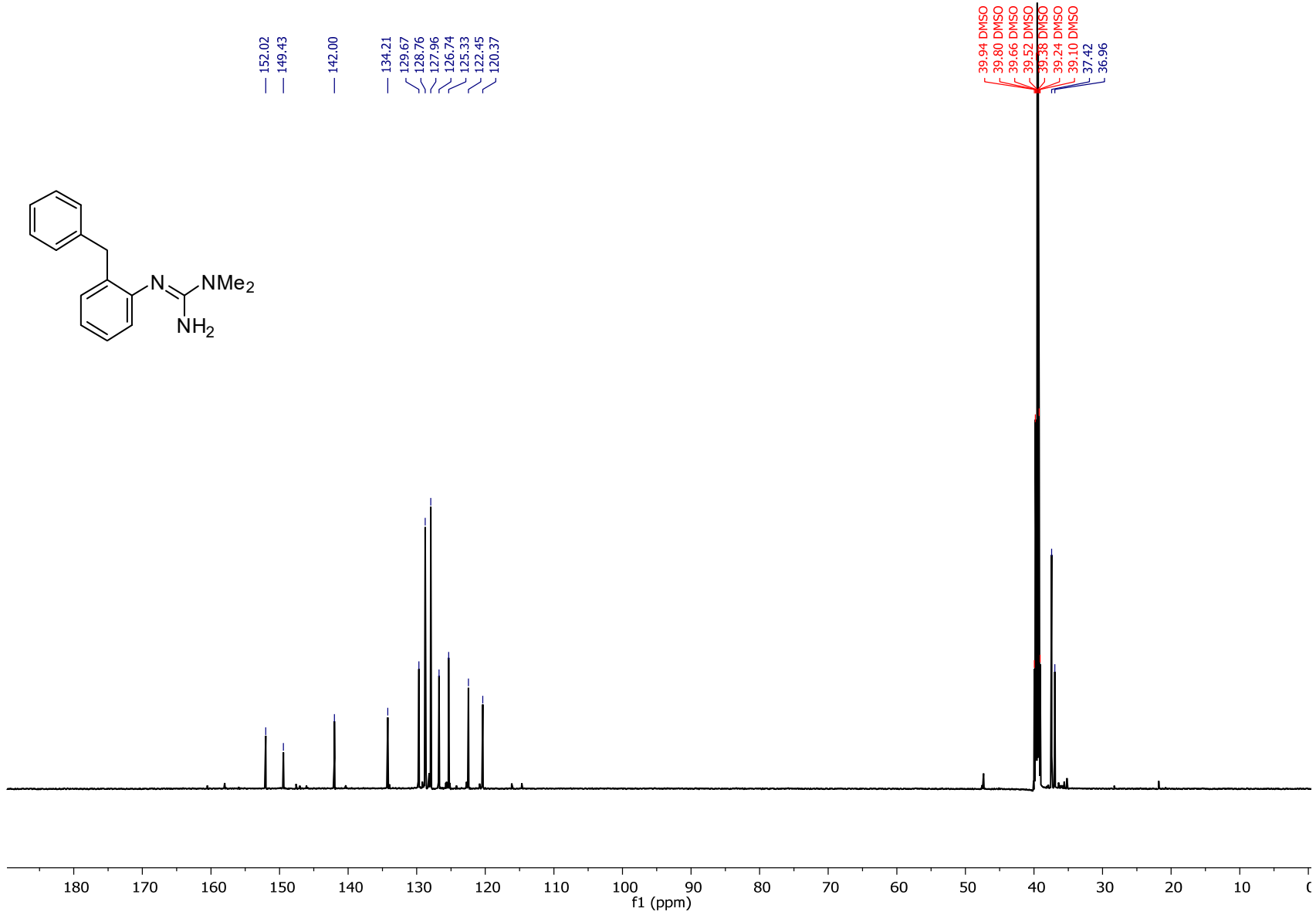

^{1}H NMR data for **8e** (600 MHz; DMSO-d_6)

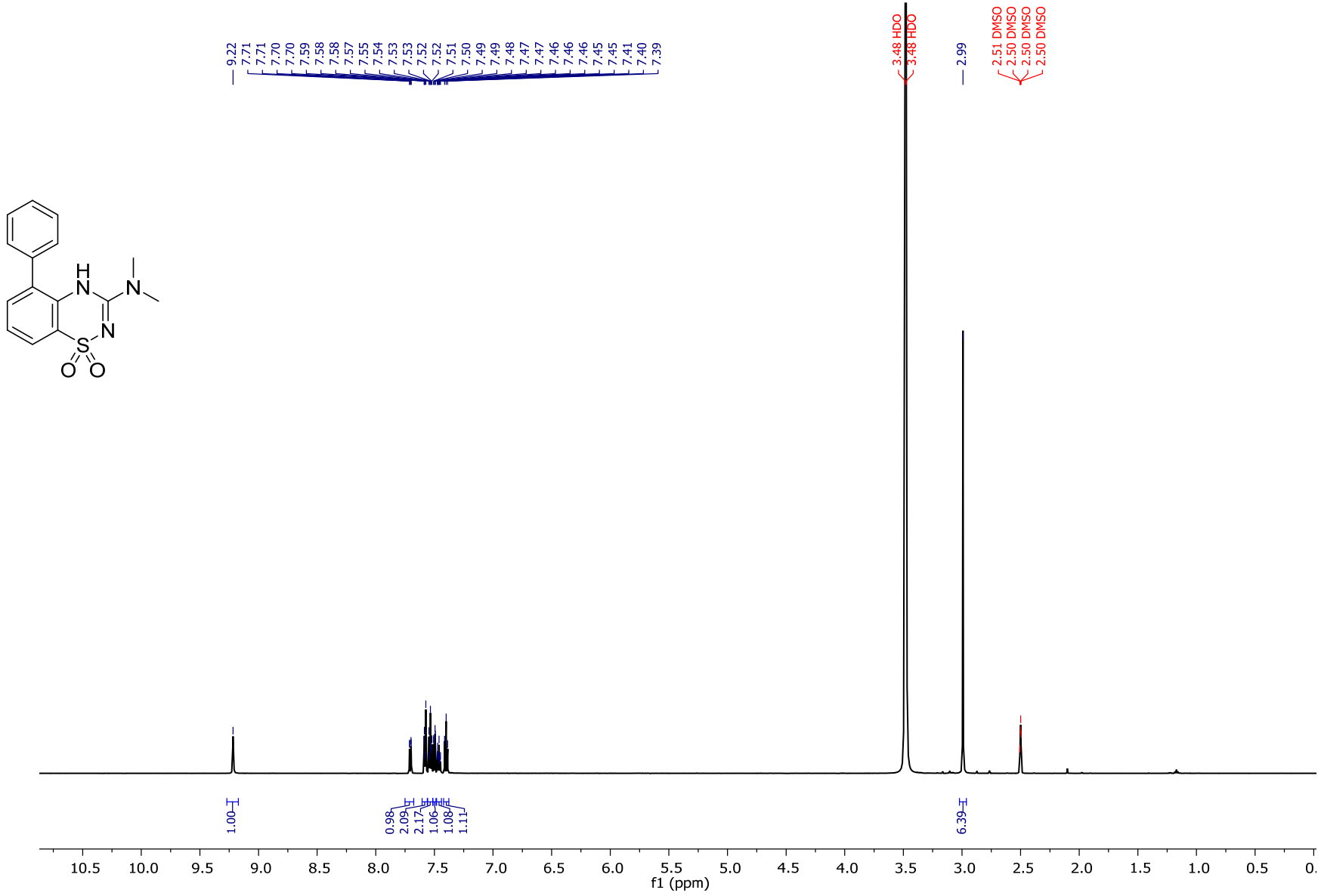

^{13}C NMR data for **8e** (150 MHz; DMSO-d_6)

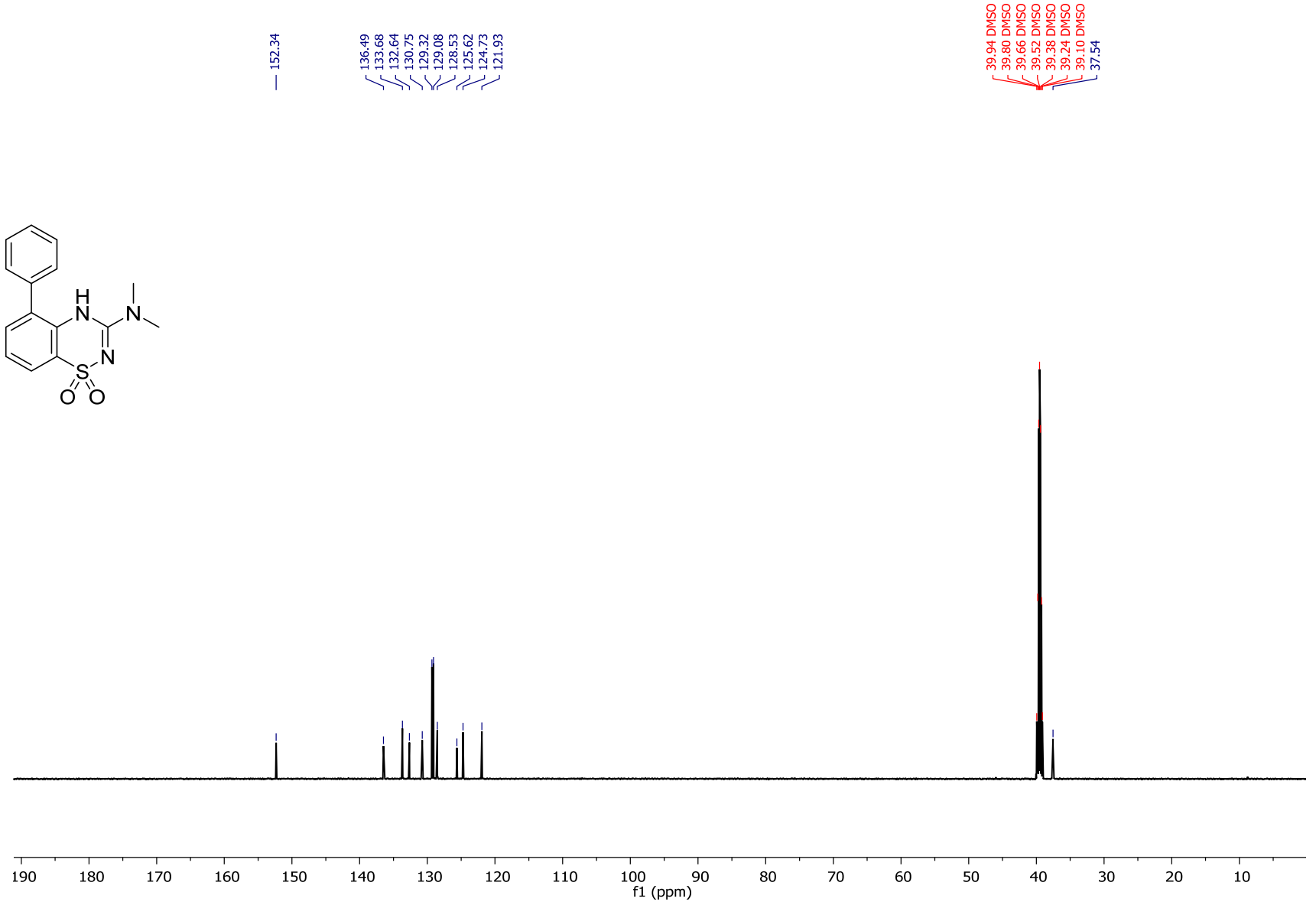

^{1}H NMR data for **17e** (400 MHz; DMSO-d_6, **120°C** (393.15 K))

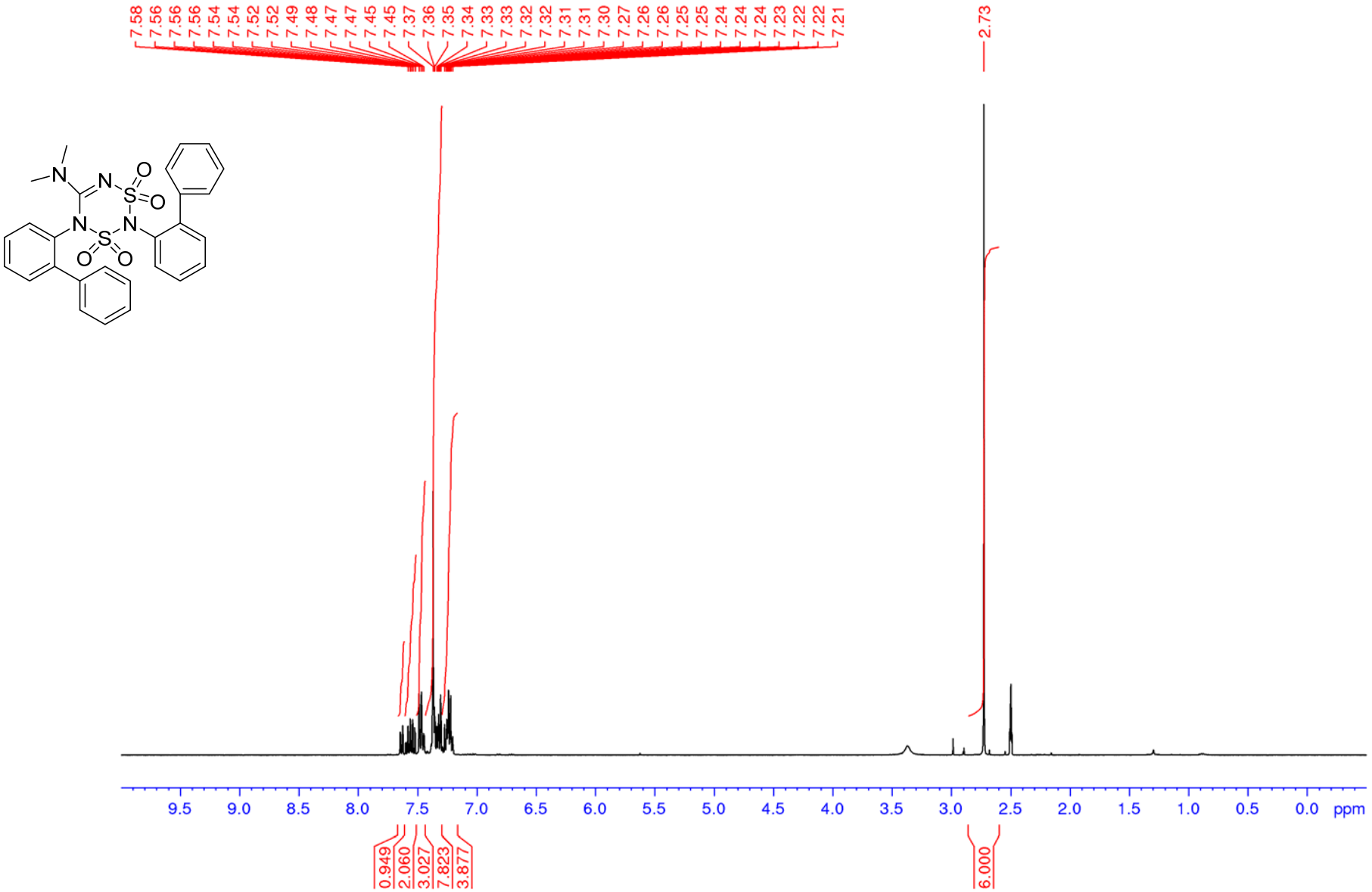

^{13}C NMR data for **17e** (100 MHz; DMSO-d_6, **120°C** (393.15 K))

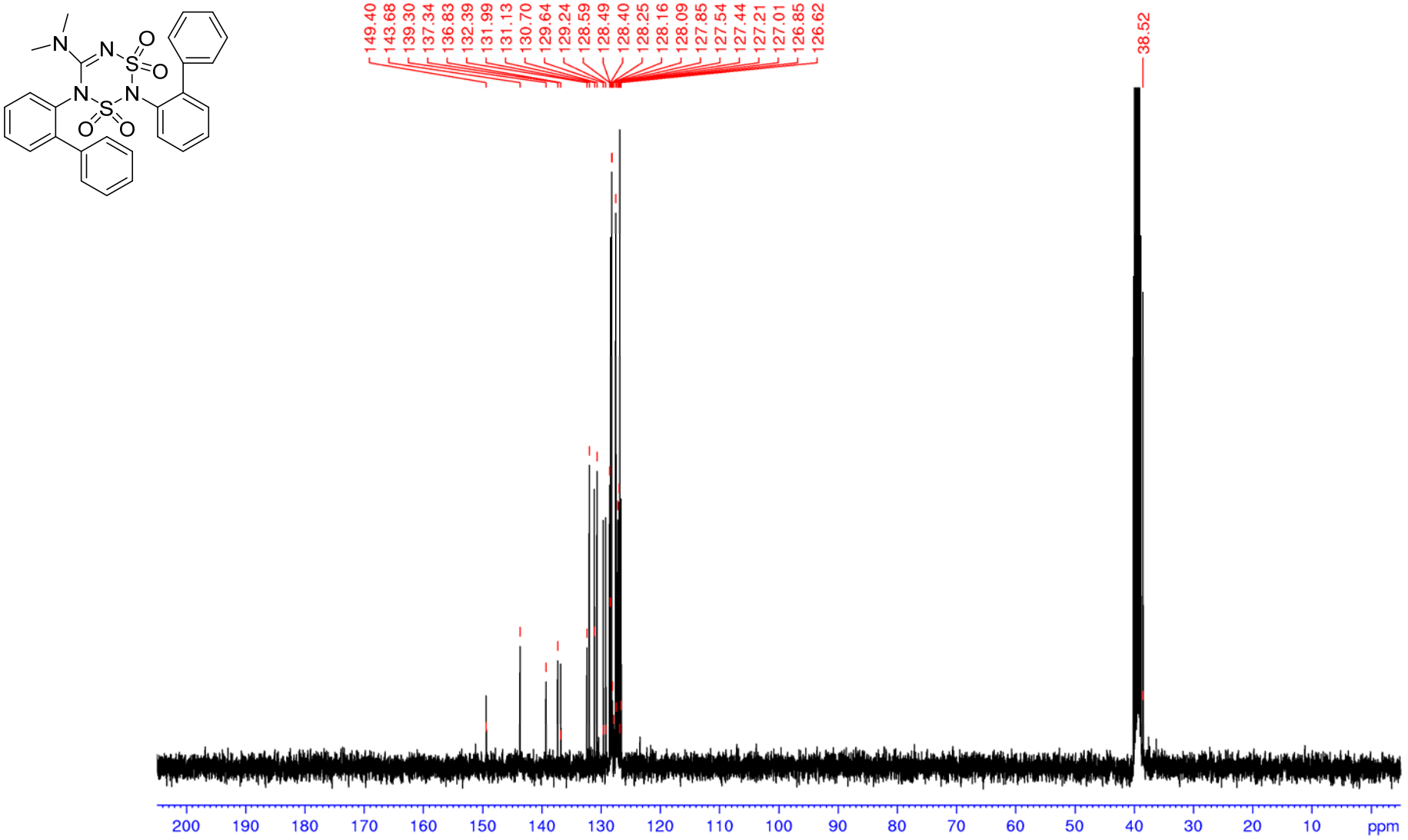

^{1}H NMR data for **14e** (600 MHz; DMSO-d_6)

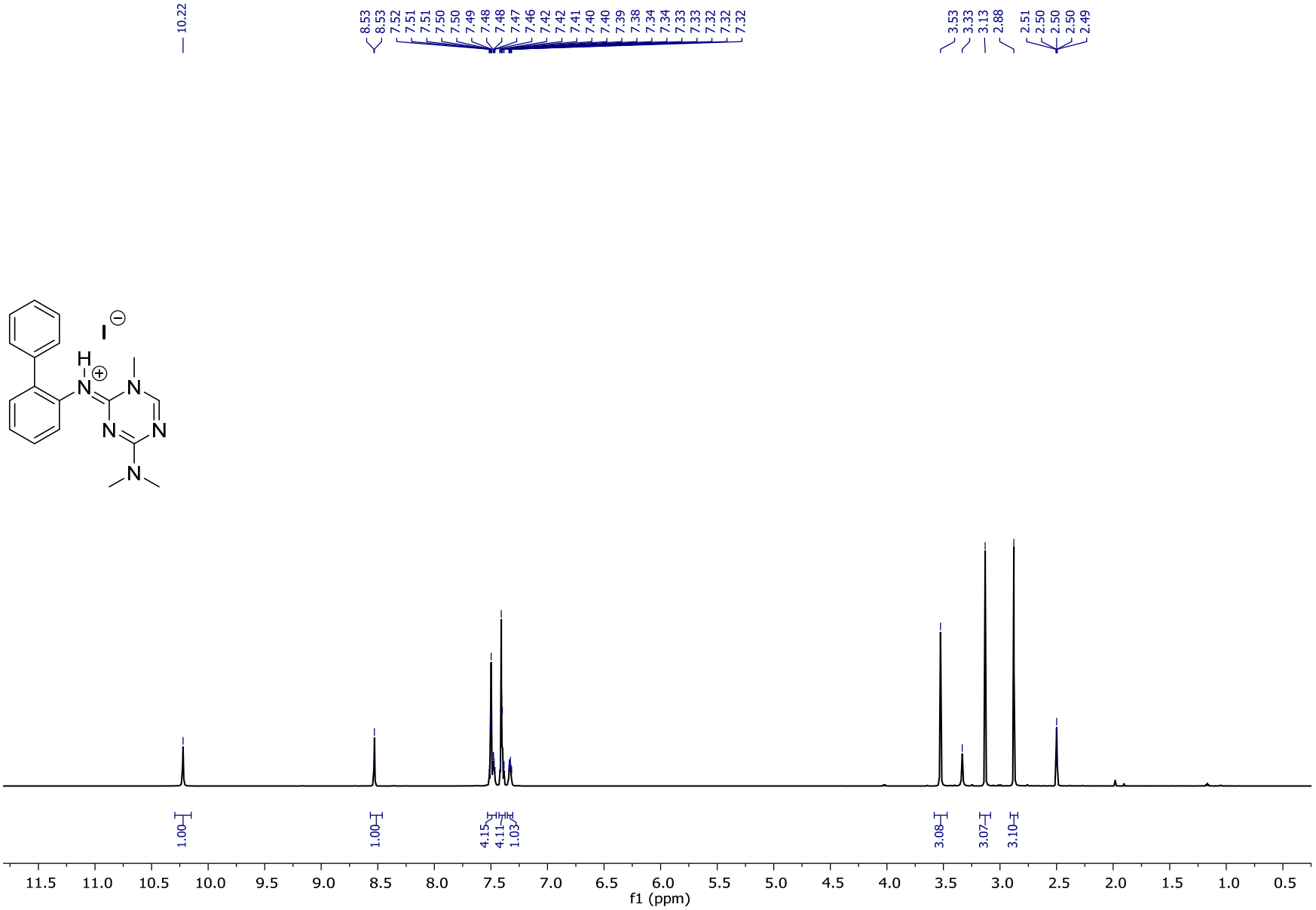

^{13}C NMR data for **14e** (150 MHz; DMSO-d_6)

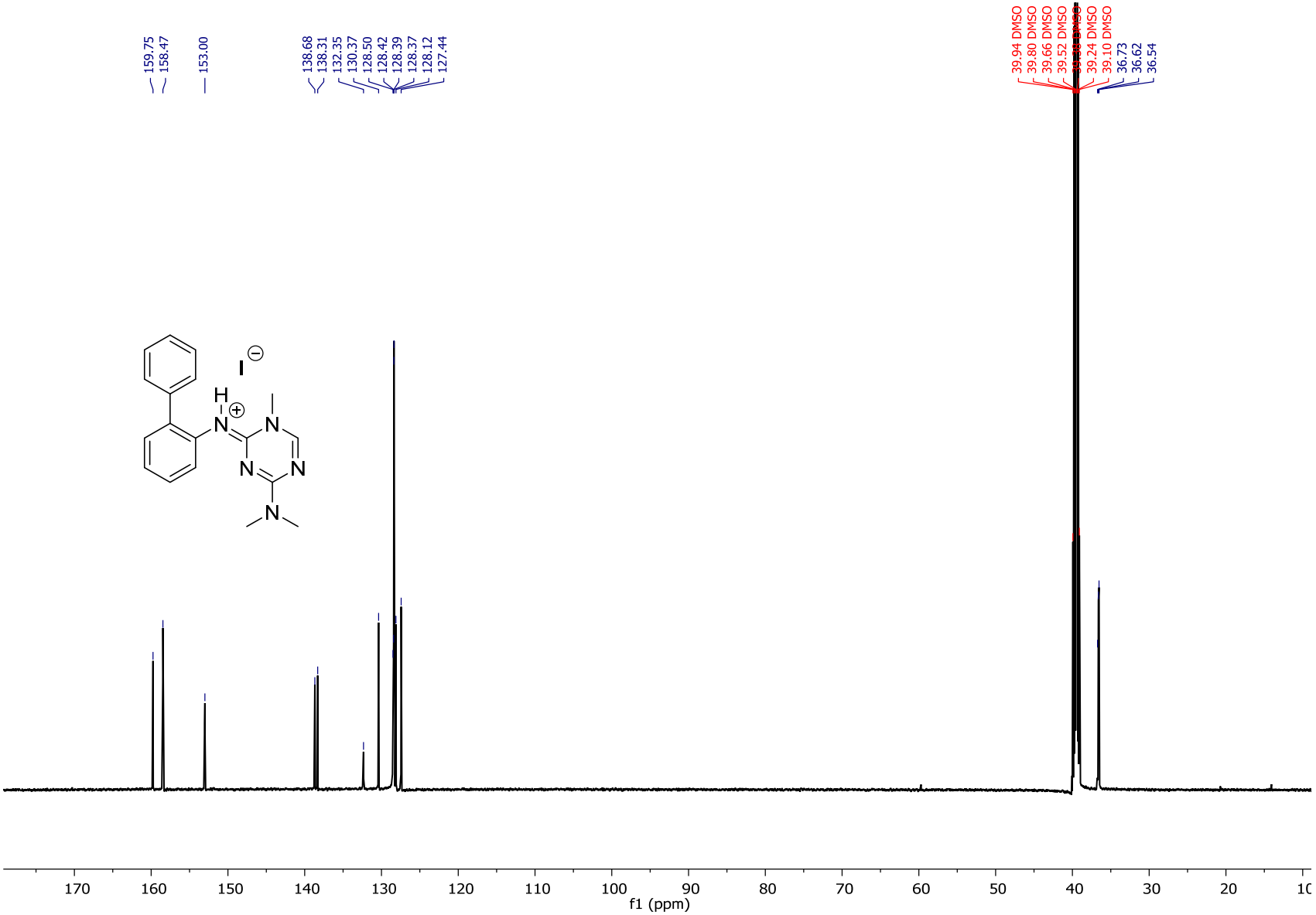

^{1}H NMR data for **17f** (600 MHz; DMSO-d_6)

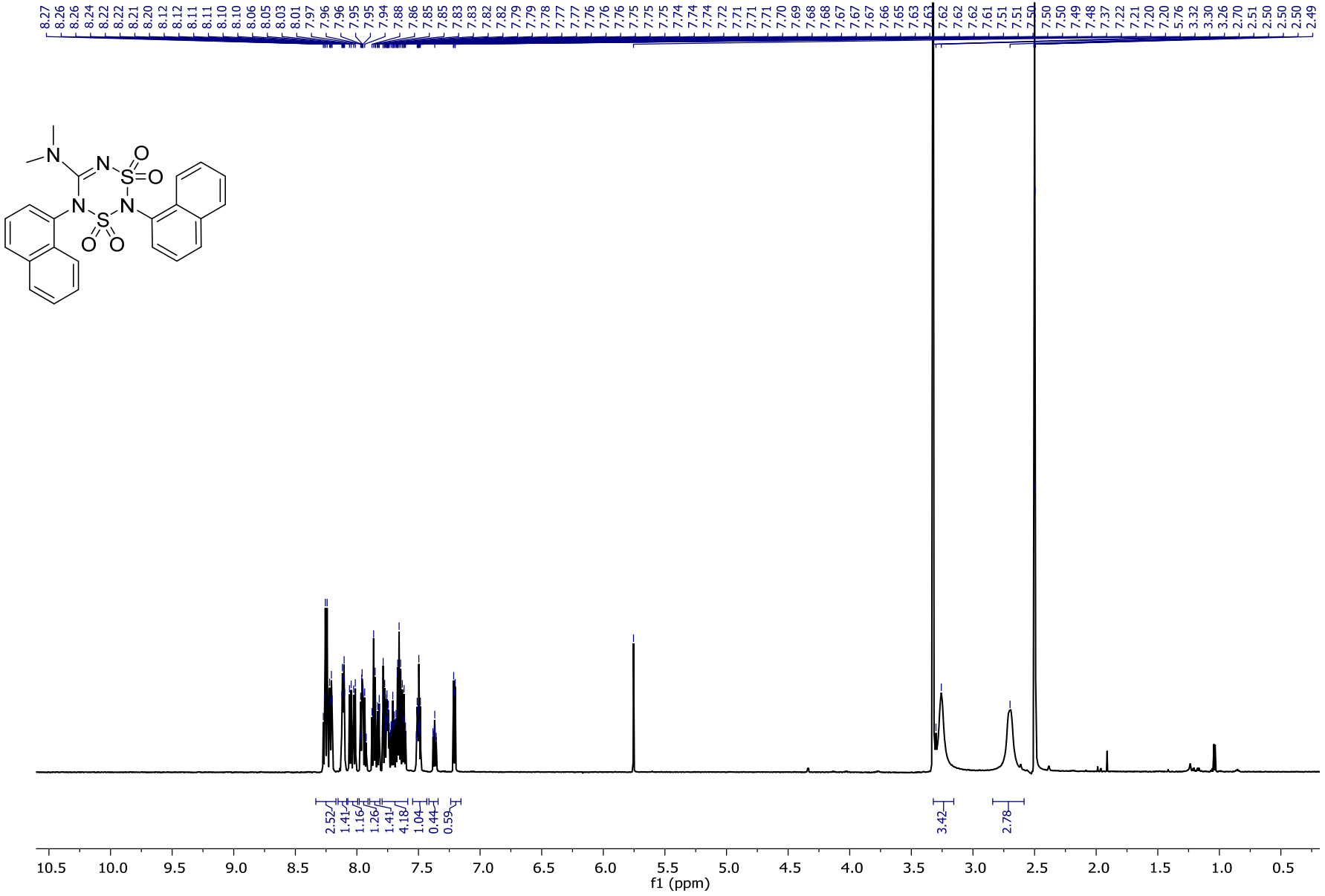

^{13}C NMR data for **17f** (150 MHz; DMSO-d_6)

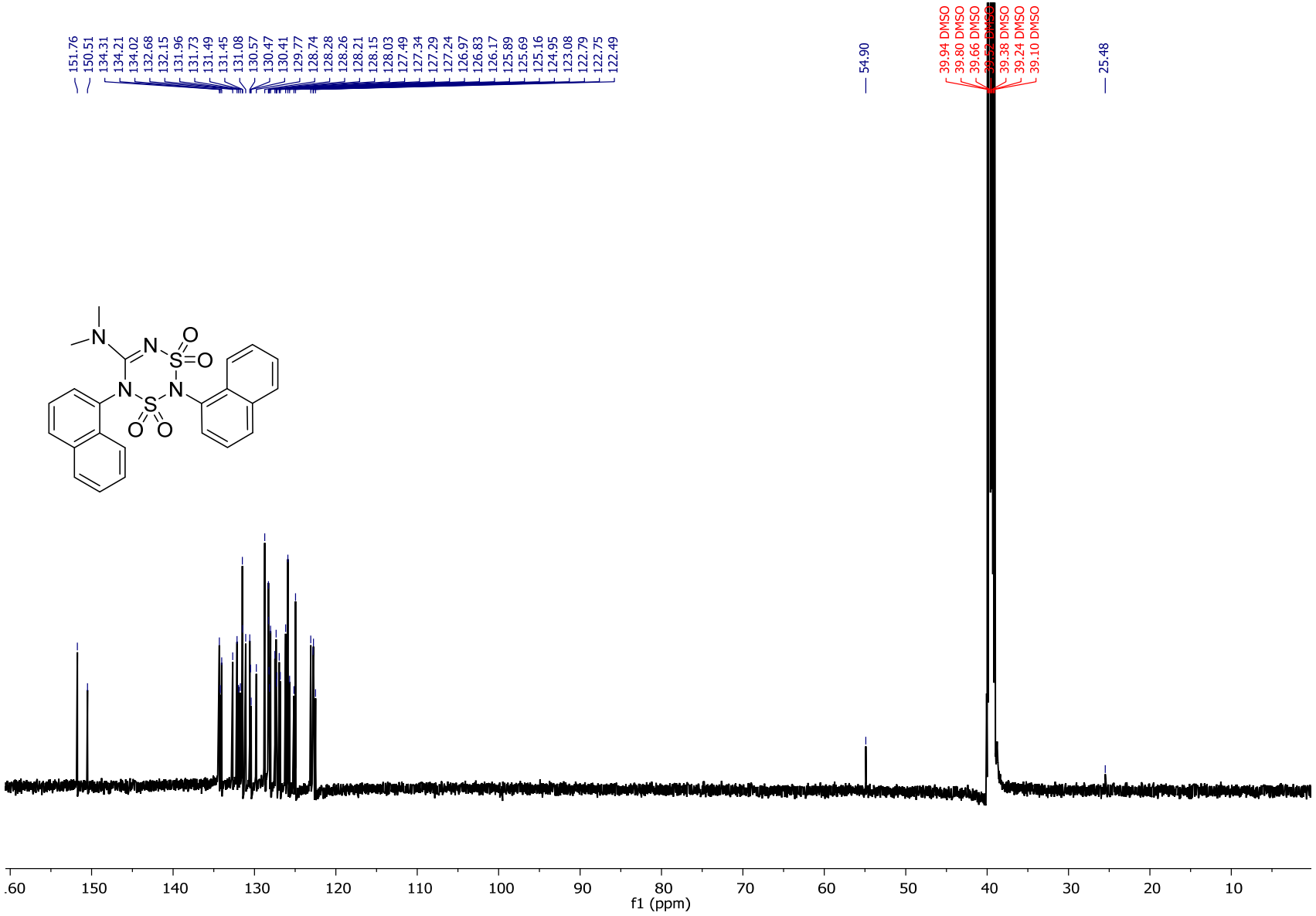

^{1}H NMR data for **9f** (400 MHz; DMSO-d_6)

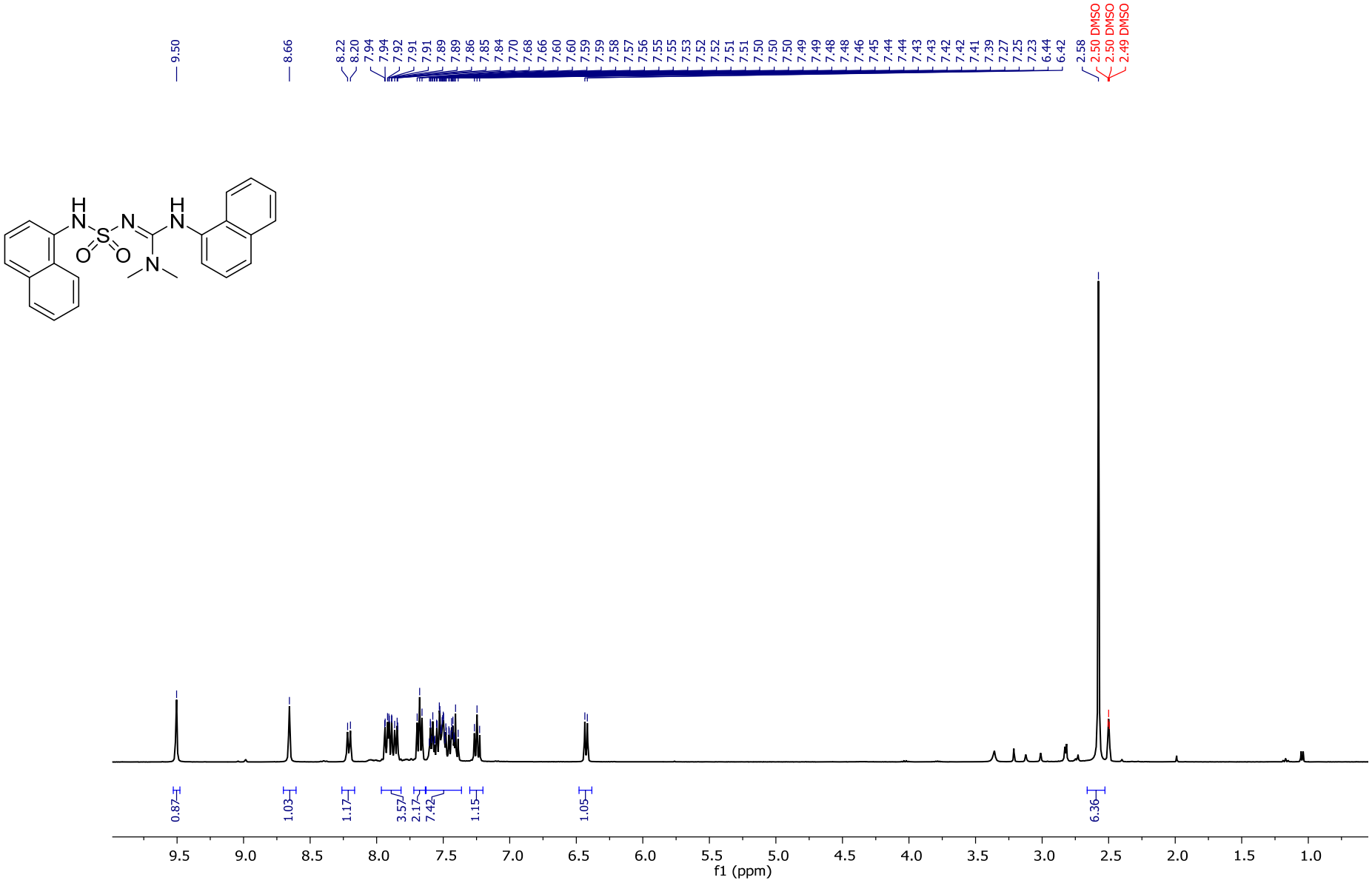

^{13}C NMR data for **9f** (100 MHz; DMSO-*d*$_6$)

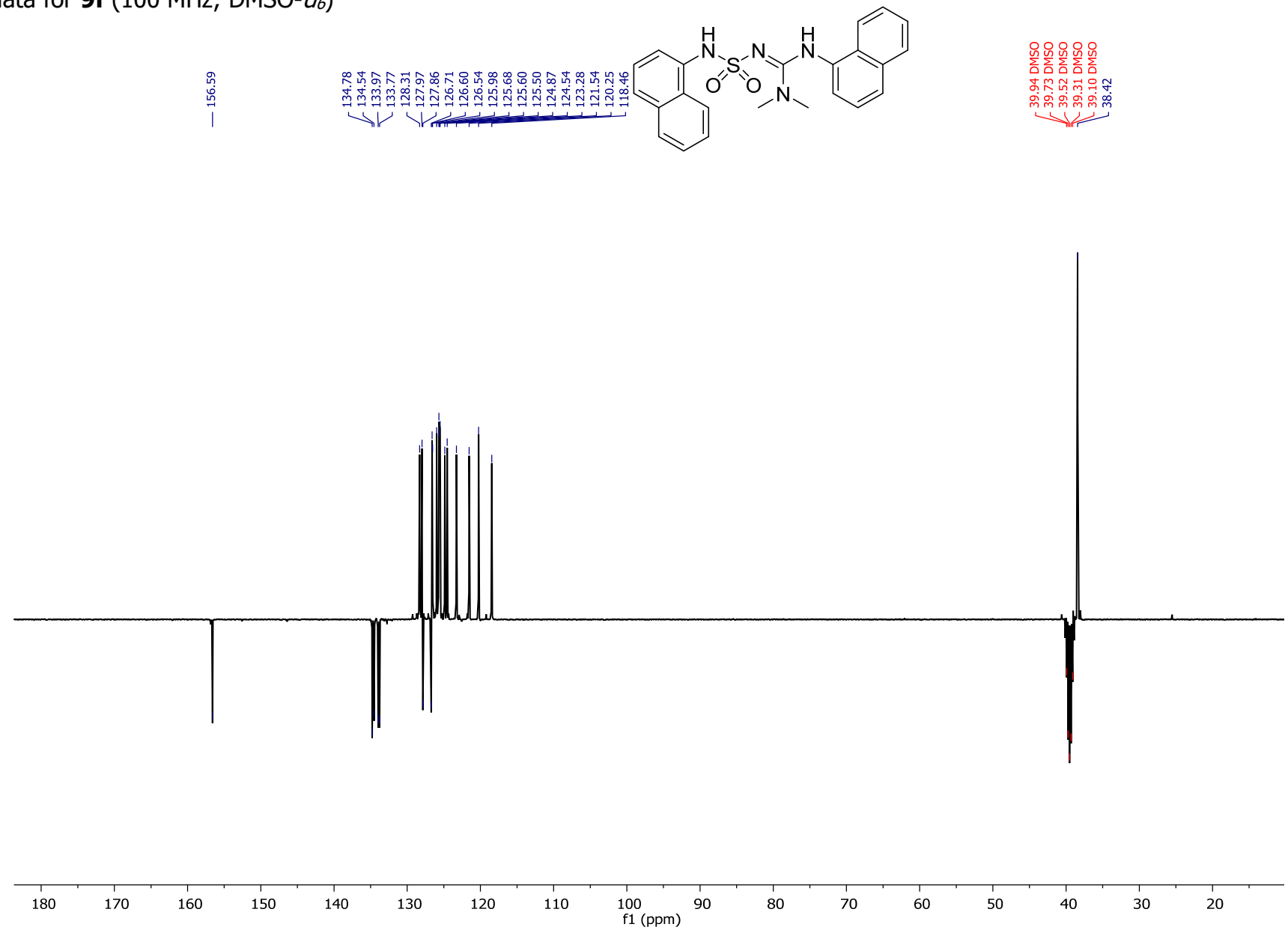

^{1}H NMR data for **14f** (600 MHz; DMSO-d_6)

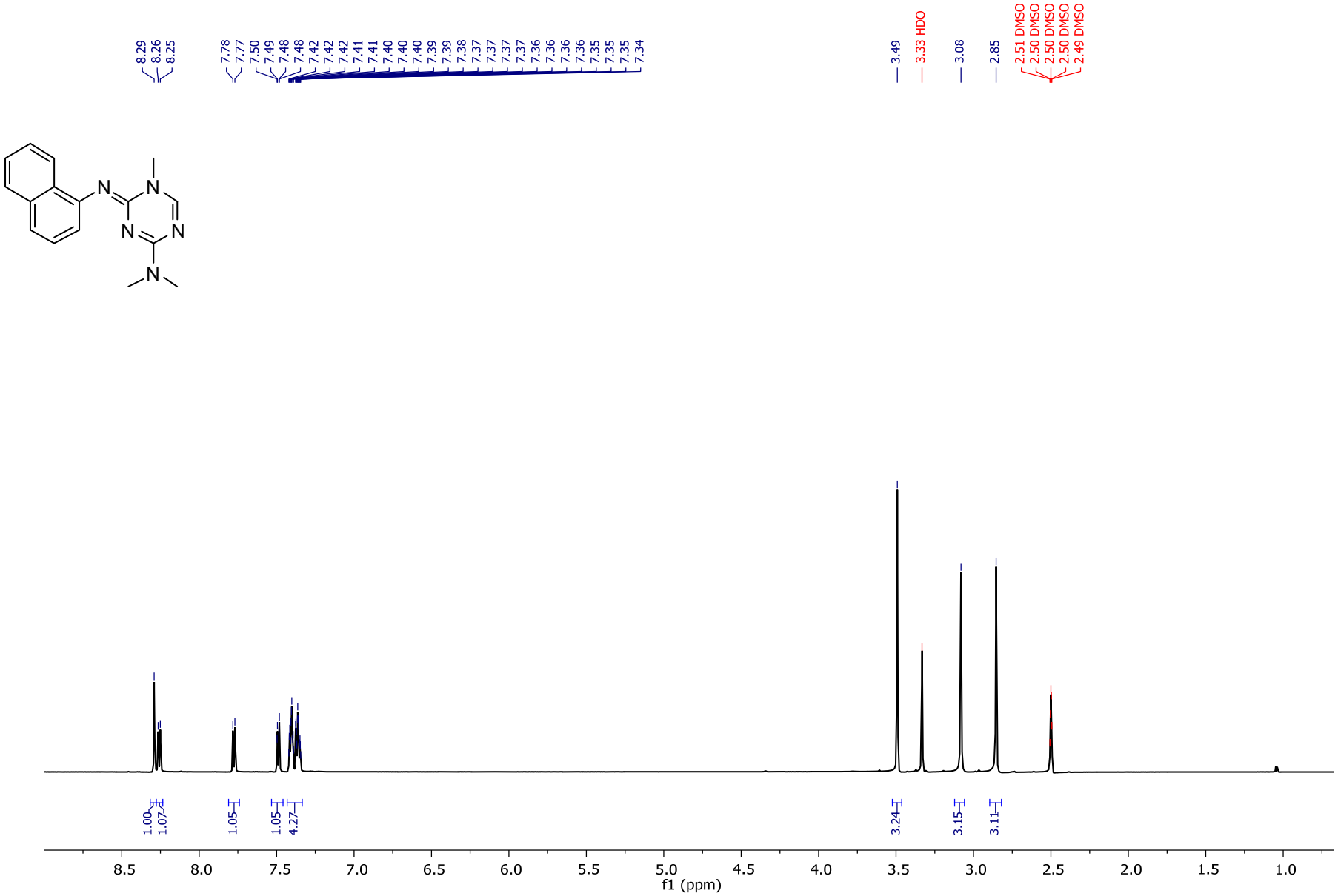

^{13}C NMR data for **14f** (150 MHz; DMSO-d_6)

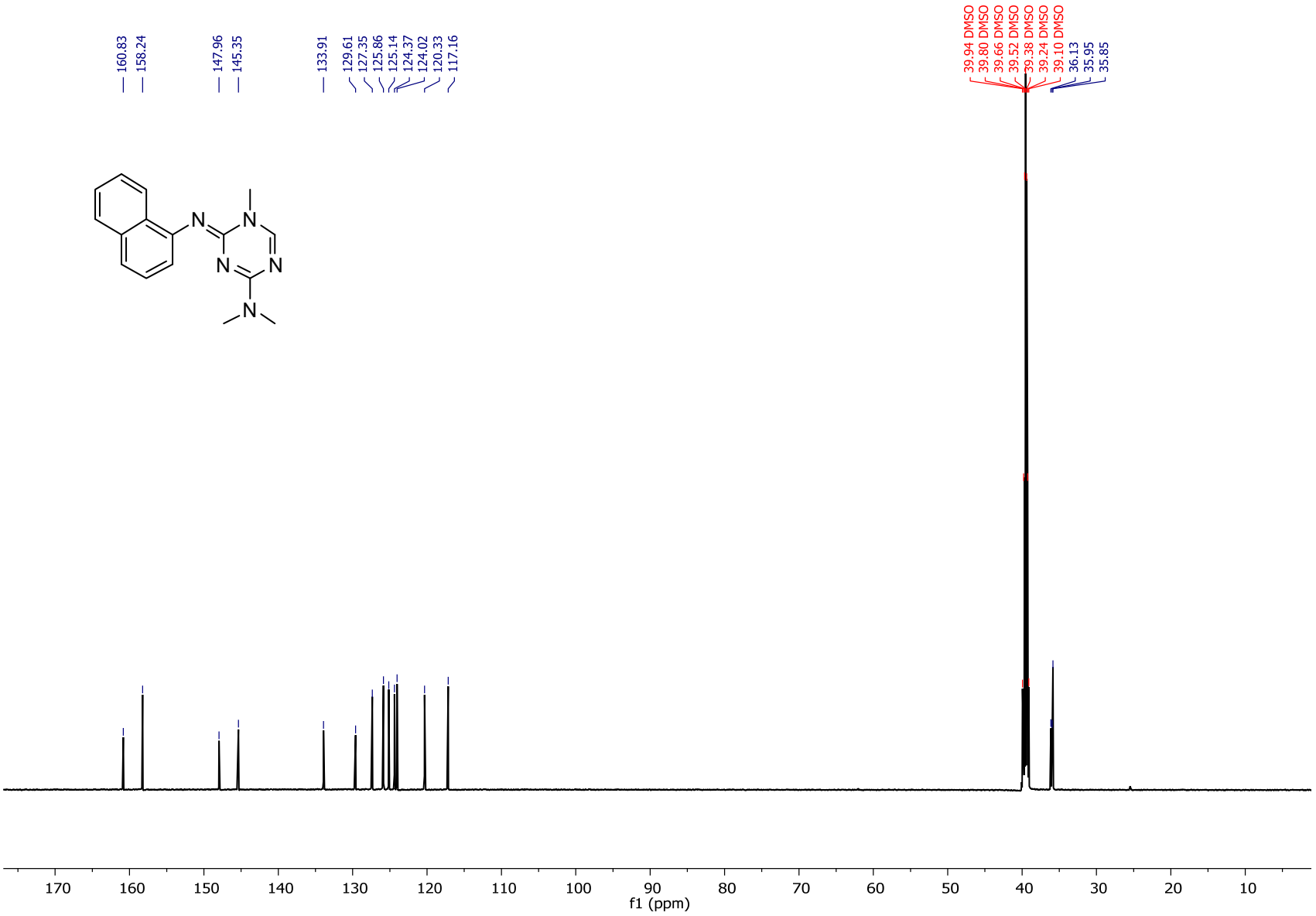

^{1}H NMR data for **8g** (600 MHz; $CDCl_3$)

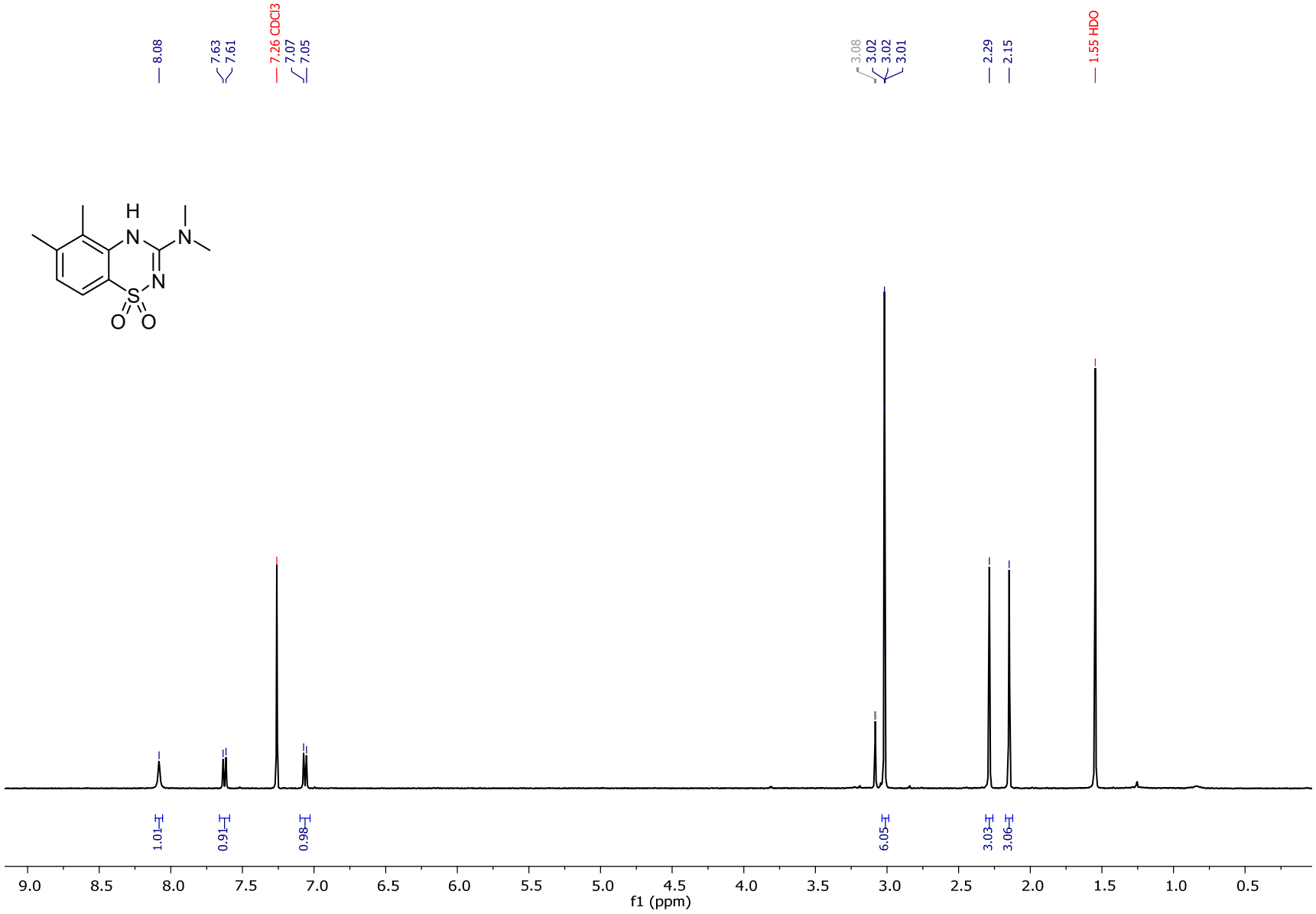

^{13}C NMR data for **8g** (150 MHz; $CDCl_3$)

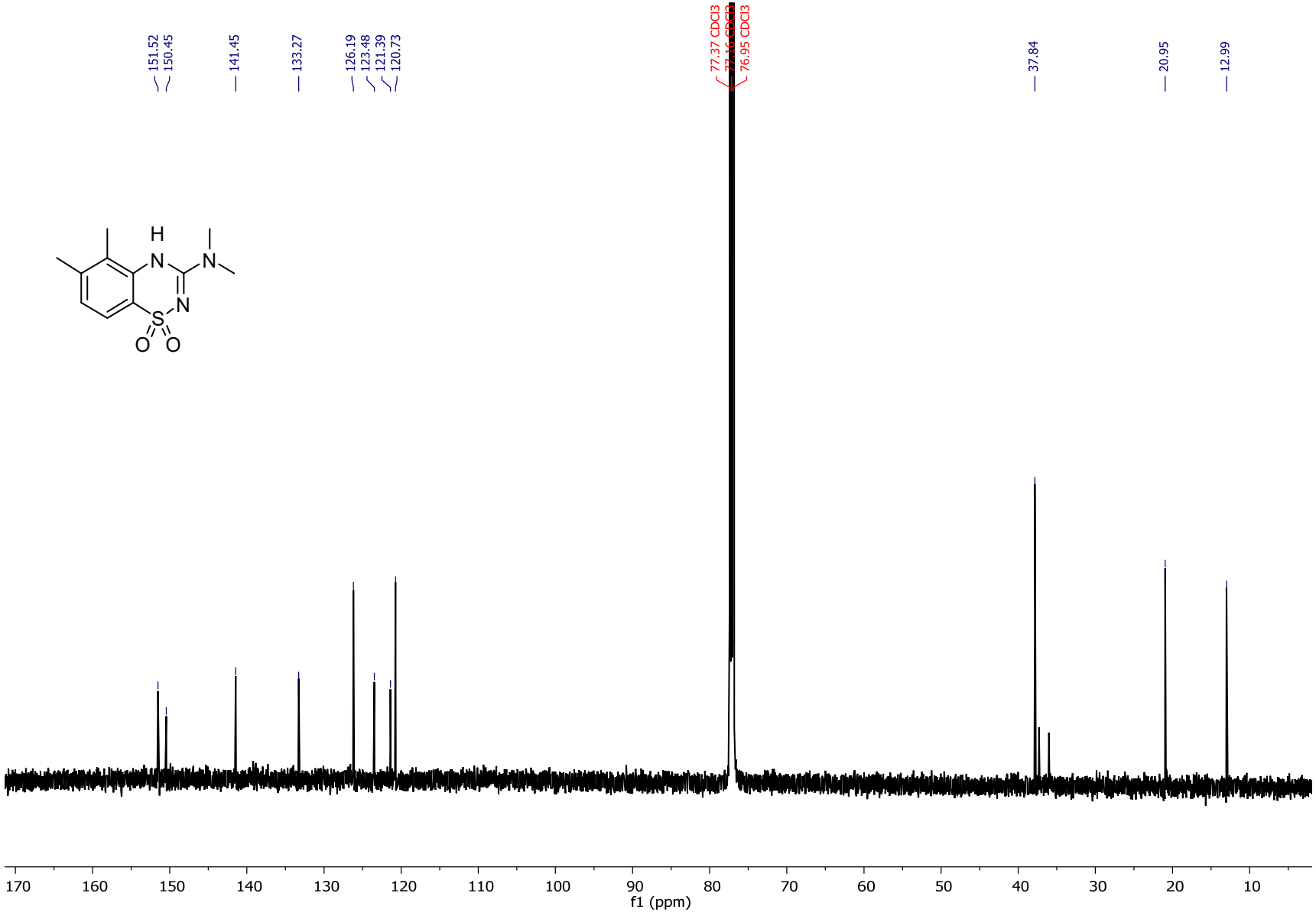

^{1}H NMR data for **14g.HBr** (600 MHz; DMSO-d_6)

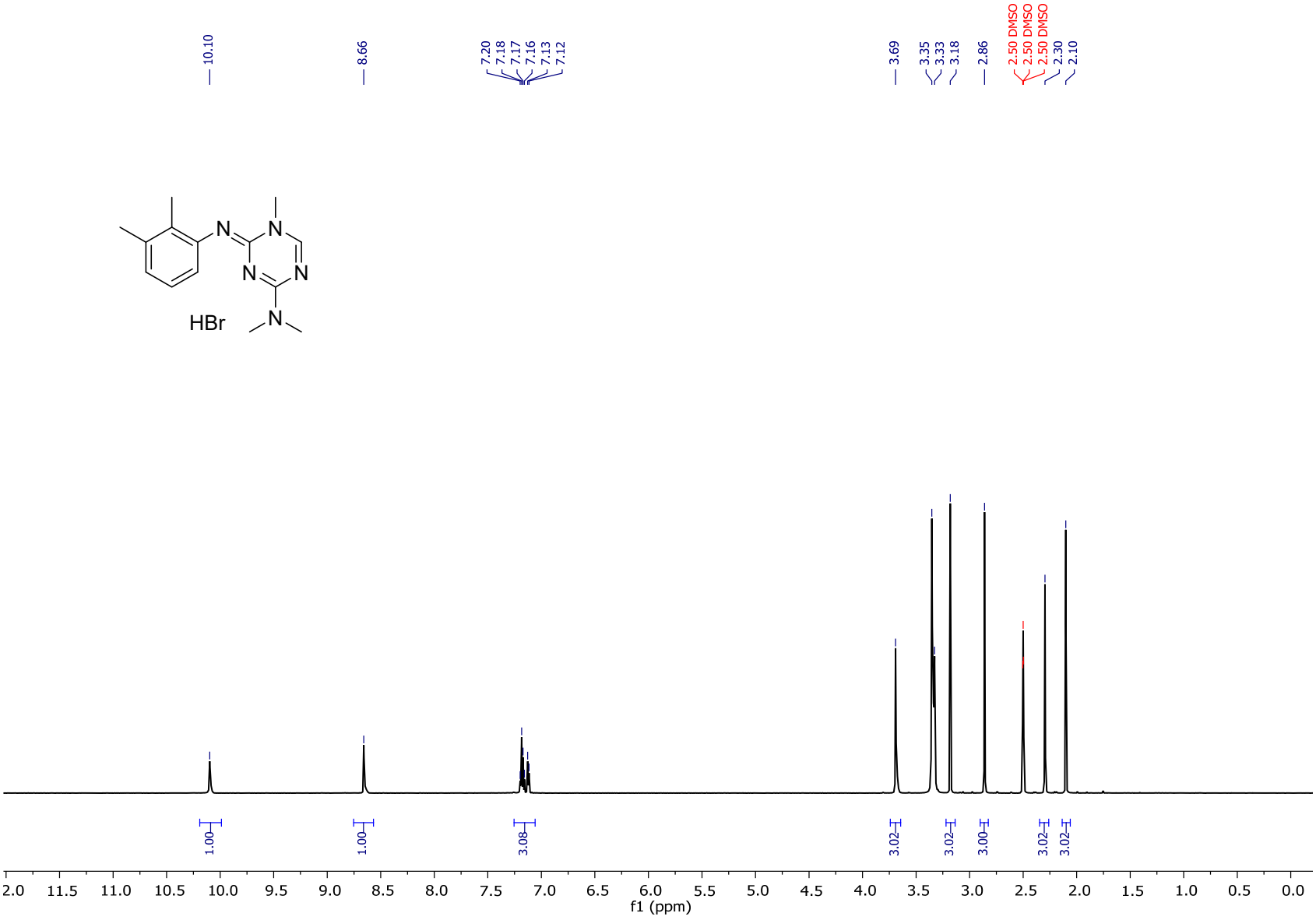

^{13}C NMR data for **14g** (150 MHz; DMSO-d_6)

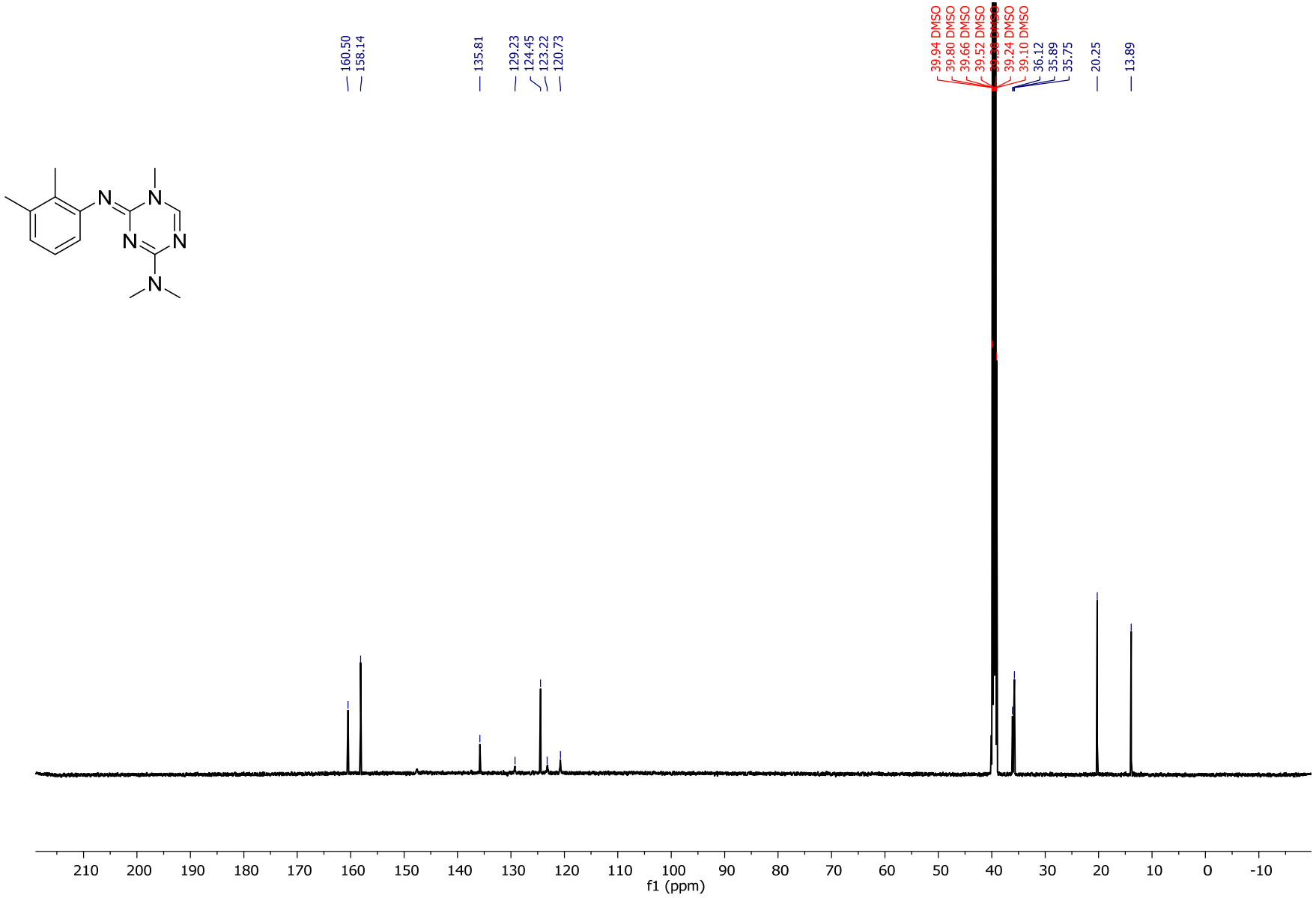

^{13}C NMR data for **14g.HBr** (150 MHz; DMSO-d_6)

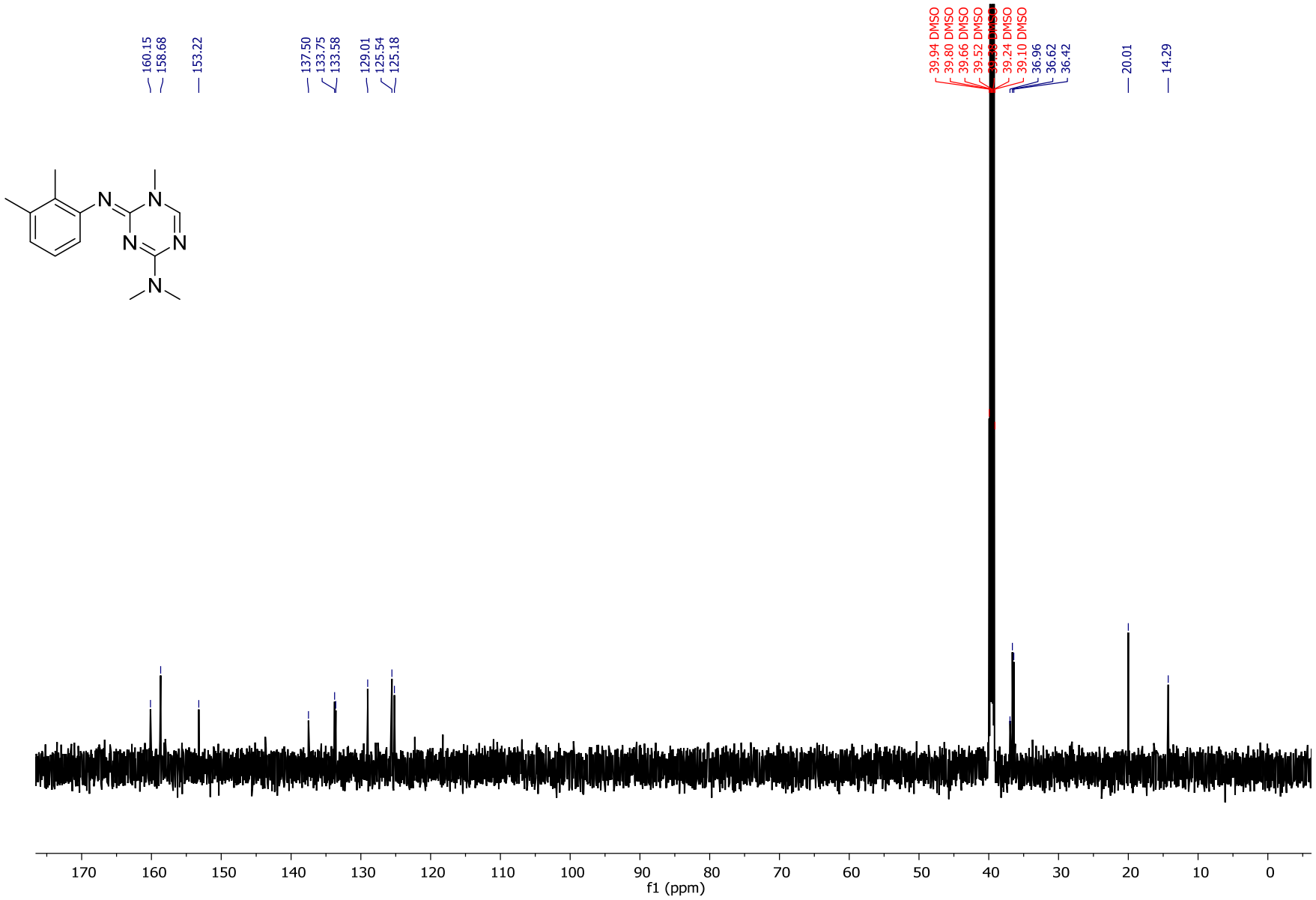

^{1}H NMR data for **17g** (600 MHz; CD_3CN, 338 K)

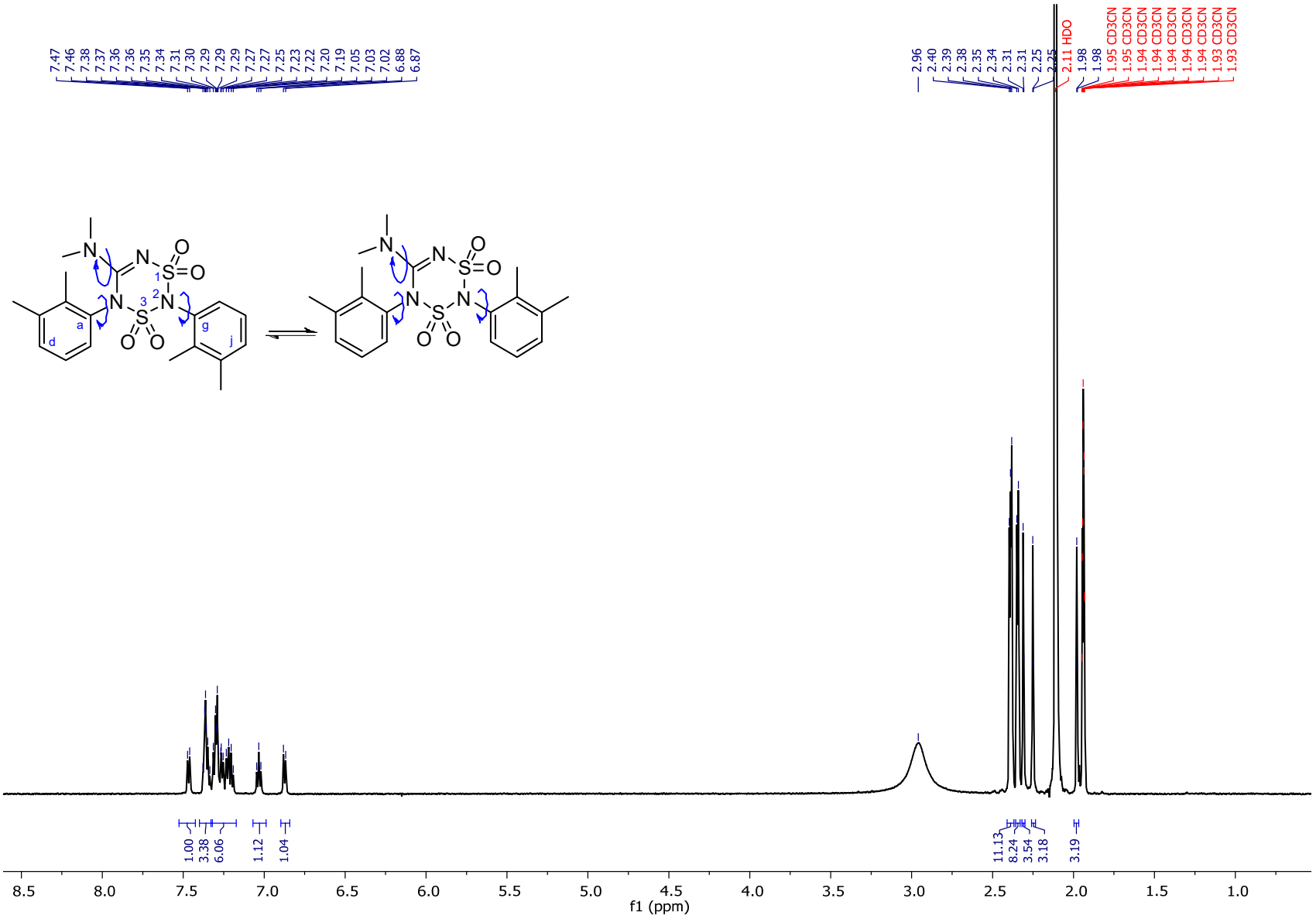

^{1}H NMR data for **17g** (600 MHz; CD_3CN, 298 K)

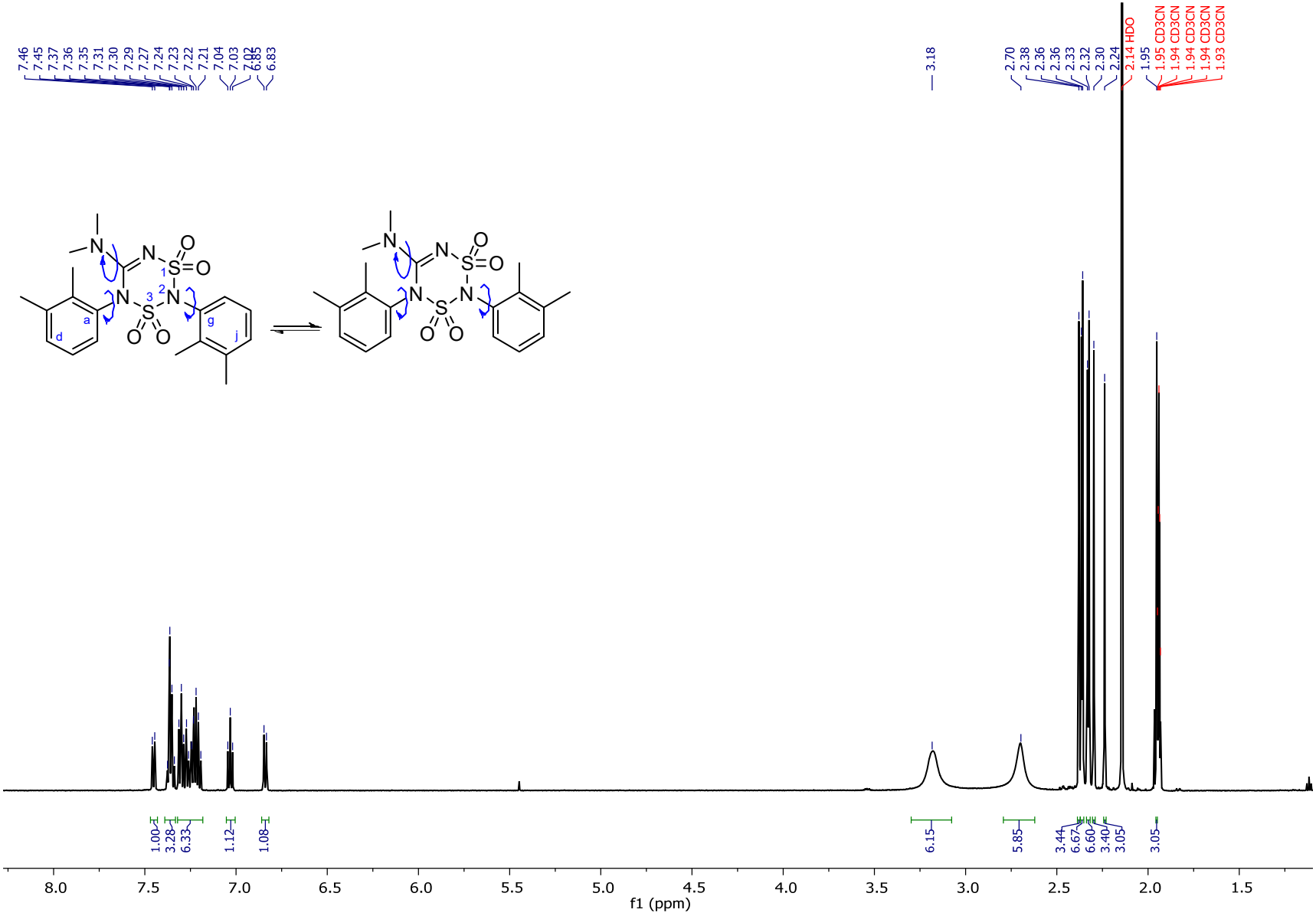

^{1}H NMR data for **17g** (600 MHz; CD_3CN, 248 K)

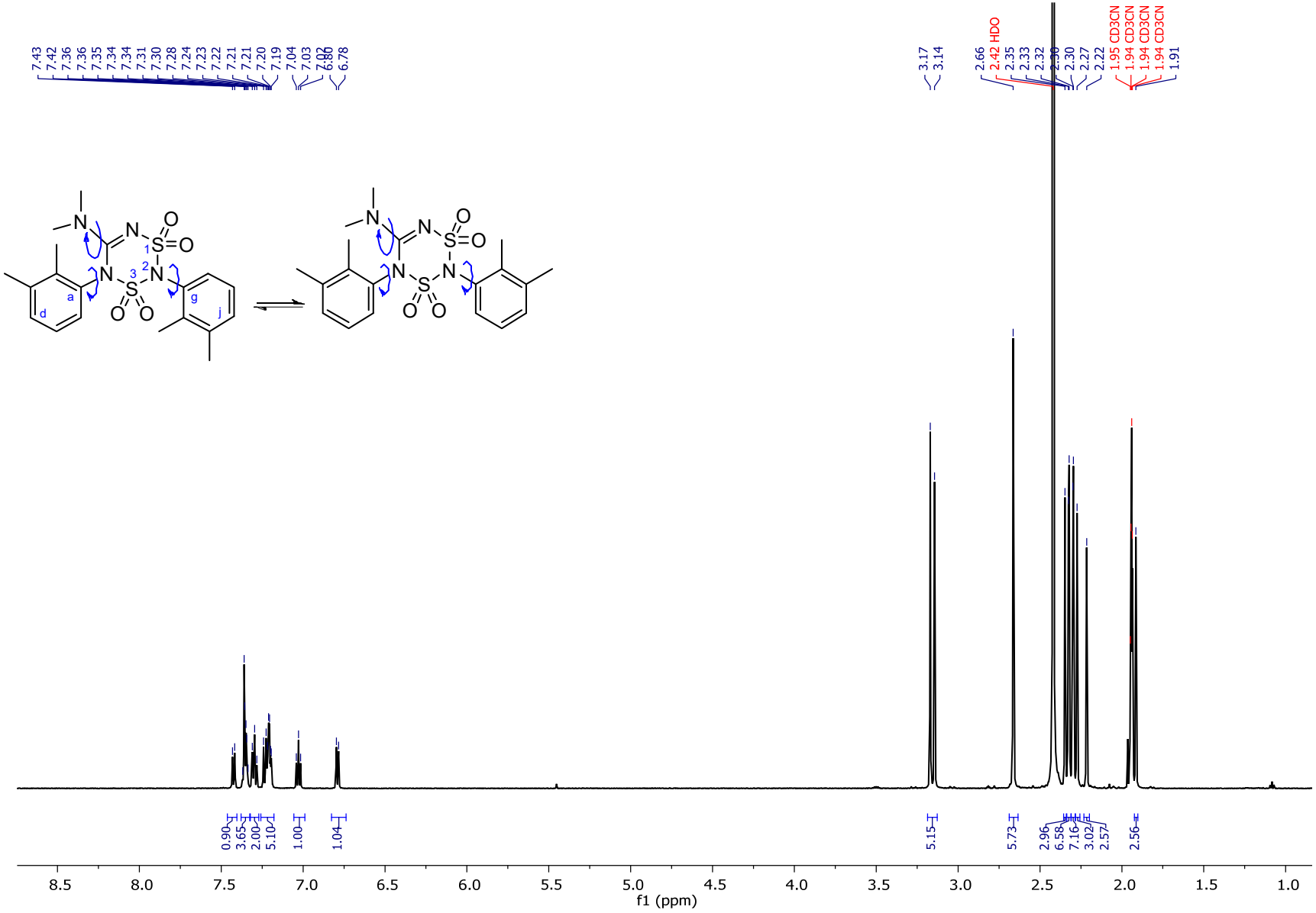

^{13}C NMR data for **17g** (150 MHz; CD_3CN, 248K)

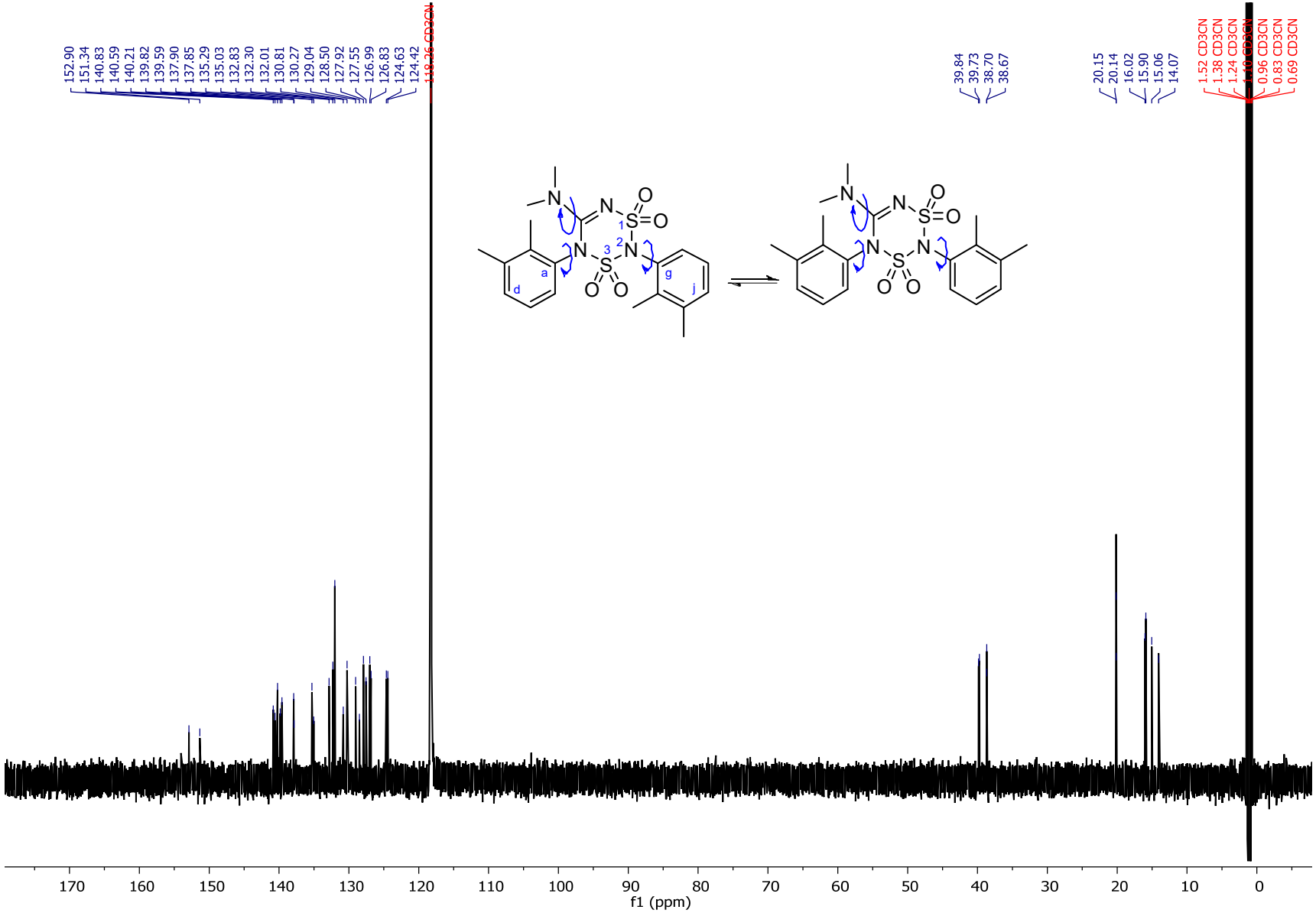

^{1}H NMR data for **17h** (600 MHz; DMSO-d_6, 328 K)

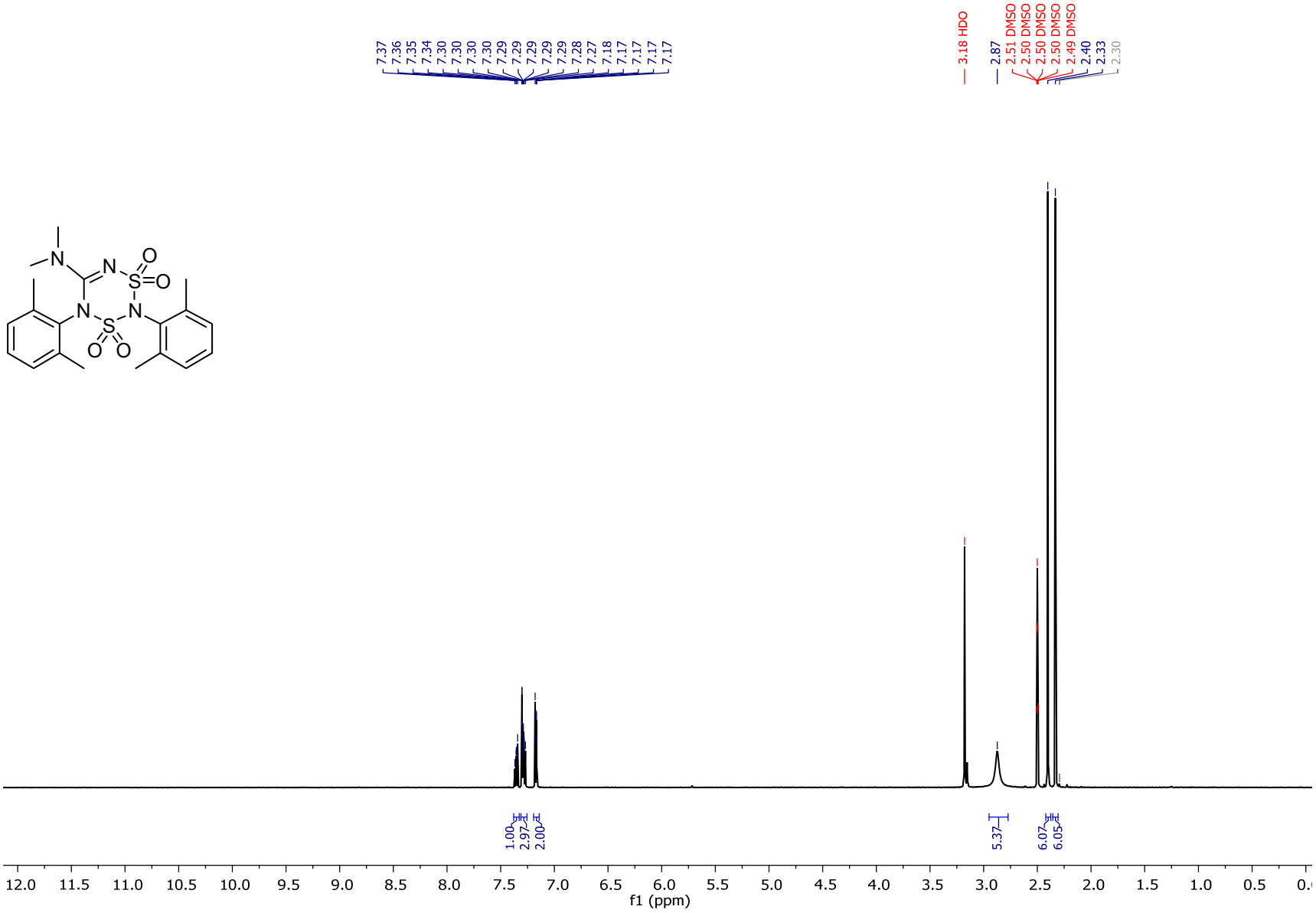

^{1}H NMR data for **17h** (600 MHz; DMSO-d_6, 298 K)

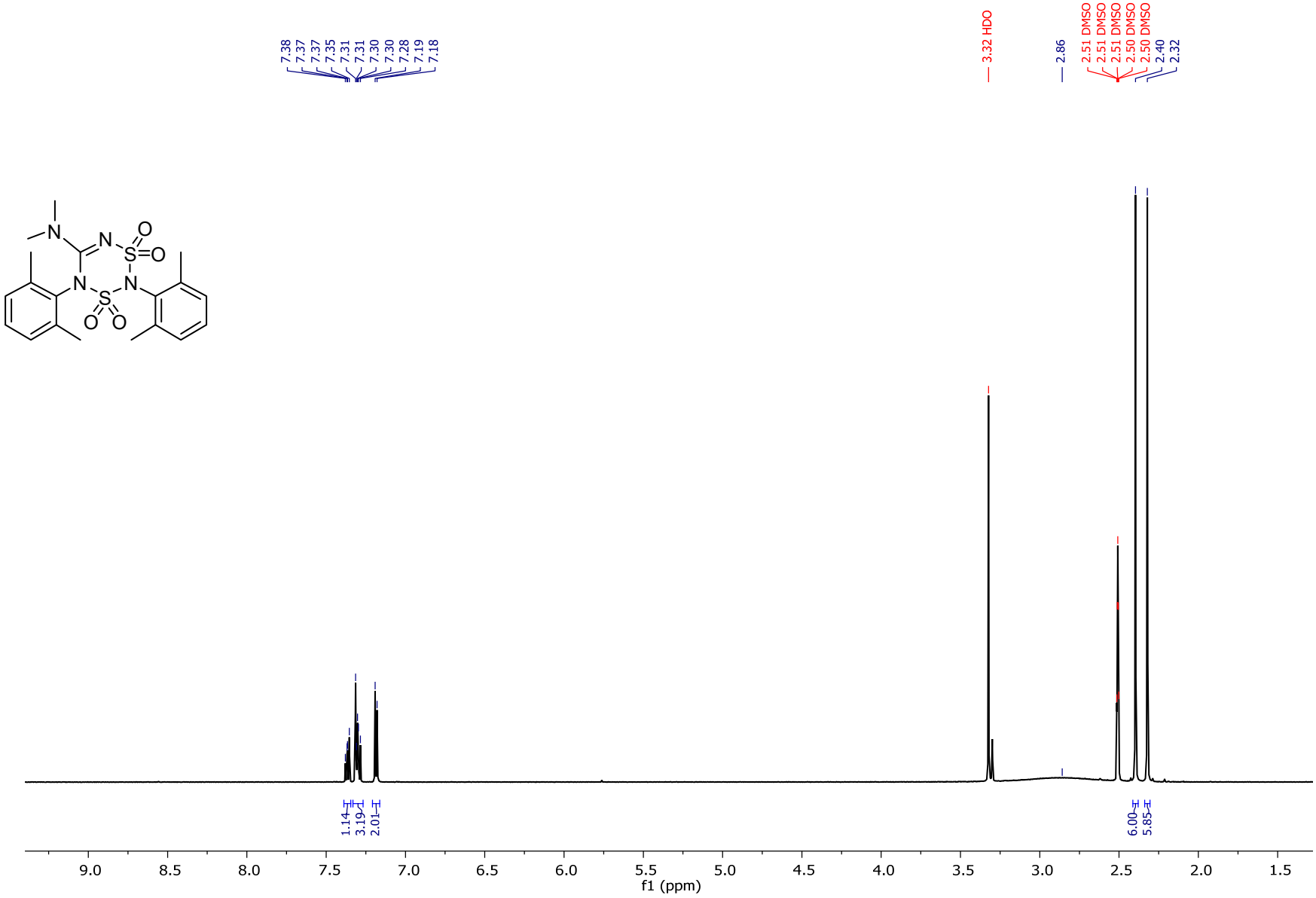

^{1}H NMR data for **17h** (600 MHz; CD_3CN, 238 K)

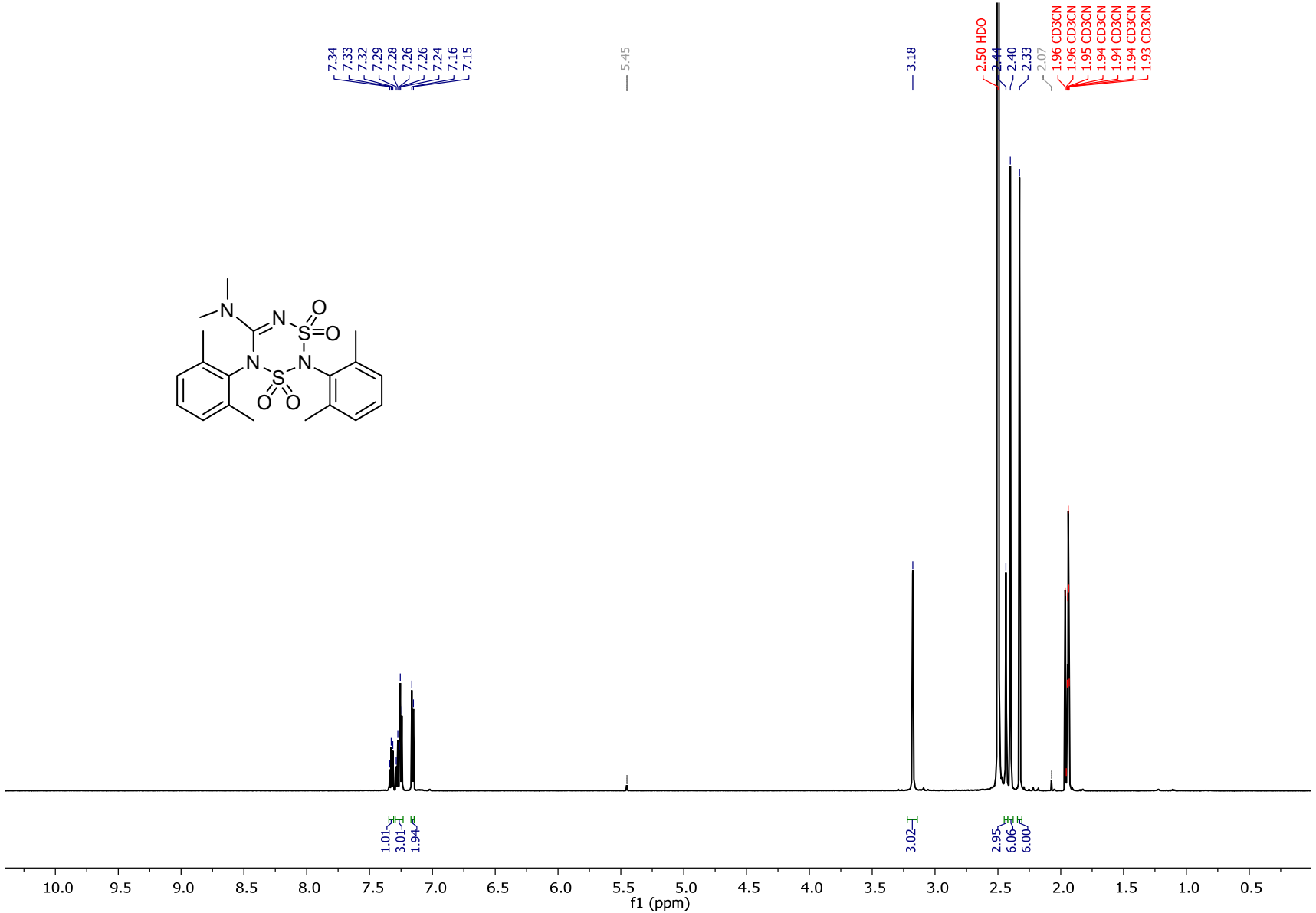

^{13}C NMR data for **17h** (150 MHz; DMSO-d_6, 298 K)

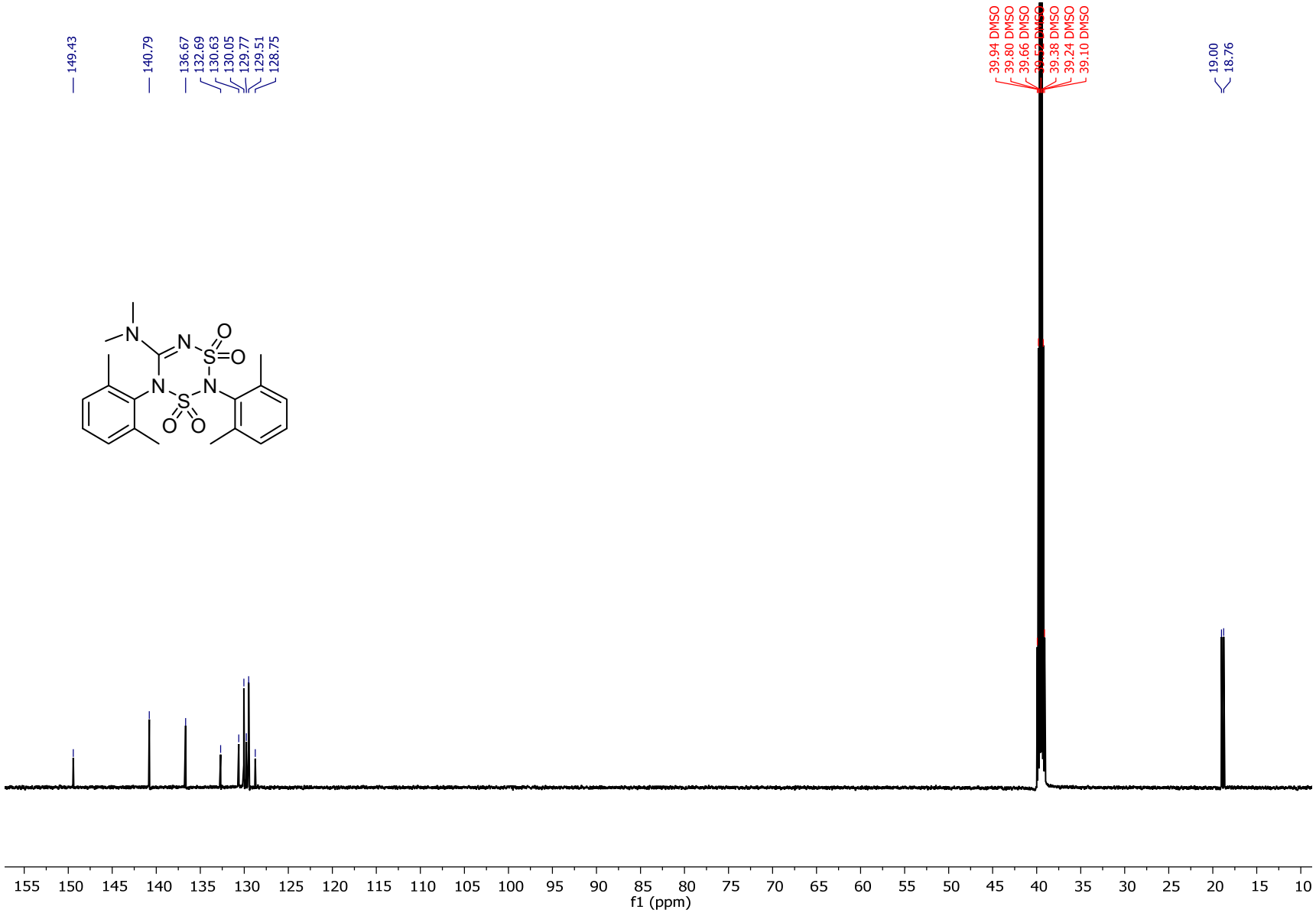

^{13}C NMR data for **17h** (150 MHz; CD_3CN, 238 K)

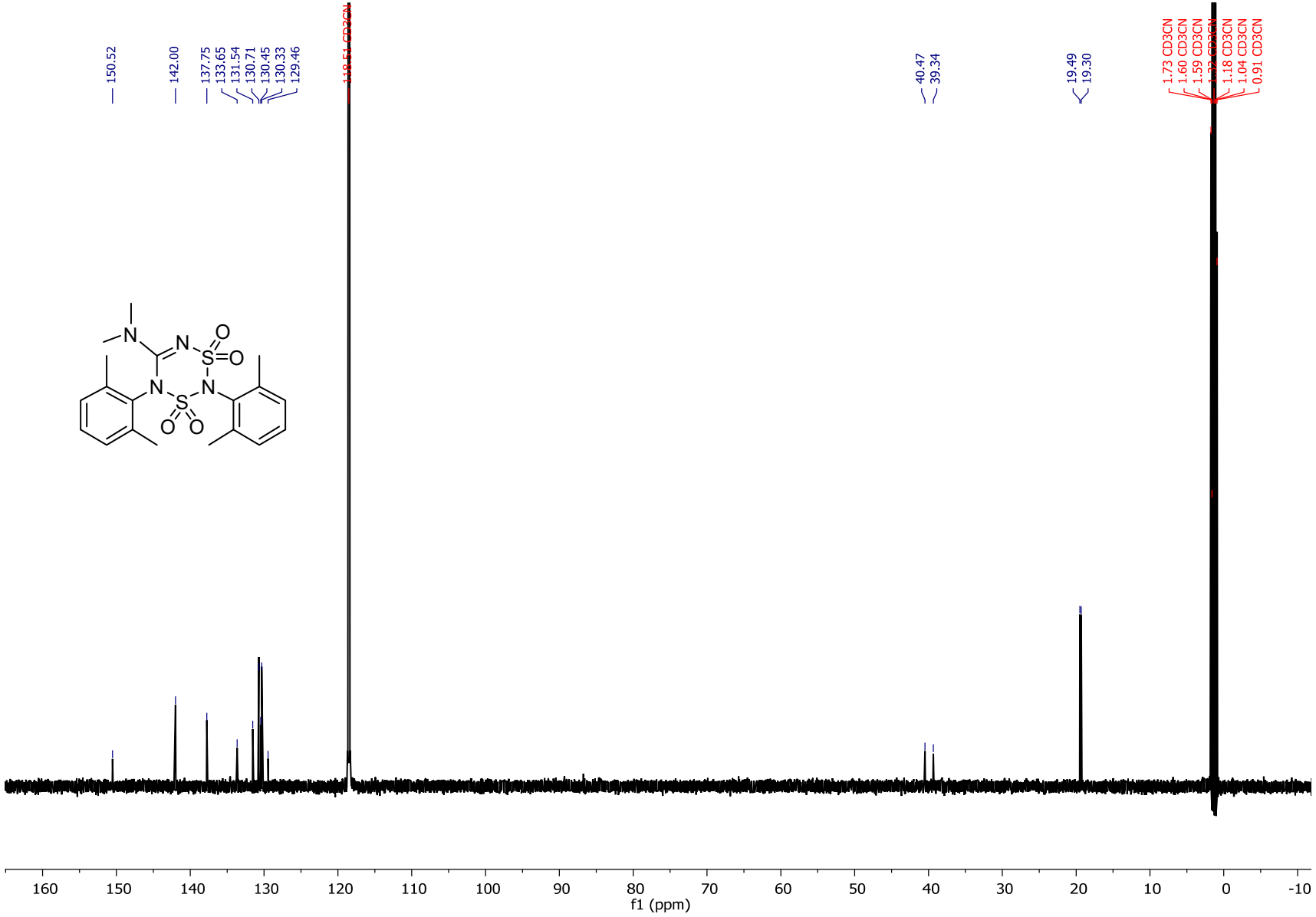

^{1}H NMR data for **8i** (600 MHz; DMSO-*d*$_6$)

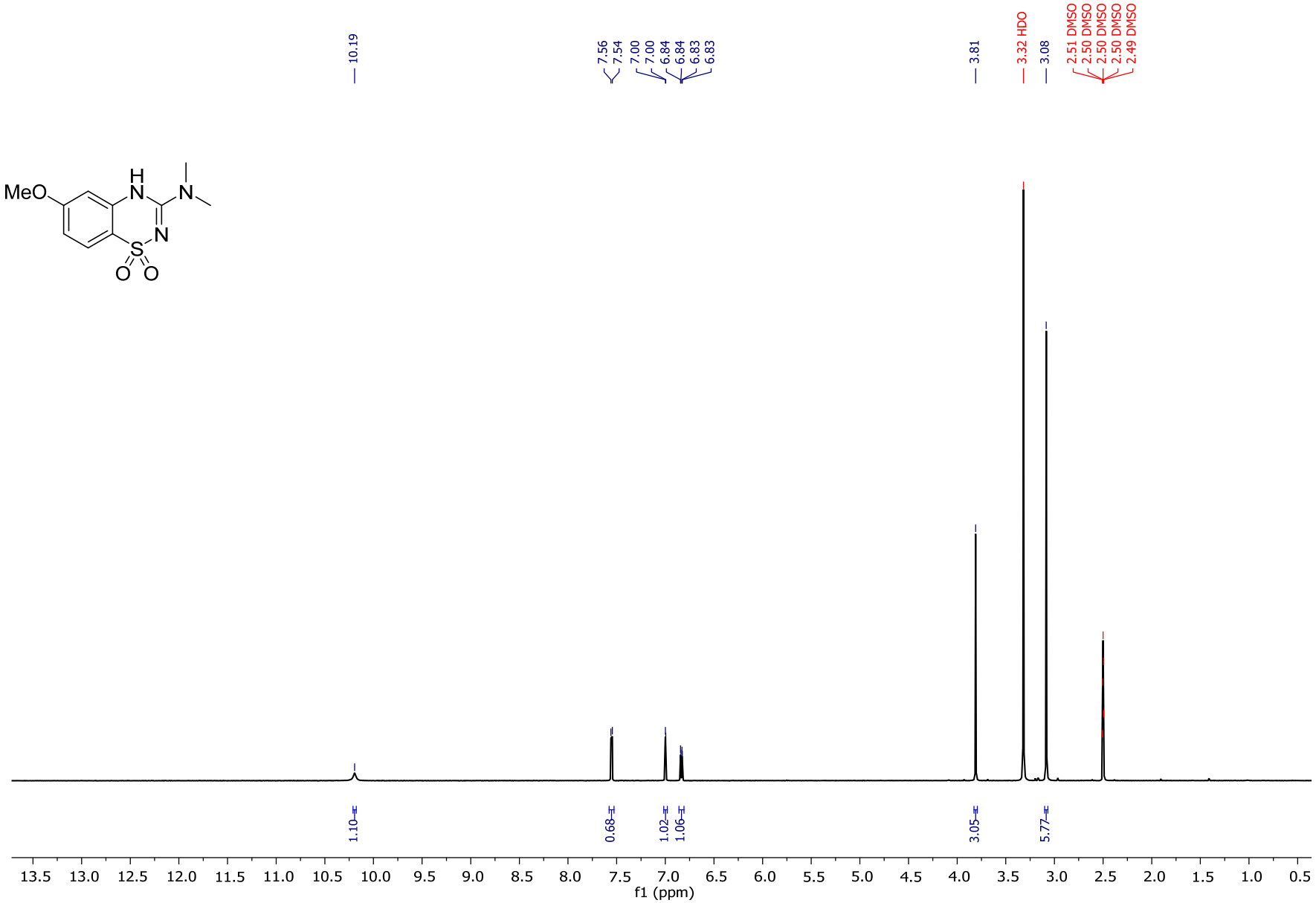

^{13}C NMR data for **8i** (150 MHz; DMSO-d_6)

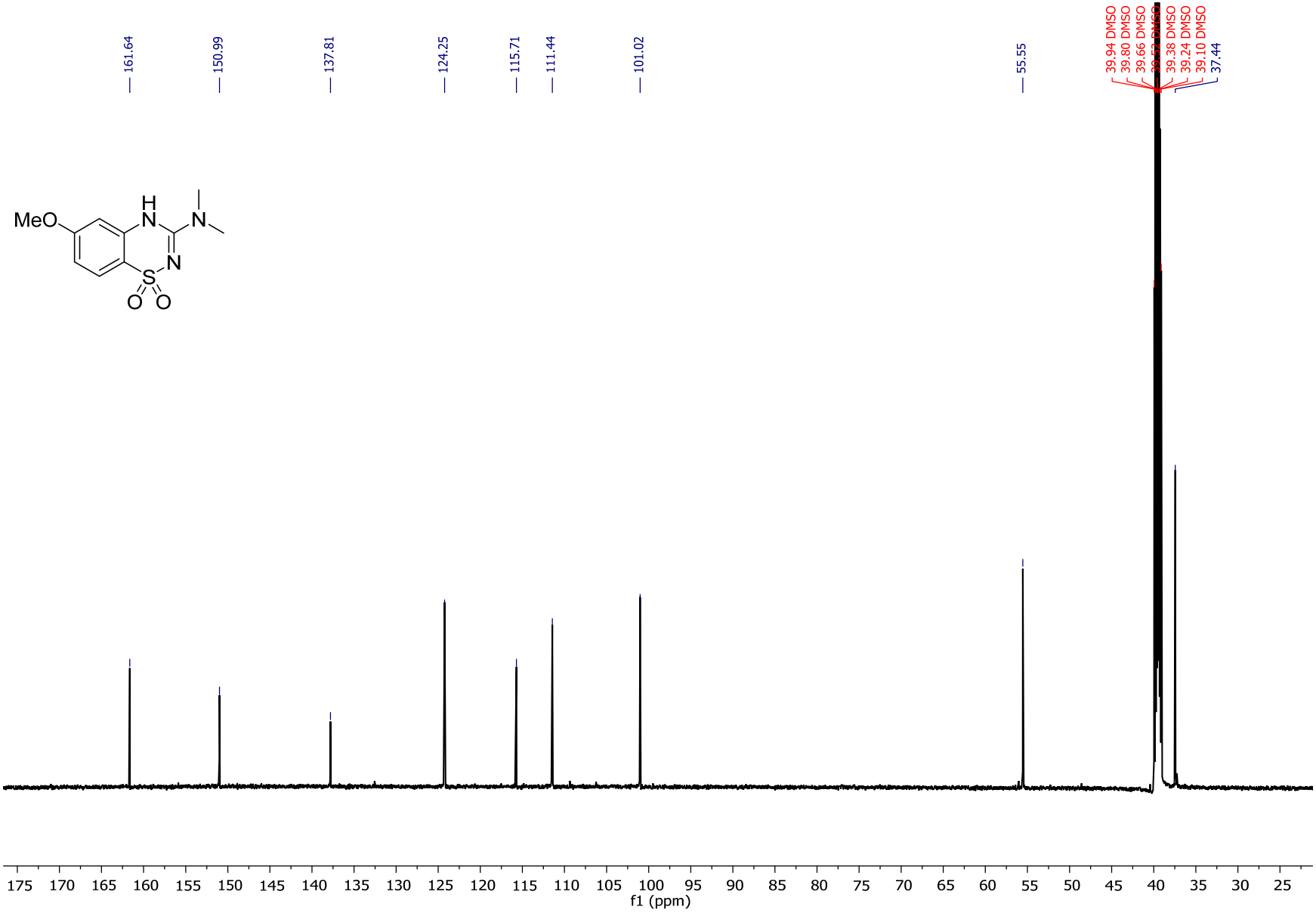

^{1}H NMR data for **24** (600 MHz; $CDCl_3$)

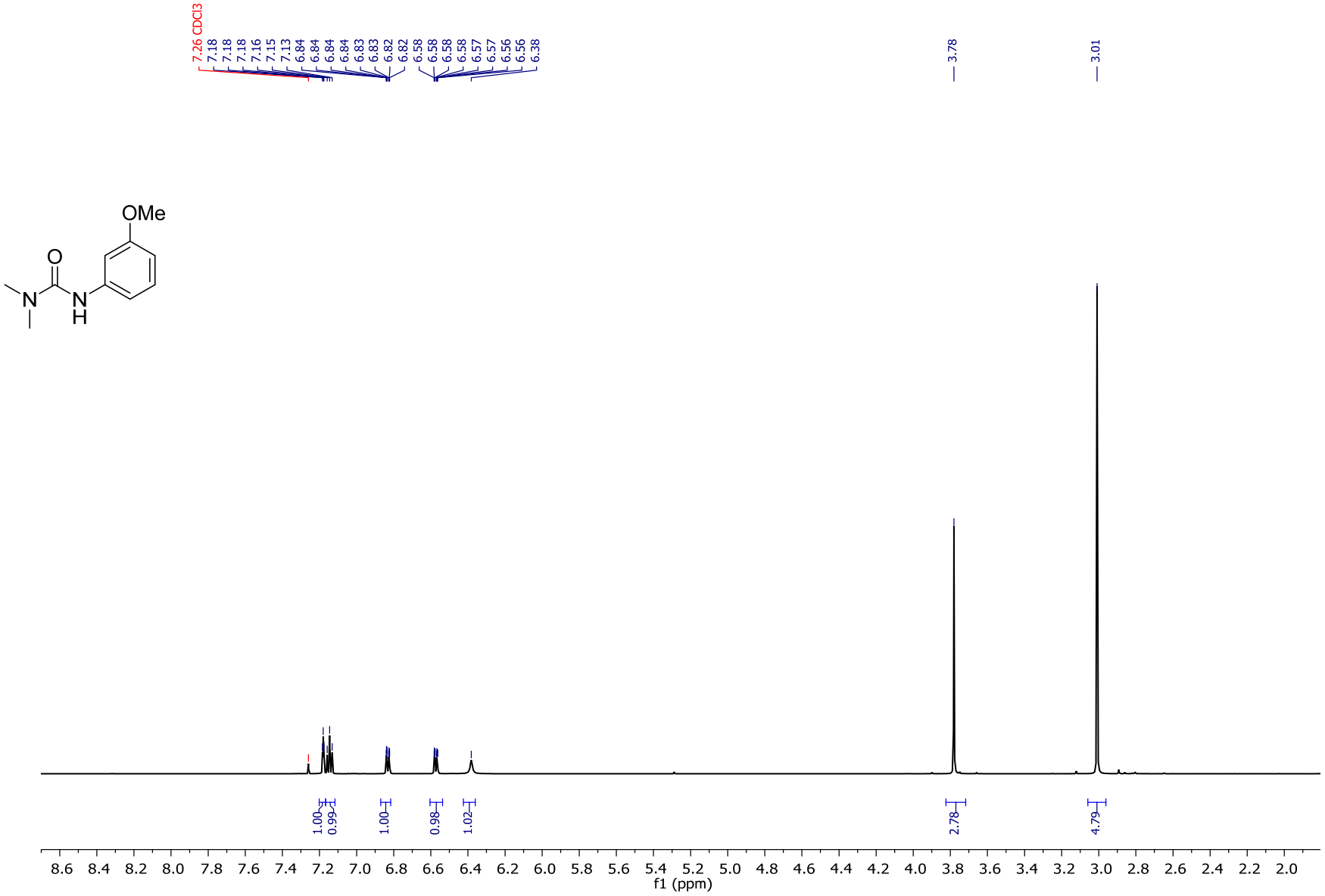

^{13}C NMR data for **24** (150 MHz; $CDCl_3$)

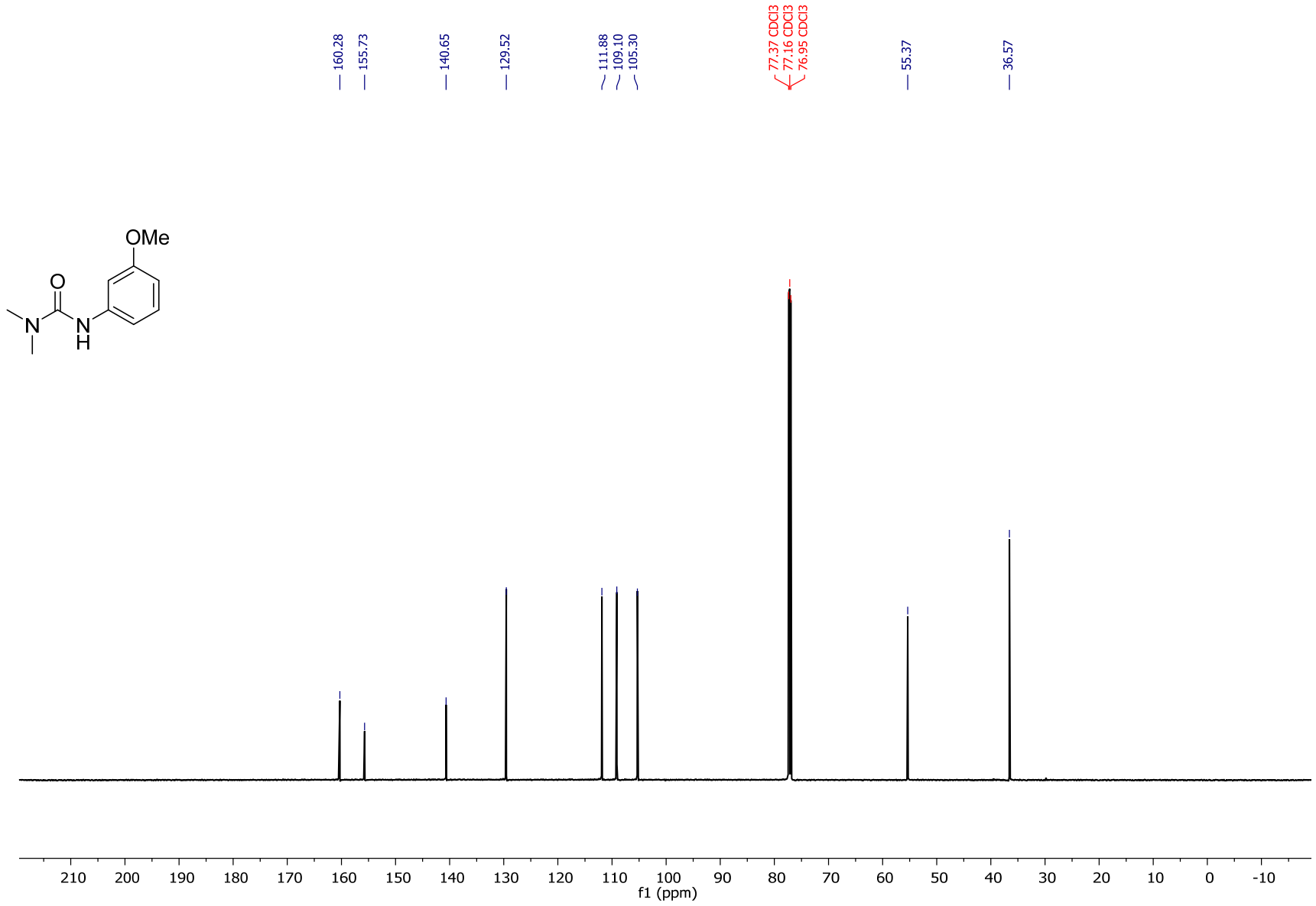

^{1}H NMR data for **25** (600 MHz; DMSO-d_6)

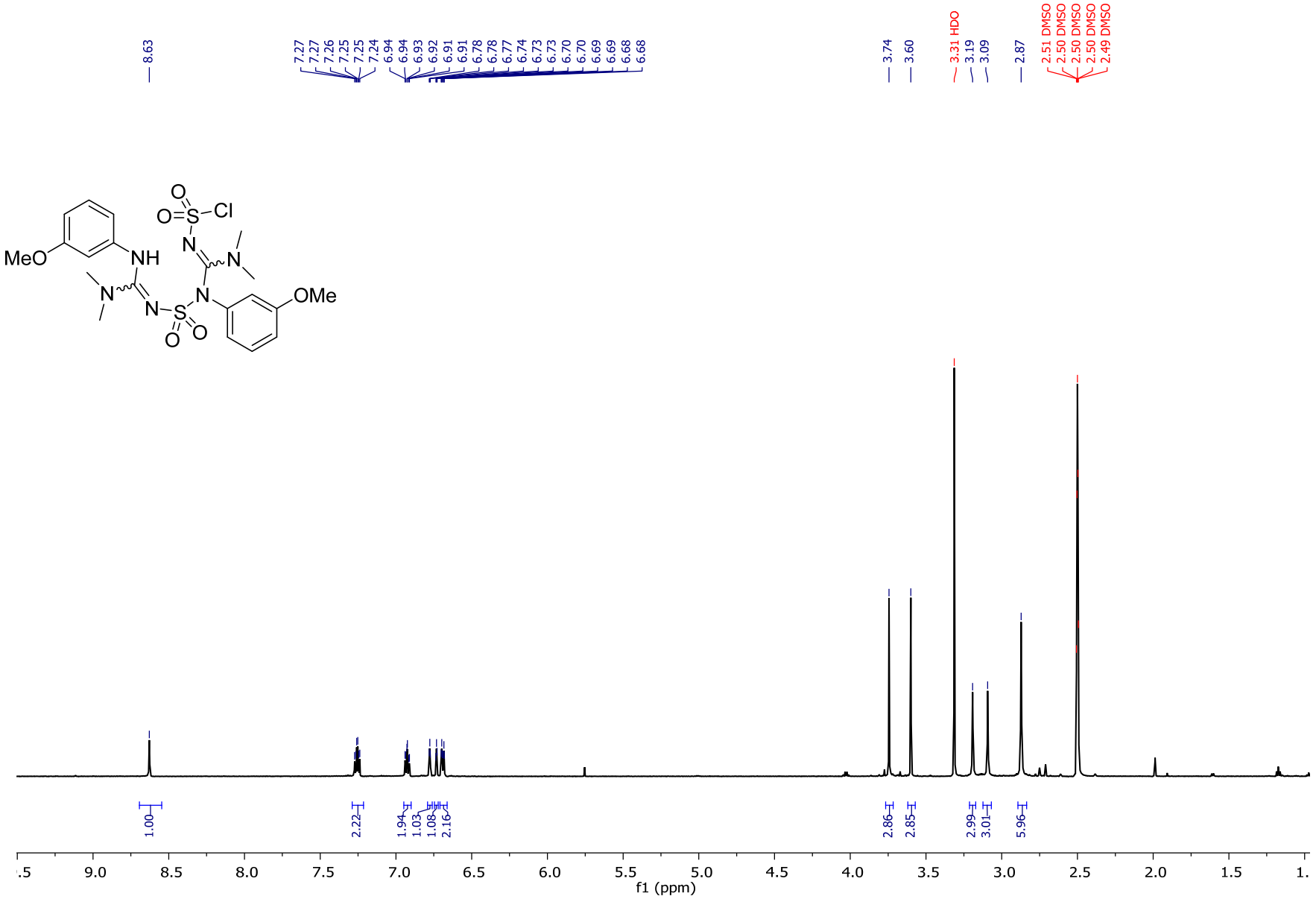

^{13}C NMR data for **25** (150 MHz; DMSO-*d*$_6$)

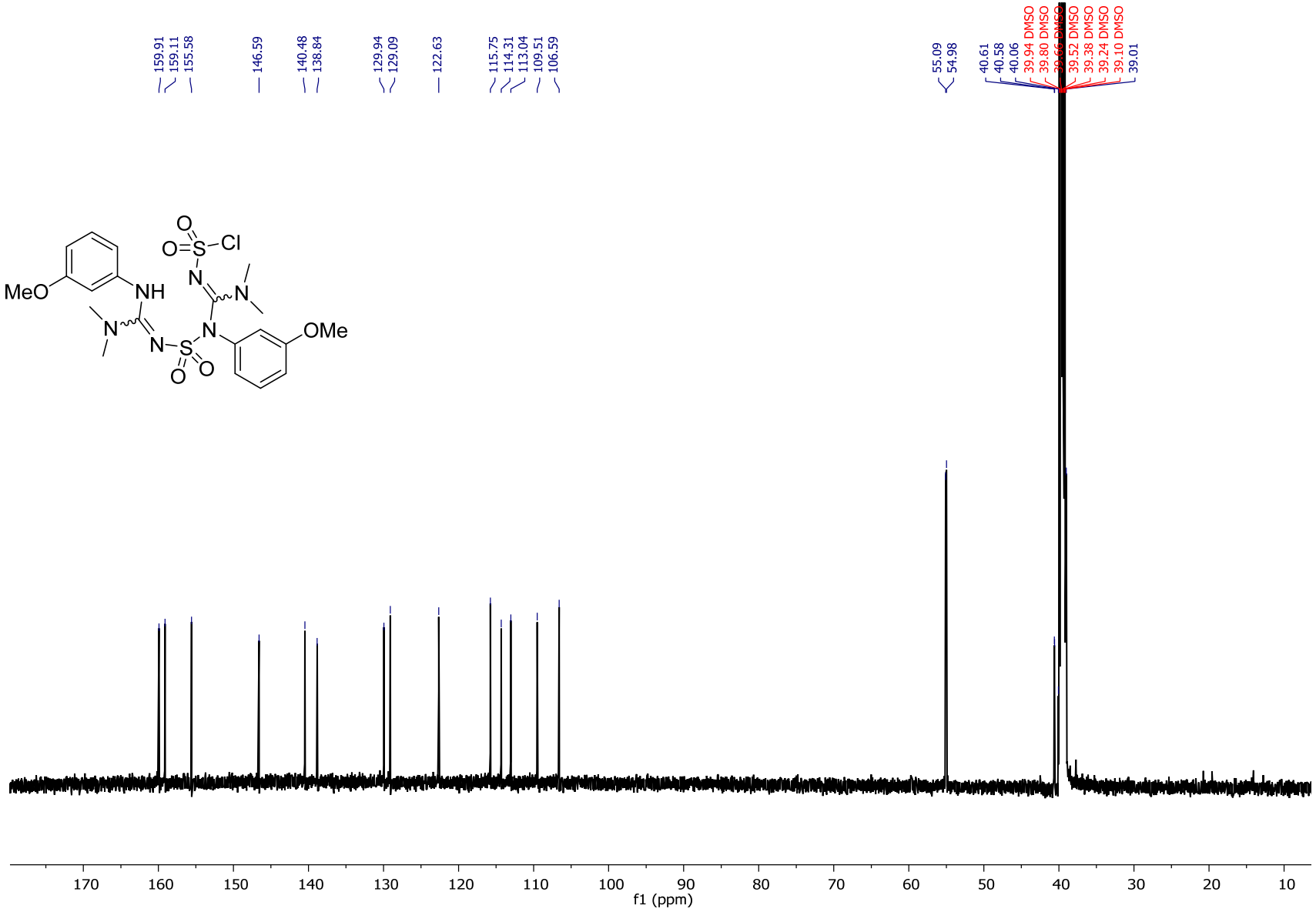

^{1}H NMR data for **8j** (600 MHz; DMSO-d_6)

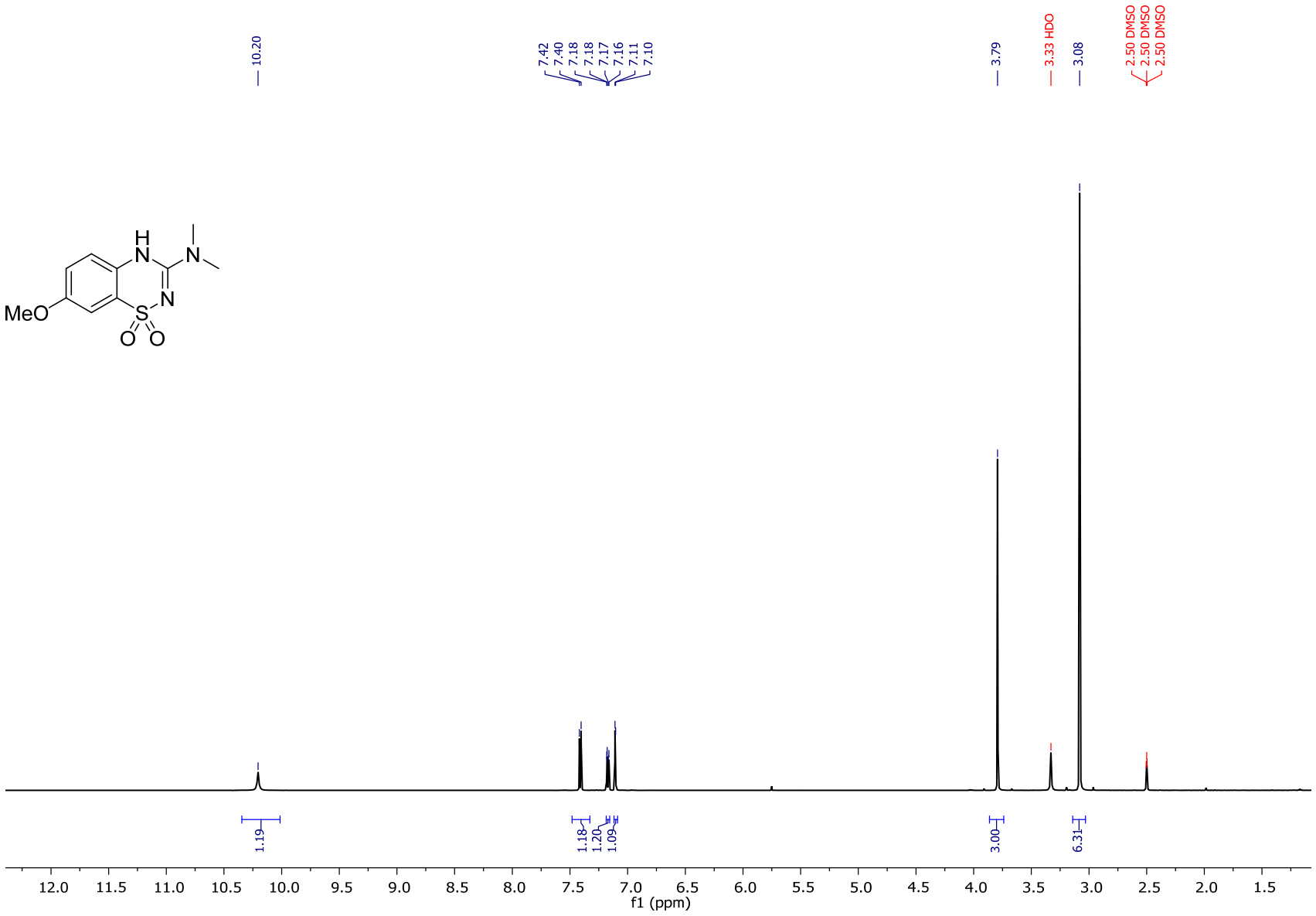

^{13}C NMR data for **8j** (150 MHz; DMSO-d_6)

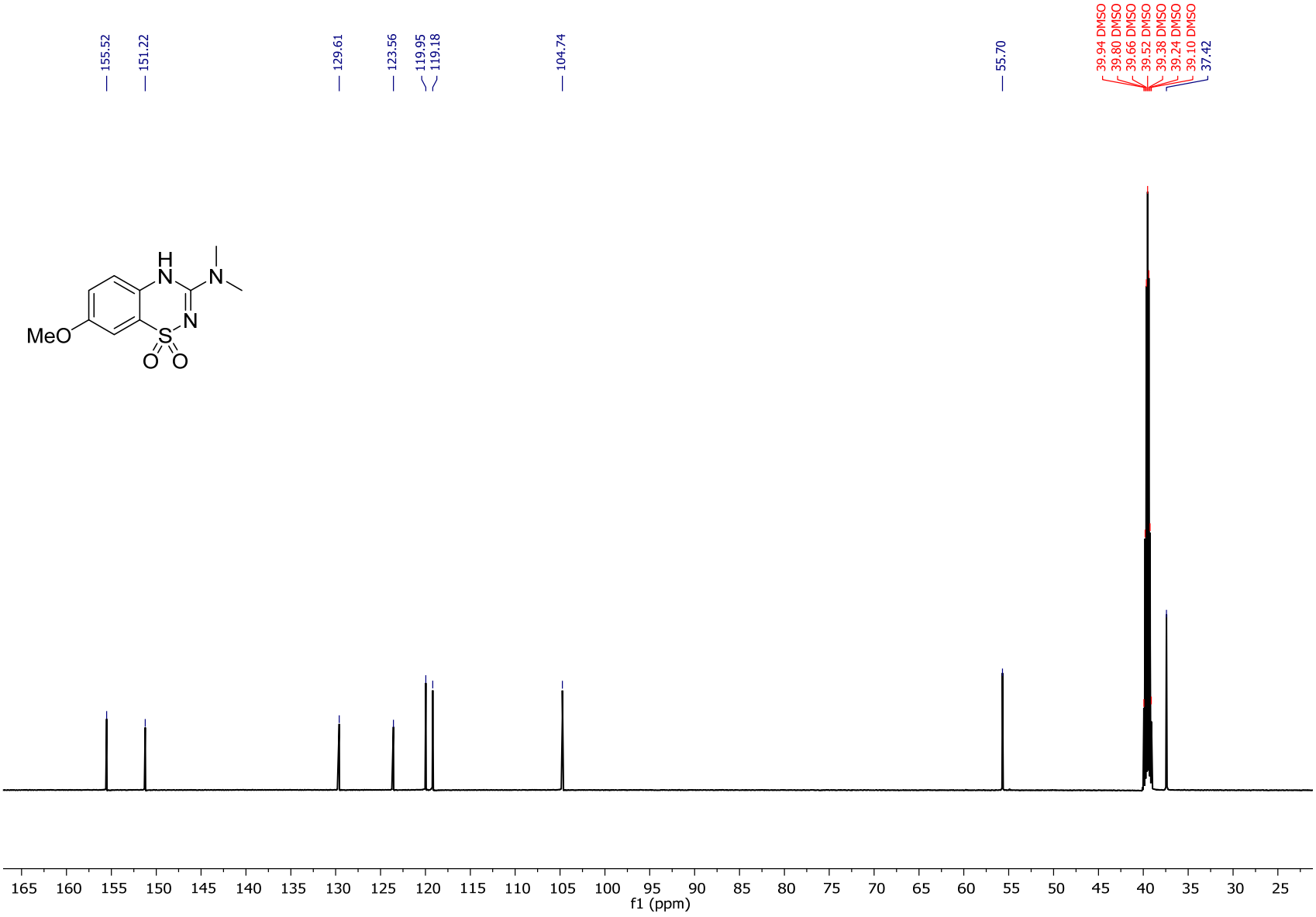

^{1}H NMR data for **9j** (600 MHz; DMSO-d_6)

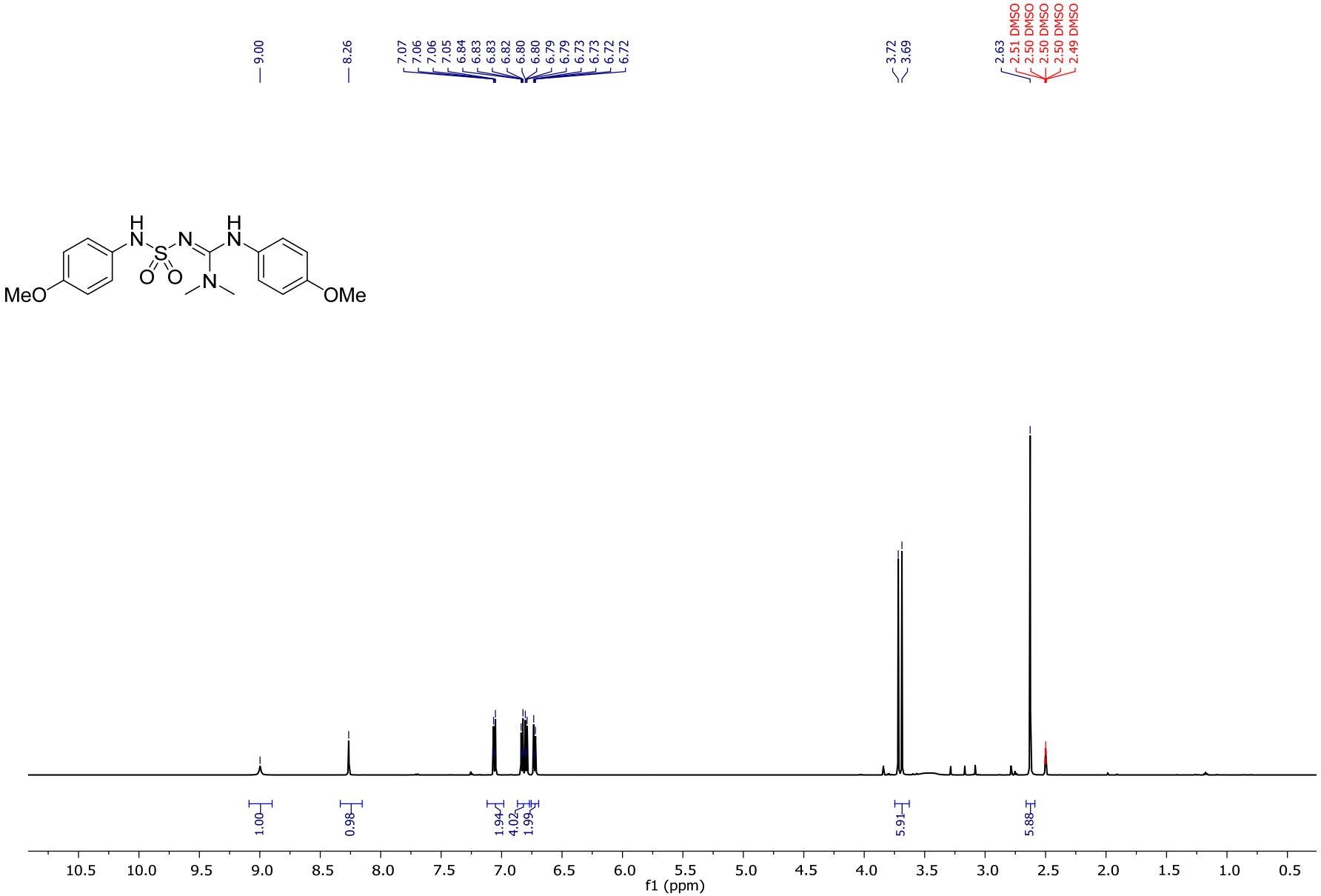

^{13}C NMR data for **9j** (150 MHz; DMSO-d_6)

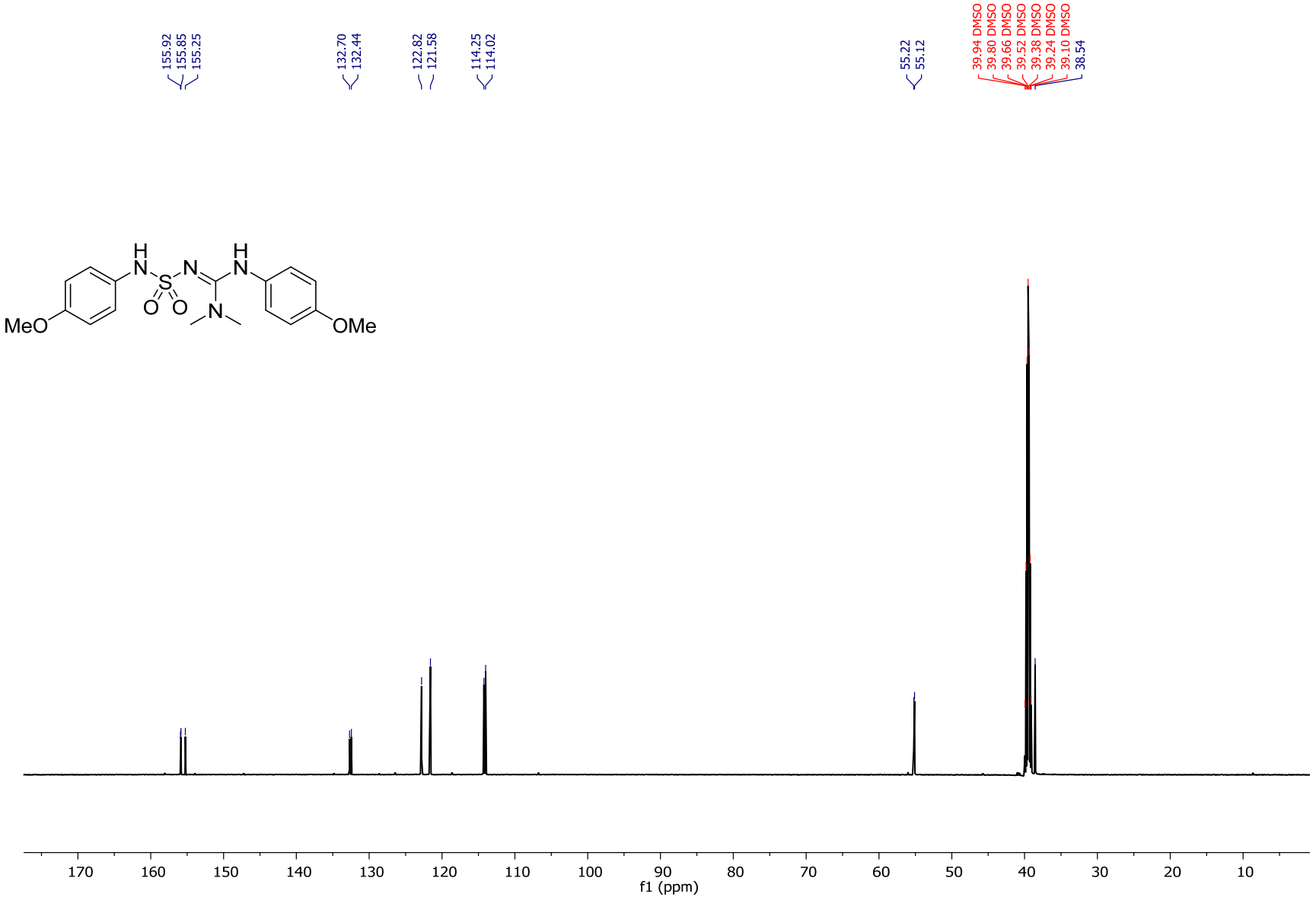

^{1}H NMR data for **14j.HBr** (600 MHz; DMSO-d_6)

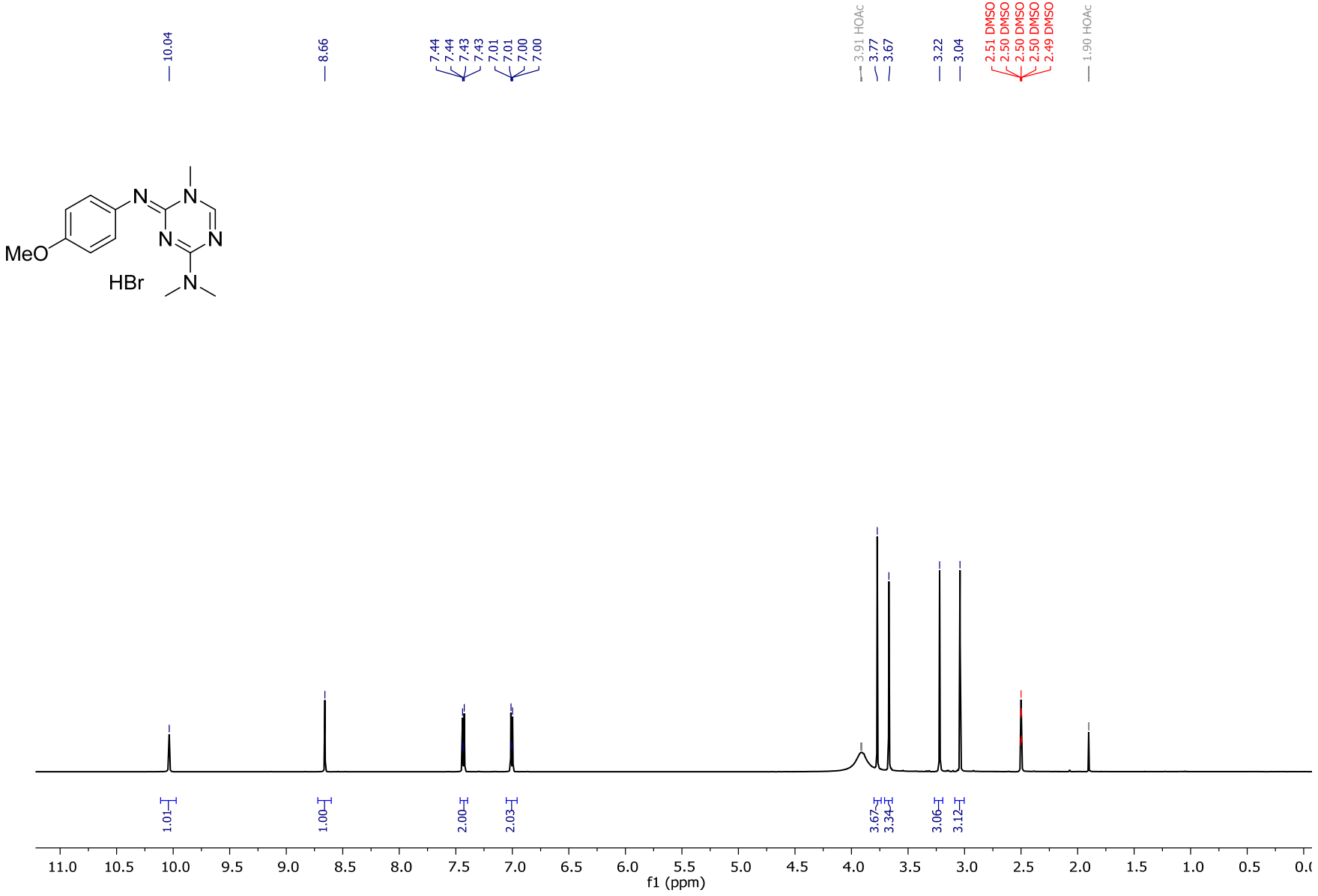

^{13}C NMR data for **14j.HBr** (150 MHz; DMSO-d_6)

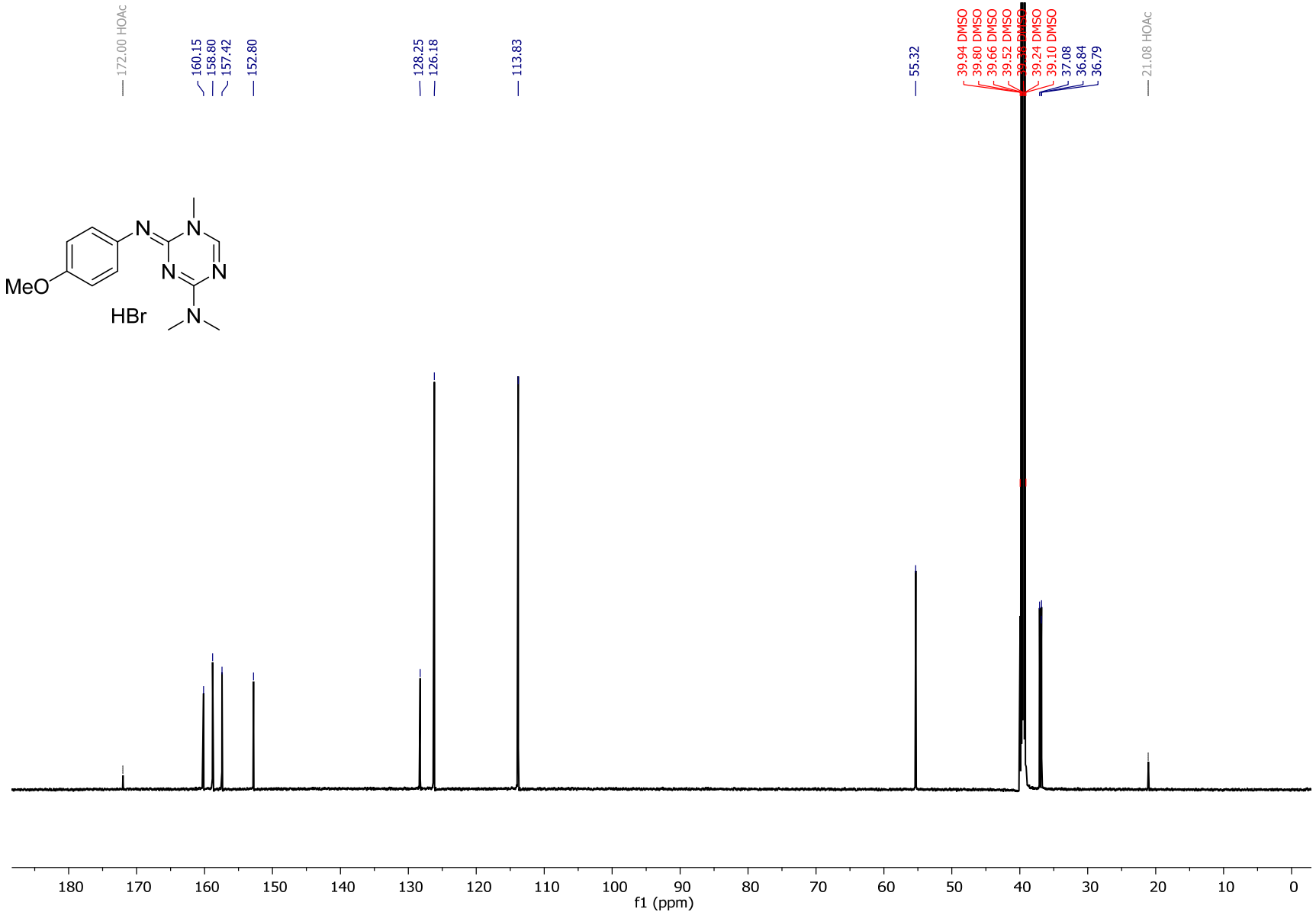

^{1}H NMR data for **28** (400 MHz; DMSO-d_6)

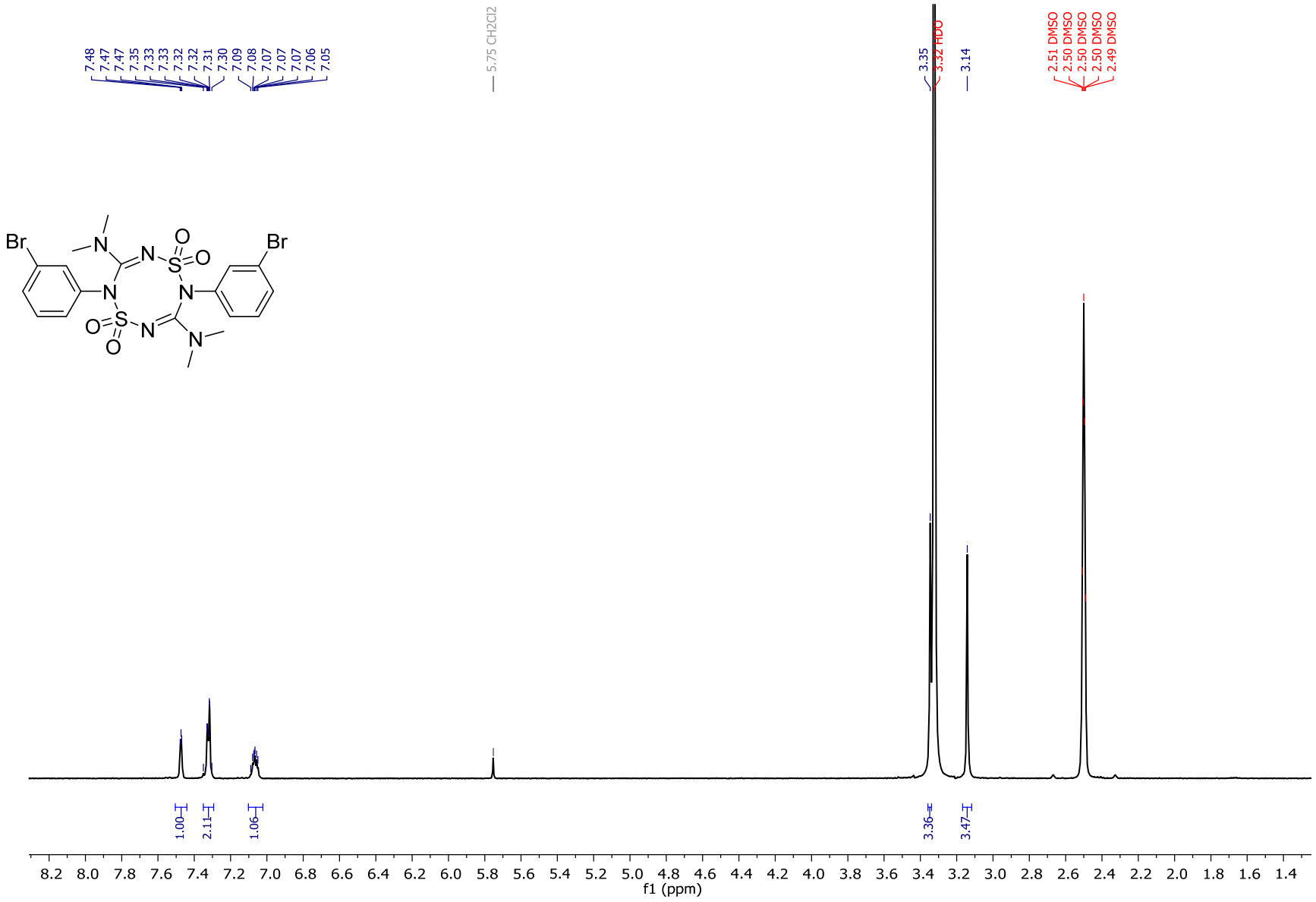

^{13}C NMR data for **28** (150 MHz; DMSO-d_6)

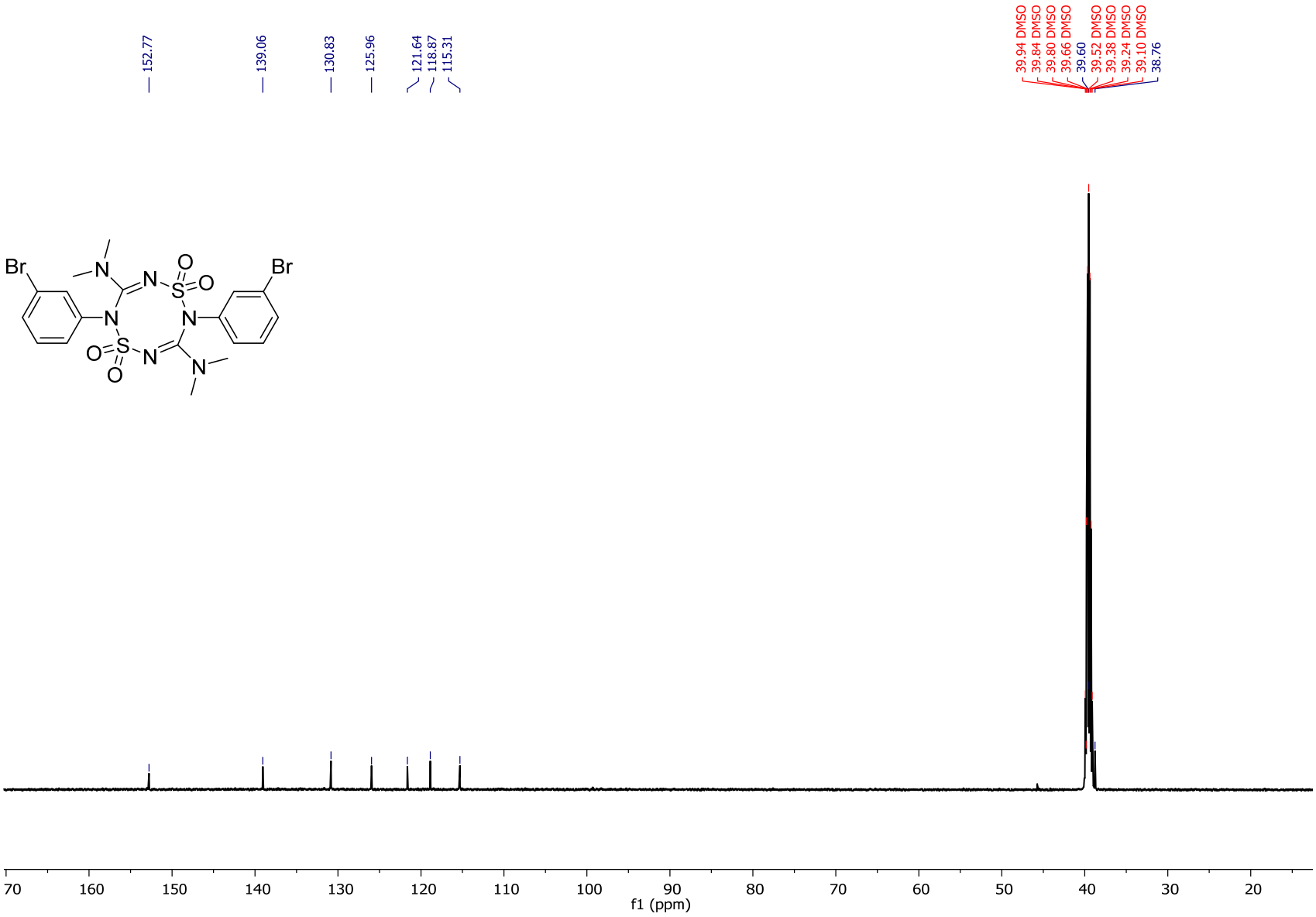

^{1}H NMR data for **17k** (600 MHz; DMSO-d$_6$)

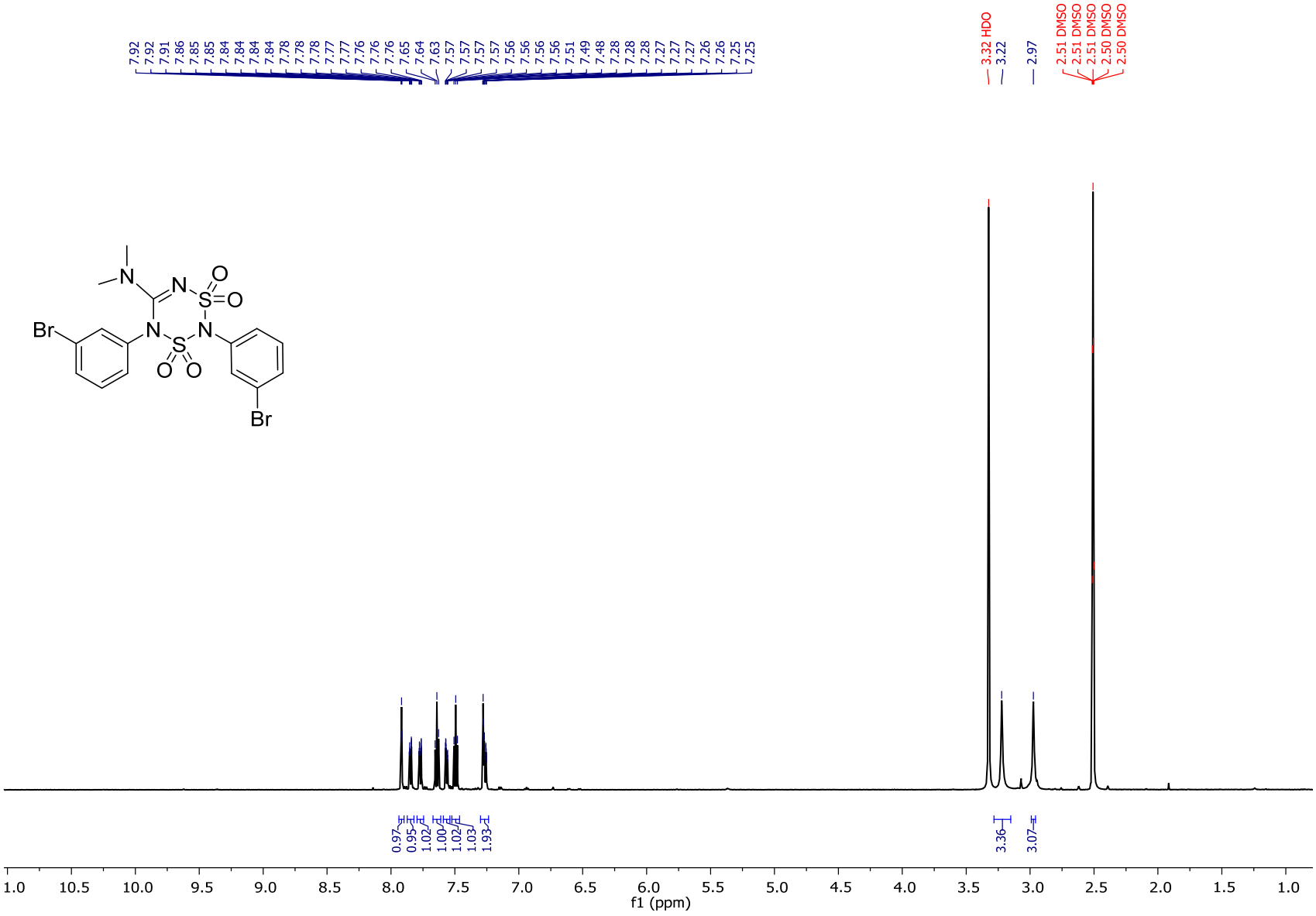

^{13}C NMR data for **17k** (150 MHz; DMSO-d_6)

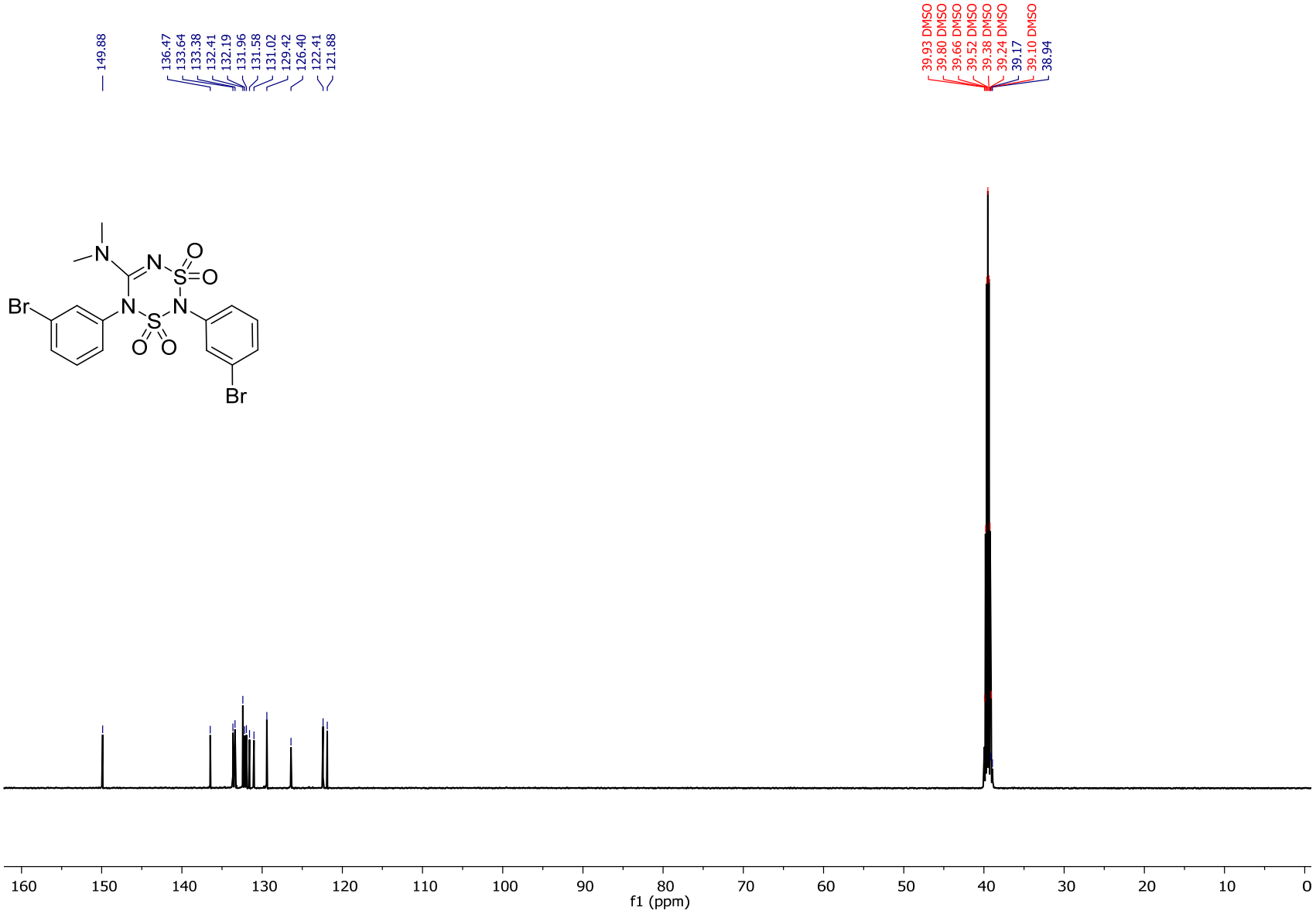

^{1}H NMR data for **27** (600 MHz; DMSO-d_6)

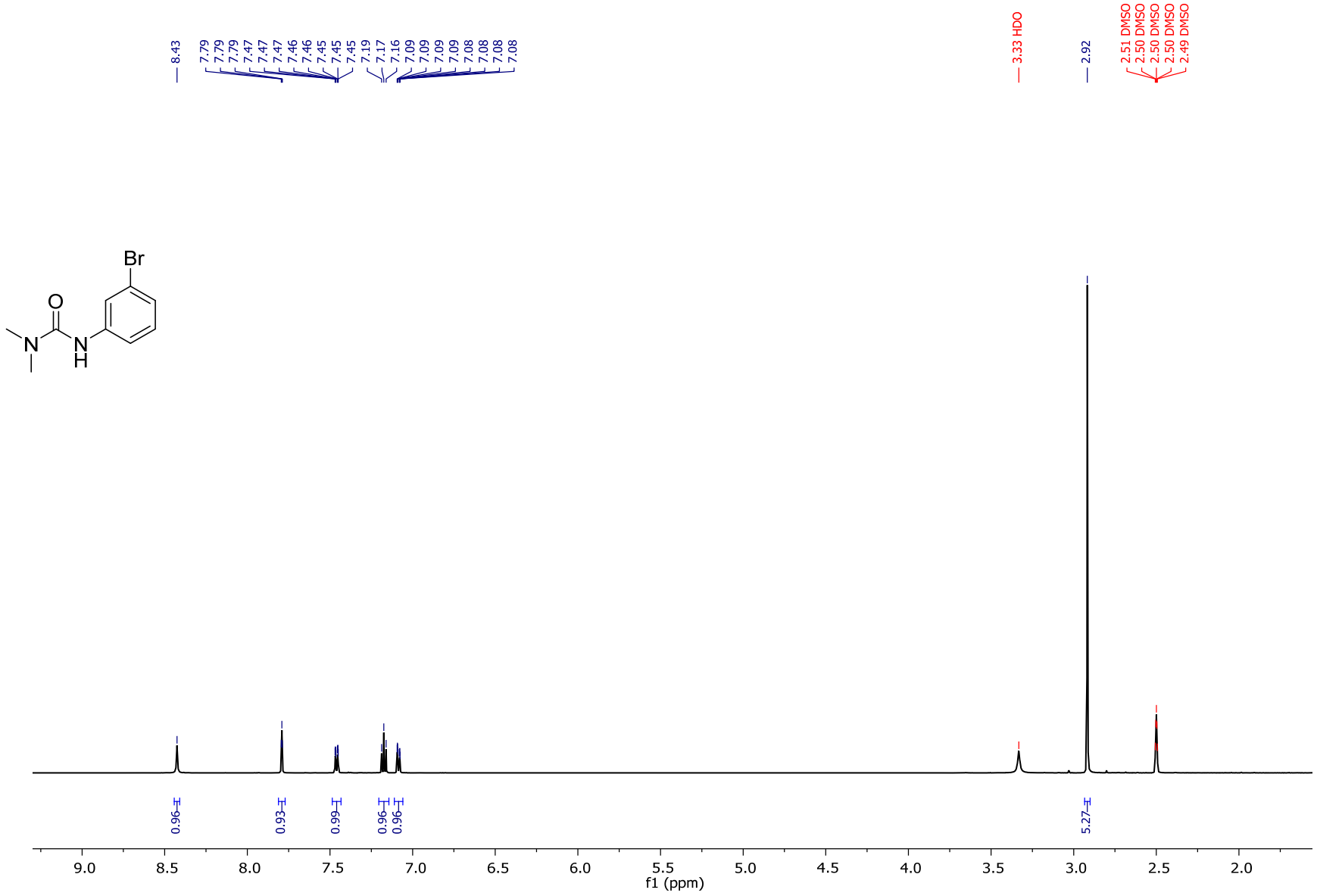

^{13}C NMR data for **27** (150 MHz; DMSO-d_6)

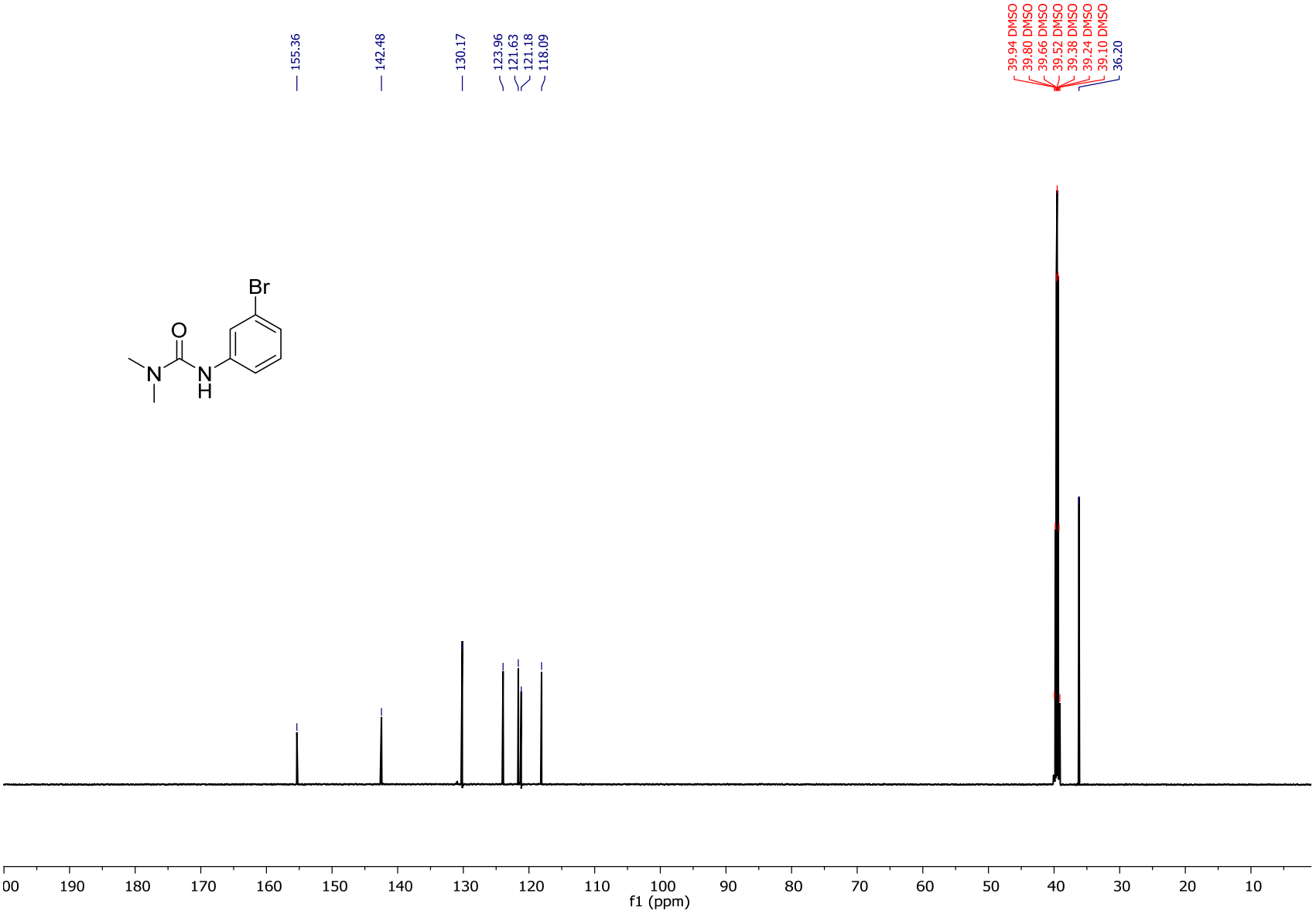

^{1}H NMR data for **8k & 8l** (600 MHz; DMSO-d_6)

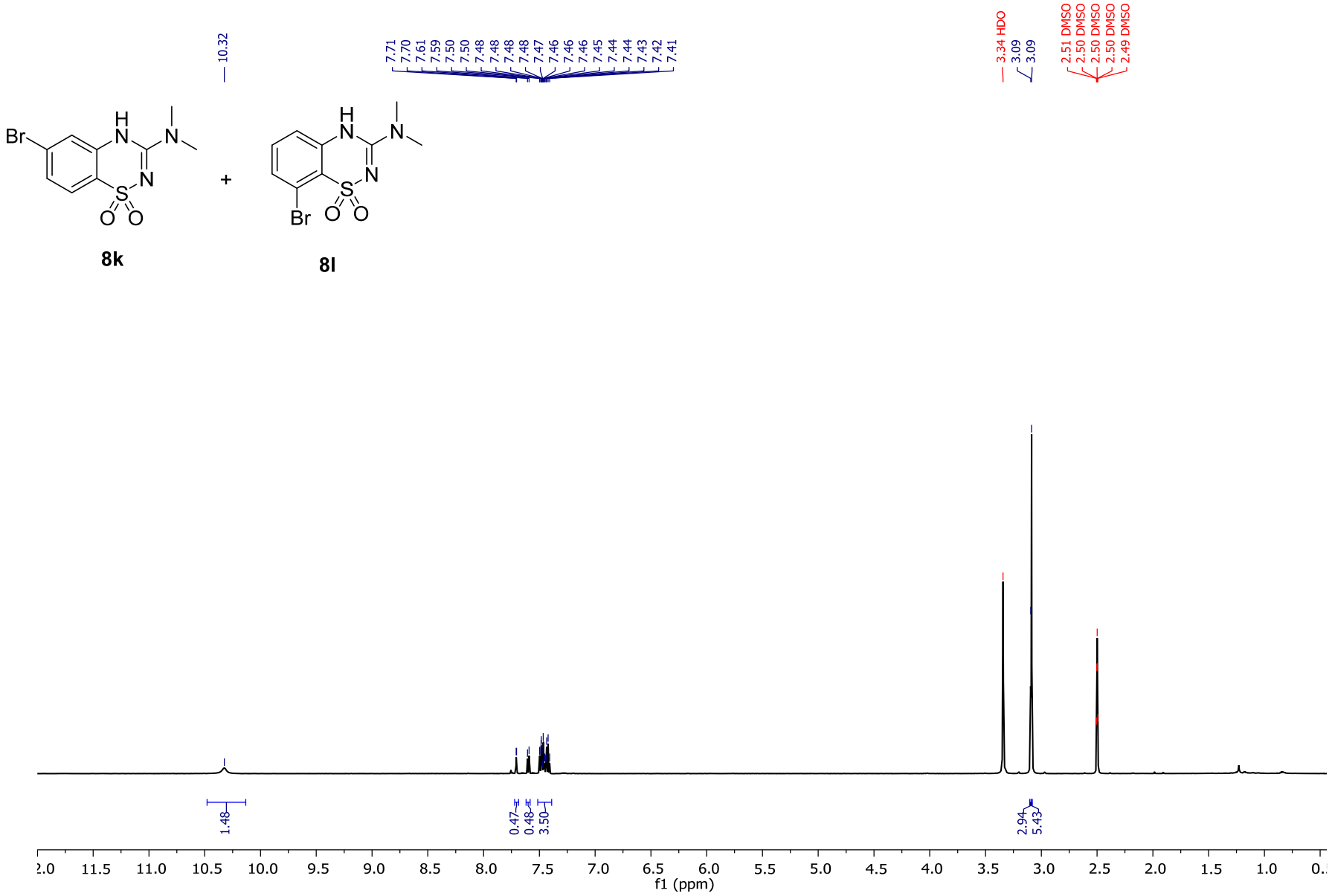

^{13}C NMR data for **8k & 8l** (150 MHz; DMSO-d_6)

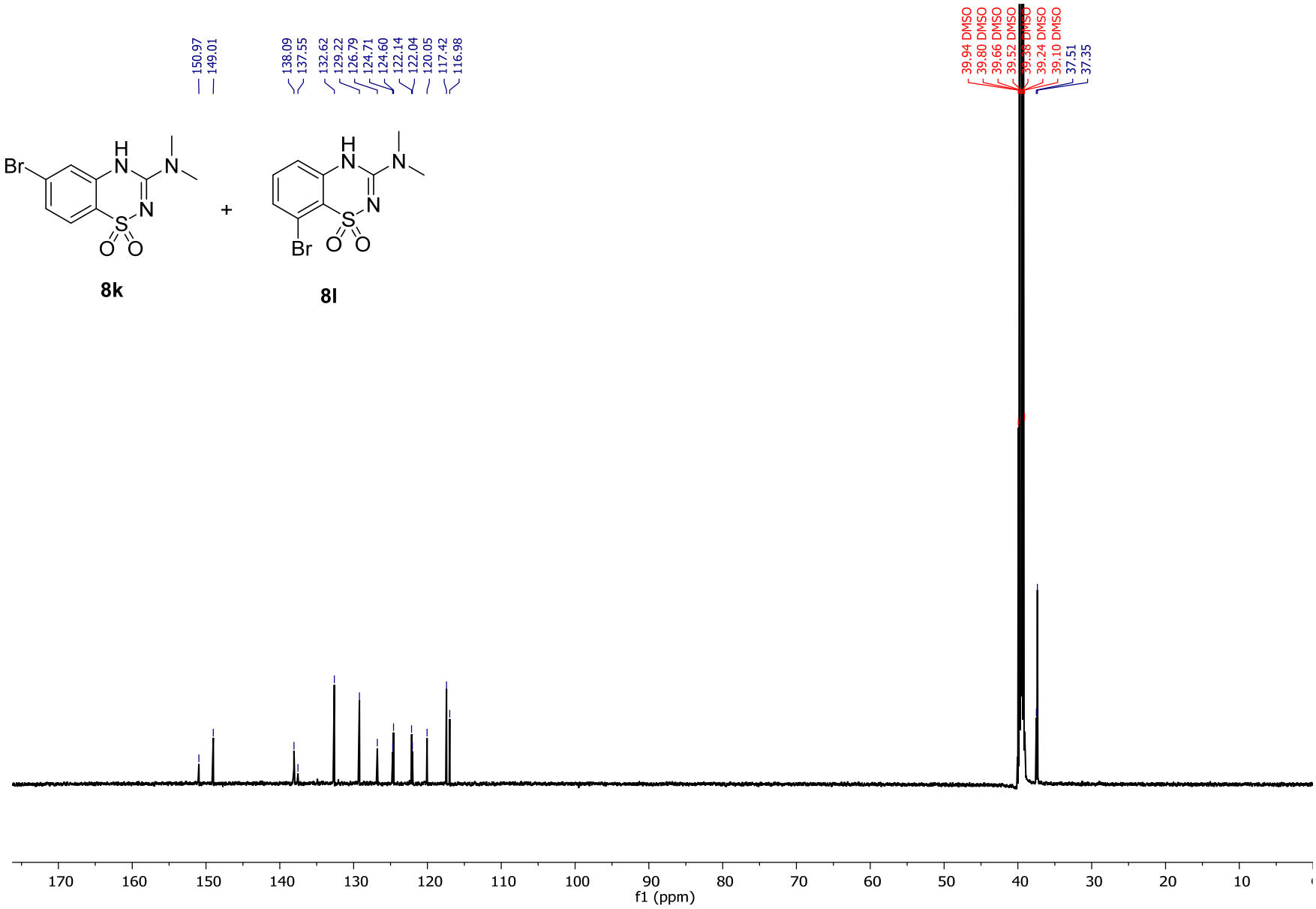

^{1}H NMR data for **8k** (600 MHz; DMSO-d_6)

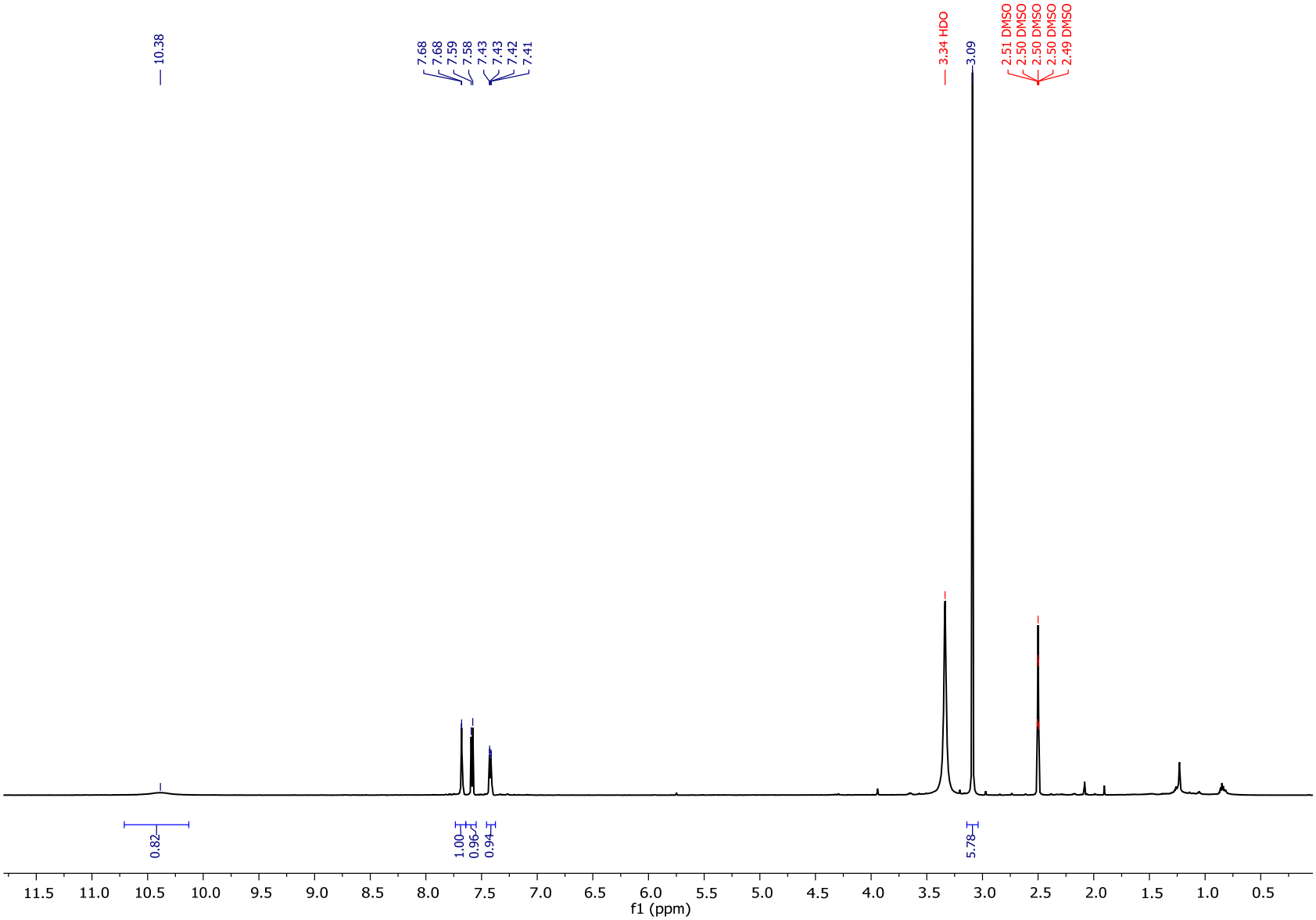

^{13}C NMR data for **8k** (150 MHz; DMSO-d_6)

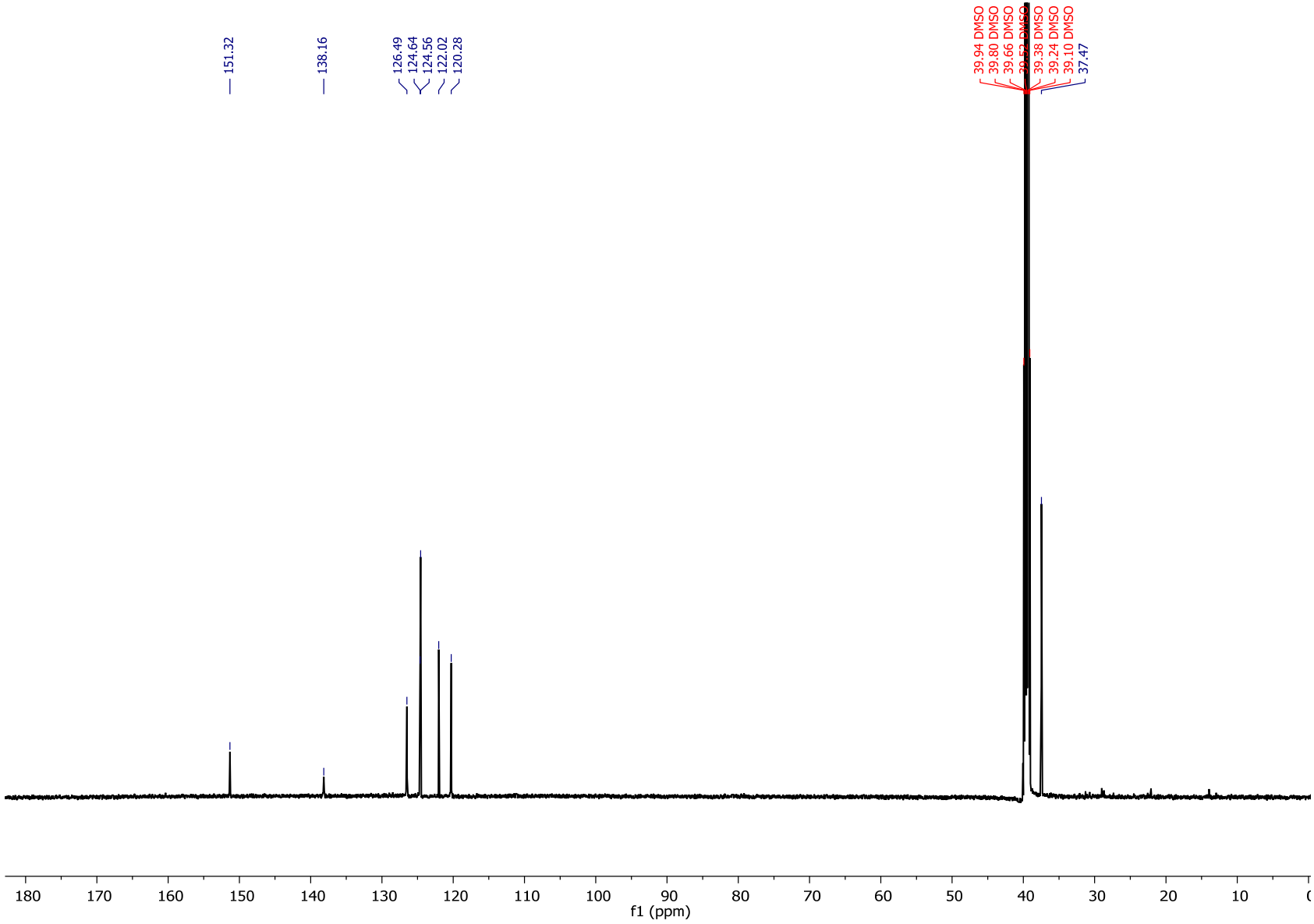

^{1}H NMR data for **9k** (600 MHz; DMSO-d$_6$)

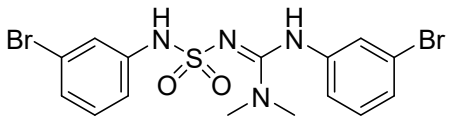

^{13}C NMR data for **9k** (150 MHz; DMSO-d_6)

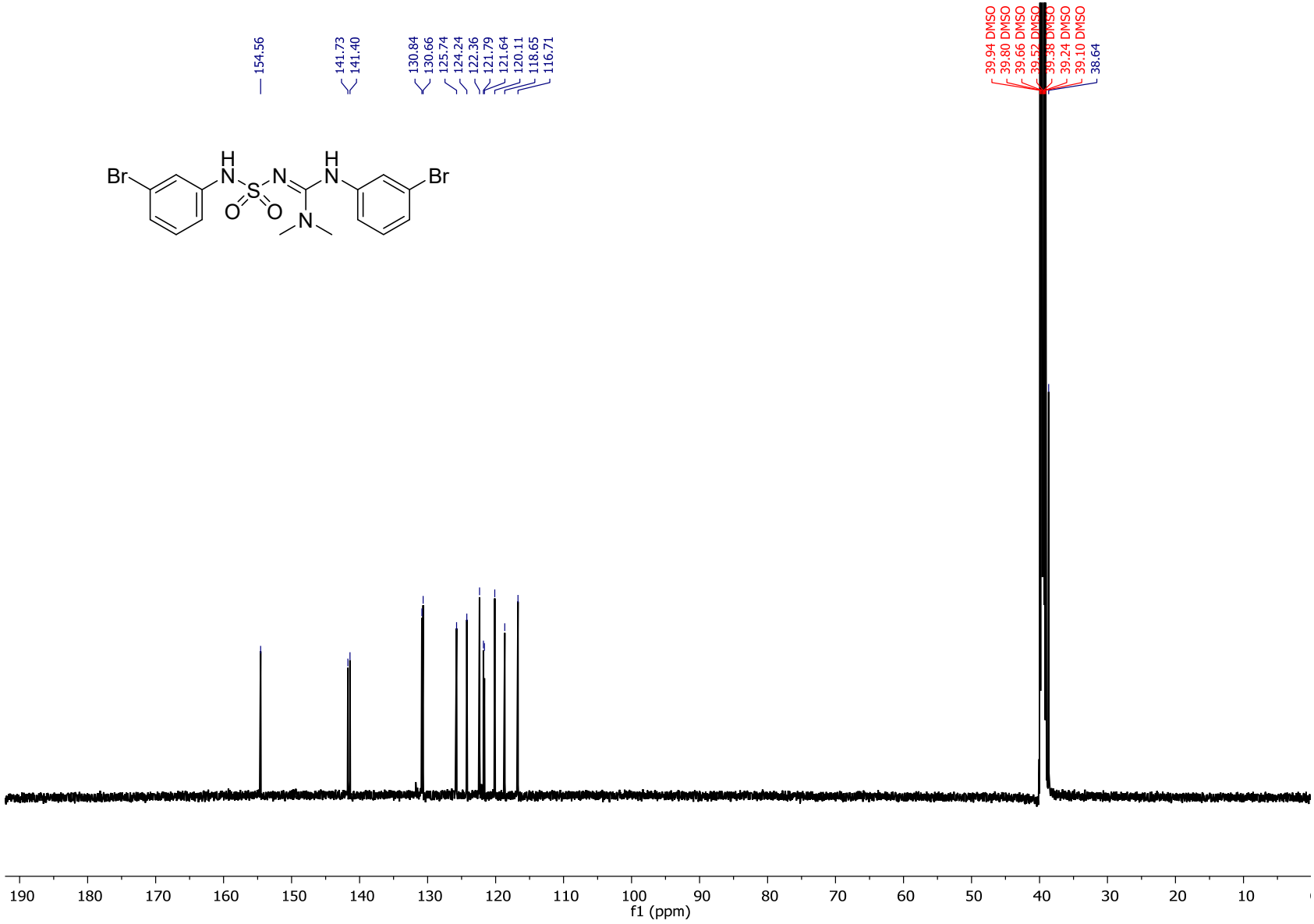

Dynamic NMR Calculations for compounds 17g and 17h.

Dynamic NMR simulations and line shape analyses for compounds **17g** and **17h** were performed with DNMR3 module of the SpinWorks program (Version 4.2.0).[17-20] Exchange rates were determined at different temperatures in the temperature range −35 to +65 °C. The activation parameters were determined from a least-squares Eyring plot by using the program Microsoft Excel 2007.

$\Delta G^{\ddagger}$ (kJ/mol) values were calculated at each temperature from the equation: $\Delta G^{\ddagger} = aT[10.319 + \log\left(\frac{T}{rate}\right)$; where a = 1.914 × 10^{-2}.[20] Arrhenius plots of ln(k) vs. 1/T ($slope = -\frac{Ea}{R}$; where R = 8.314) were used to determine the E_a value for each of the slow-exchange processes. Eyring plots of ln(k/T) vs. 1/T provided values for $\Delta H^{\ddagger}$ and $\Delta S^{\ddagger}$ (slope = $\frac{\Delta H}{R}$; intercept = $\frac{\Delta S}{R} + \ln\left(\frac{kb}{h}\right)$; where R = 8.314, kb = Boltzmann's constant and h = Planck's constant).

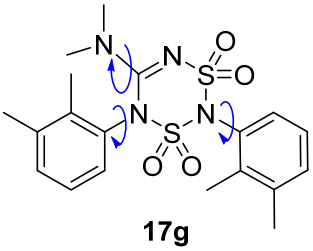

17g

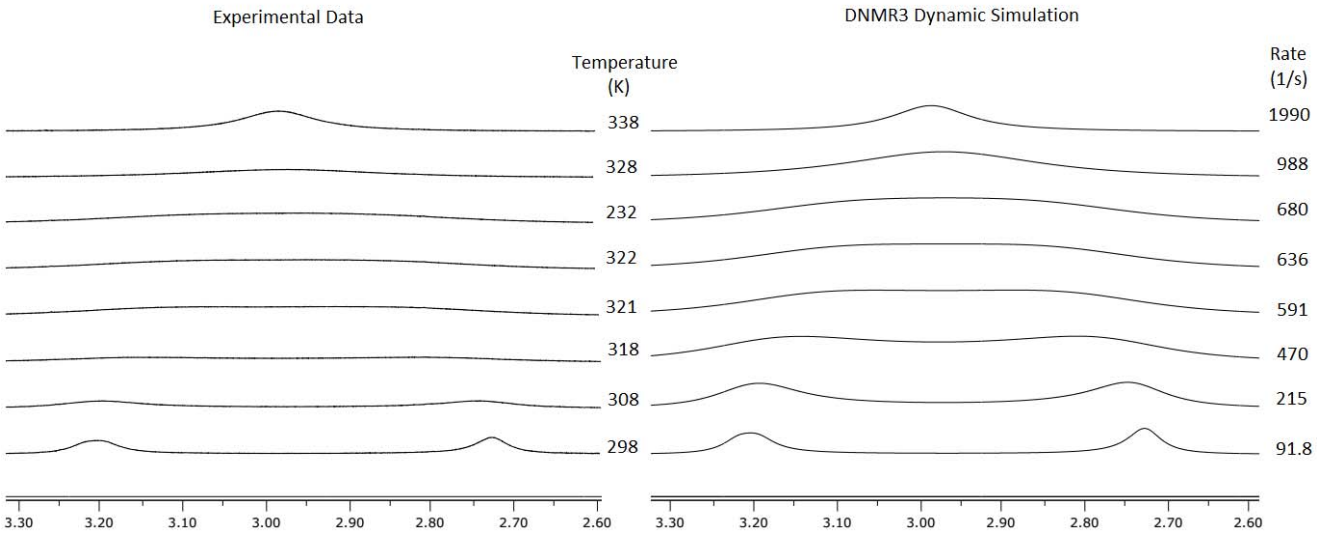

Figure 1. DNMR3 Simulation and determination of rates for compound 17g at 25–65 °C.

Table 1. $\Delta G^{\ddagger}$ (kJ/mol) Values for compound 17g at 25–65 °C.

T (K)	Rate (1/s)	$\Delta G^{\ddagger}$ (kJ/mol)
298.2	91.85	61.82
308.3	215.0	61.81
318.2	470.0	61.81
321.2	591.0	61.81
322.2	636.0	61.82
323.1	680.0	61.82
328.2	988.0	61.81
338.2	1990.0	61.81
	Average =	61.81

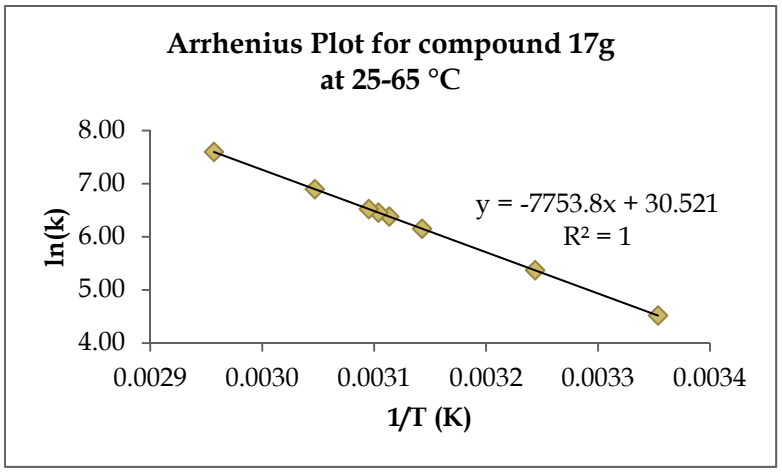

Figure 2. Arrhenius Plot for compound 17g at 25-65 °C. Provides: E_a = 64.47 kJ/mol.

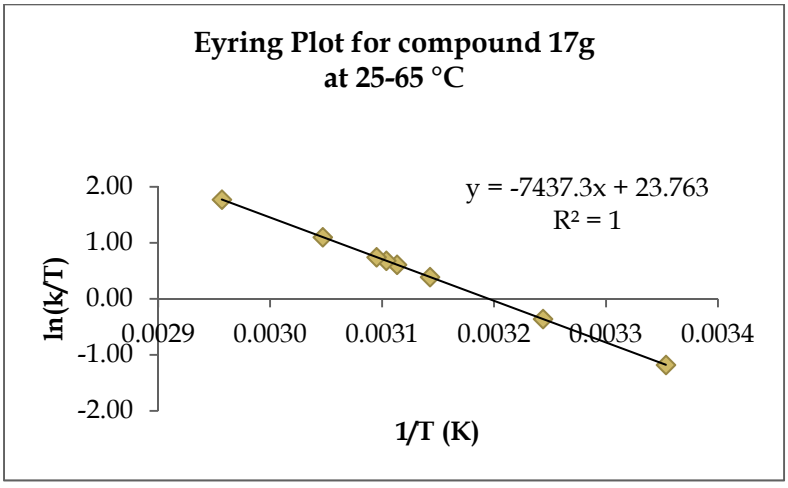

Figure 3. Eyring Plot for compound 17g at 25-65 °C. Provides: $\Delta H^{\ddagger}$ = 61.84 kJ/mol and $\Delta S^{\ddagger}$ = 0.026 J/mol.K

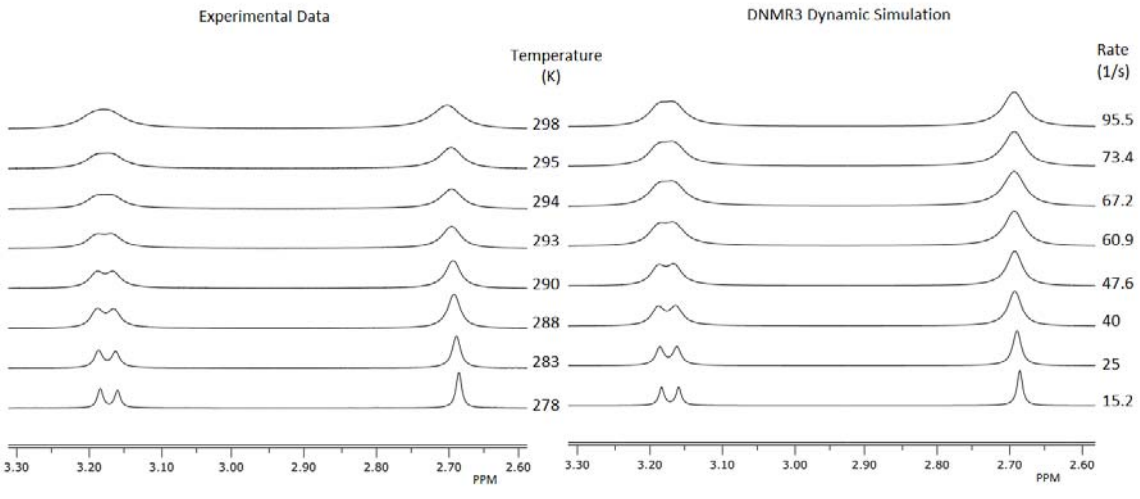

Figure 4. DNMR3 Simulation and determination of rates for compound 17g at 5–25 °C.

Table 2. $\Delta G^{\ddagger}$ (kJ/mol) Values for compound 17g at 5–25 °C.

T (K)	Rate (1/s)	$\Delta G^{\ddagger}$ (kJ/mol)
278.4	15.2	61.71
283.5	25.0	61.72
288.5	40.0	61.72
290.4	47.6	61.72
293.1	60.9	61.72
294.2	67.2	61.72
295.2	73.4	61.72
298.2	95.5	61.72
	Average =	61.72

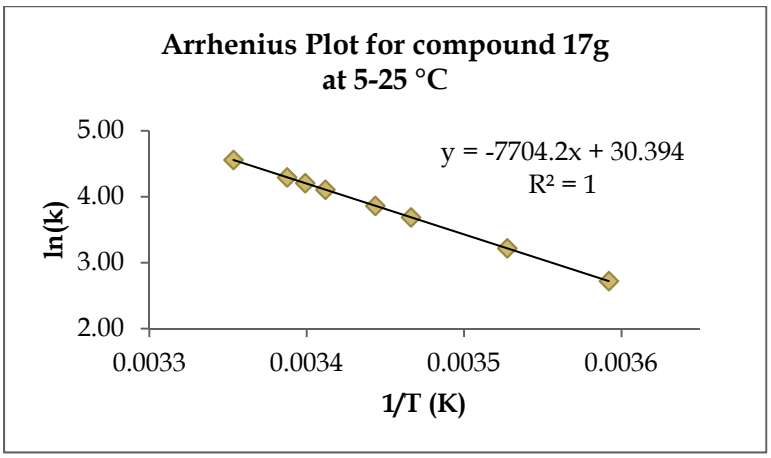

Figure 5. Arrhenius Plot for compound 17g at 5-25 °C. Provides: E_a = 64.05 kJ/mol.

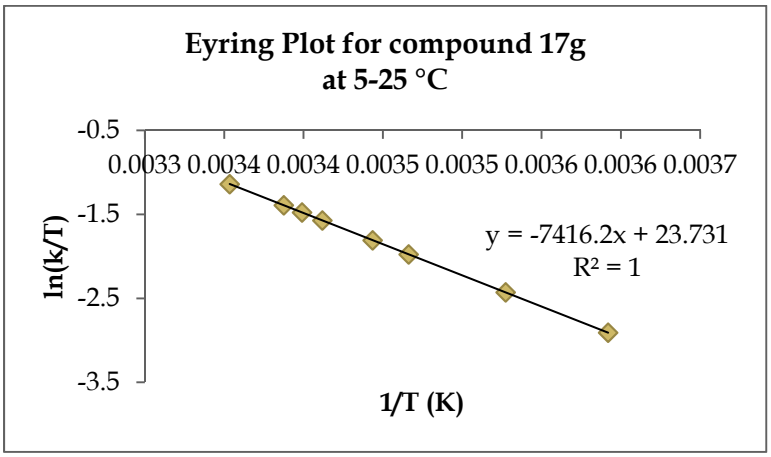

Figure 6. Eyring Plot for compound 17g at 5-25 °C. Provides: $\Delta H^{\ddagger}$ = 61.66 kJ/mol and $\Delta S^{\ddagger}$ = −0.24 J/mol,K

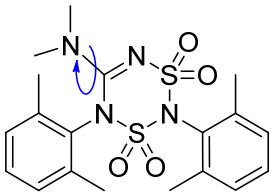

17h

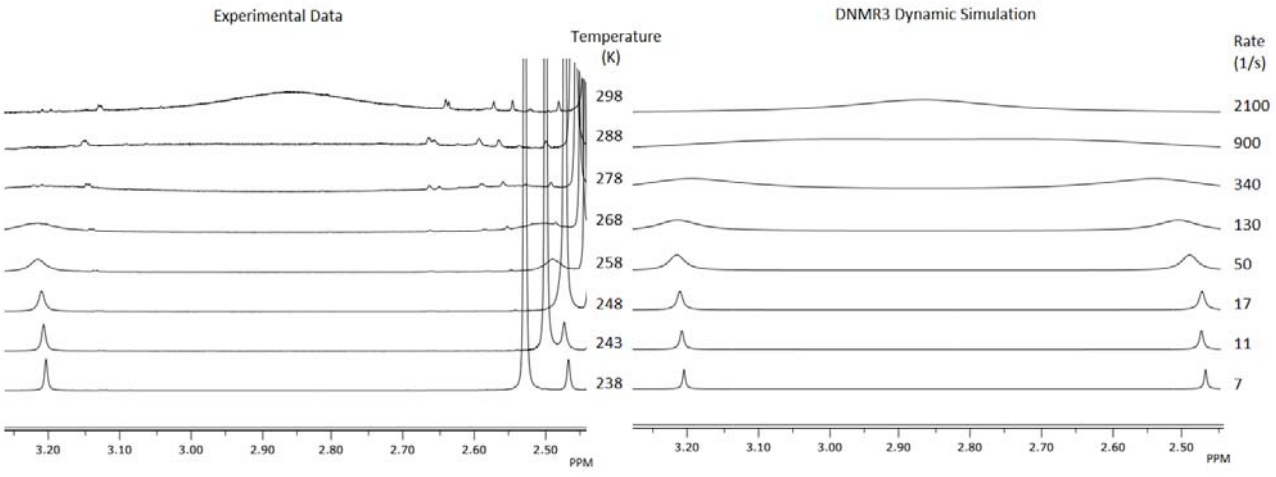

Figure 7. DNMR3 Simulation and determination of rates for compound 17h at −35–25 °C.

Table 3. $\Delta G^{\ddagger}$ (kJ/mol) values for compound 17h at −35–25 °C.

T (K)	Rate (1/s)	$\Delta G^{\ddagger}$ (kJ/mol)
238	7	53.98
243.1	11	54.27
248.2	17	54.55
258.2	50	54.52
268	130	54.54
278.1	340	54.46
287.9	900	54.13
298.1	2100	54.04
	Average =	54.31

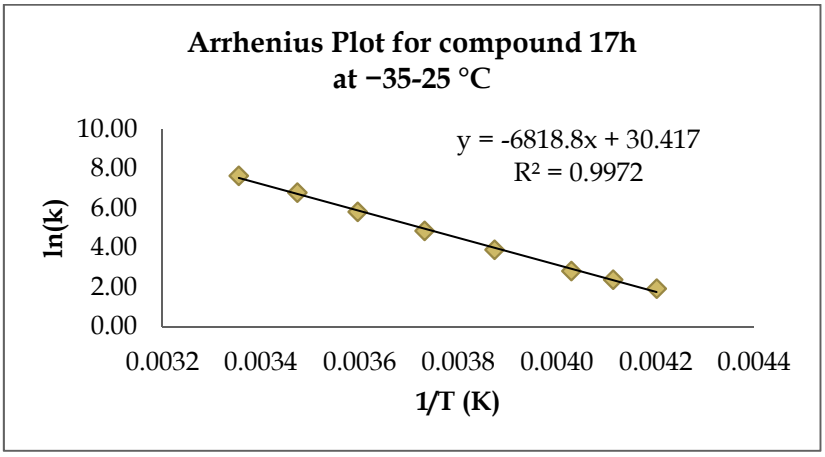

Figure 8. Arrhenius Plot for compound 17h at −35–25 °C. Provides: E_a = 56.69 kJ/mol.

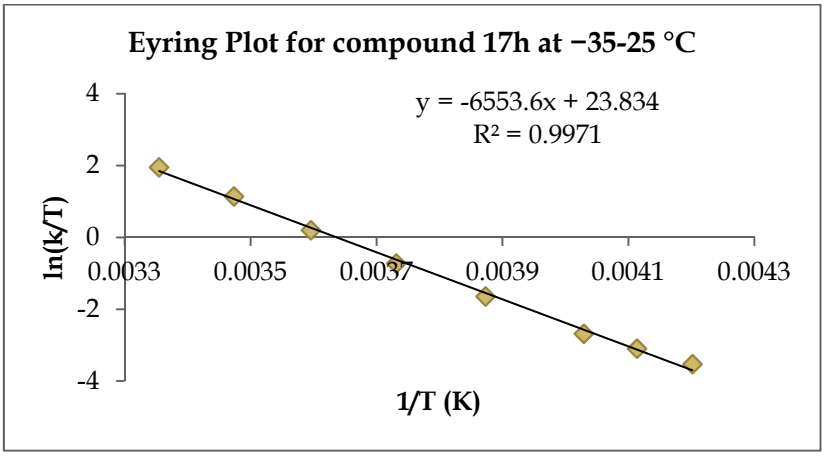

Figure 9. Eyring Plot for compound 17h at −35–25 °C. Provides: $\Delta H^{\ddagger}$ = 54.49 kJ/mol and $\Delta S^{\ddagger}$ = 0.62 J/mol,K